Robust Control via Adaptive, Learning, and Switching Controllers

Laurence S. Irlicht

B.Sc. Hons. (Melb), Dip. Ed. (Melb)

November 1992

A thesis submitted for the degree of Doctor of Philosophy of the Australian National University

Department of Systems Engineering

Research School of Physical Sciences and Engineering,

Co-operative Research Centre for Robust and Adaptive Systems

The Australian National University

Acknowledgements

I would like to thank the students and staff of the Systems Engineering Department for providing a stimulating environment in which to work. More specifically, I thank my supervisor, John Moore, for having the patience to guide me in the initial stages of my course, and the wisdom to allow my independence to grow toward the end. John taught me a lot about engineering, and also a lot about living.

I would also like to thank Iven Mareels for helping me to develop my ideas, for a shared enthusiasm to research, and for many fruitful discussions on matters well beyond those contained in this thesis.

This acknowledgement would not be complete without reference to the many friends who have been there for me during the last 3 years, especially Perry Blackmore, and also Brian Ewert, David Ekselman, and Simon Inglis.

Finally, but not least, I thank my parents, Ted and Sylvia, and my sister, Sari. I thank them for their support and especially their encouragement. Thanks for believing in me - it made a difference.

Statement of Originality.

The work presented in this thesis is the result of original research done by myself in collaboration with others in the time I have been enrolled in the Department of Systems Engineering as a Doctor of Philosophy student. It has not been submitted for any other degree or award in any other university or educational institution. Much of it has been published or accepted for publication in refereed journals and conference proceedings, [28, 30, 33, 43], or submitted for publication [31]. At times, I worked on developing ideas by supervisors, and at other times they gave me help on my own ideas. Certainly, I identify very closely with 100% of the thesis content, and yet my supervisors probably also identify closely with large portions of the thesis as well. The specific contributions I particularly identify with are summarized as follows:

- The nonlinear Q, S stabilization results of Chapter 2 were carried out jointly by myself and Prof. Moore. I also developed the simulation section by streamlining the original code, and extending it to cope with various disturbances, repeated trajectories and unmodelled dynamics.

- The idea of utilising a functional-learning Q scheme was Prof. Moore's. We worked together on the implementation issues, and I extended the developed methods to the vector case, created the programs used to implement functional learning theory, spliced them into the adaptive-Q program and designed and implemented the simulations.

- The problem of extending time-varying factorization results to a nonlinear context was suggested by Prof. Moore. The key observations that state dependent systems could in the right factorization case, and in inversion and cascade, behave like linear time-varying systems are mine. Prof. Moore suggested the augmentation approach, and I designed the augmentations, and formulated and proved the limitations of this approach. Prof. Moore and I worked together to incorporate the known non-linear stability results, and I designed and implemented the simulations.

- The idea that fast time varying systems would behave like time-invariant systems arose from discussions between myself, Dr. Mareels, and Prof. Moore. The idea of using this to achieve model order reduction, and hybrid control, and the methods of implementation are mine. Iven and I worked together on the convergence results.

- Prof. Moore suggested the idea of using switched controllers for resonance suppression, and initial discussions as to implementation were held between Prof. Moore, Dr. Mareels, and myself. I carried out the rest of the work almost independently.

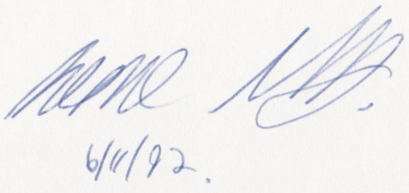

6/11/92.

Abstract

In this thesis we investigate new methods of analysis, design, and application of adaptive, learning, and switched controllers. We view these controllers as examples of state dependent systems, *i.e.* systems with a state space description in matrix form with the system matrices being functions of the state of the system. This viewpoint encourages their application to the robust control of state-dependent, and uncertain plants, and leads to new stability results.

In the first part of the thesis, we build upon known linear and nonlinear factorization theory, and the Youla-Kucera parametrization, to study the blending of off-line designed optimal controllers with adaptive and learning controllers. The feedback controller is designed for a state dependent system, namely the actual plant linearized about an optimal trajectory. The inclusion of this controller results in robustness enhancement, with performance enhancement in the non-nominal case.

Motivated by this work, a more complete factorization theory for state dependent systems is developed. Stabilization results are recalled which require such factorizations to achieve the identification of classes of all stable pairs of state-dependent plants and controllers. These classes are parametrised by the so called $\{Q, S\}$ parametrisation.

Further stability results are then generated for linear time-varying (periodic) systems. These results, which bound the difference between the trajectories of these systems and the trajectory of stable "averaged" linear time-invariant systems, provide results which are shown to achieve dramatic reduction in controller order, and effective implementation of hybrid control.

Finally, resonance suppression via "switched" controllers is proposed. It appears that such systems, although very effective, are beyond the scope of present analysis techniques. In this thesis they are put forward as an area for future research with preliminary simulation studies. Key arguments are provided to illustrate the importance of such switched systems, which are themselves an example of state-dependent, adaptive controllers. It is

suggested and partially shown that this type of control design may be important in applications which present large model uncertainty, large model order, or severe restrictions on computational load.

Contents

List of Figures

Chapter 1

Introduction

1.1 General Background

Feedback controllers are often designed to operate within certain hard constraints such as total energy utilised, maximal allowed acceleration, etc. Beyond this, the controller may be optimised for one, or a combination of three objectives:

1. Robustness to Plant Uncertainty:
   The actual plant may not be identical to the nominal one. Usually, it is assumed that the actual plant will be within some *uncertainty region* of the nominal. The controller must be designed to stabilize all plants within this region.

2. Robustness to Noise:
   The controller must stabilize the plants in the uncertainty region in the presence of some form of stochastic noise.

3. Performance Objective:
   Given a specific controller, plant and noise environment, the quality of control may be measured via the application of a cost function. This function quantifies the performance by comparing the state and output of the plant and utilised control energy with desired values. The controller must stabilize the plants within the uncertainty region in some economical manner with respect to the cost function.

During the operation of a plant, measured signals become available which can permit restriction of plant uncertainty. Since the knowledge of the plant or of the closed loop is improving, new or modified controllers may be designed, perhaps on-line, to incorporate this knowledge, and therefore provide improved performance and robustness. To this end,

for our purposes, we define two classes of controllers which are designed to make use of the increasing information.

Adaptive controllers are those designed to modify their dynamics based on measured signals. This is generally done in one of two ways. Direct adaptive control adjusts parameters of a fixed controller to achieve performance objectives. For example, Model Reference Adaptive Controllers modify their behaviour to attempt to force the closed loop system to approximate a given model. Alternately, indirect adaptive controllers estimate the plant parameters, and then modify the controller according to some design method using plant model estimators.

Learning controllers are also adaptive, but have the ability to more effectively learn from their experience. To achieve this, they store large amounts of data, such as input-output maps, and use this to generate behavioural information. They differ from standard adaptive controllers both in their ability to choose the data they work with, and also in their capacity to generate and extrapolate knowledge of the system. This added complexity results in a sophisticated adaptive controller which intelligently controls its own adaptation process.

Another very common type of controller which modifies its behaviour on-line, is a *gain scheduled* or *switched* controller. More generally this may be structured as an adaptive or learning system. The switched controller consists of a bank of (usually) a-priori designed controllers, and a switching rule which decides which controller is to be active at a given time. One appeal of switched controllers is their stability for plants with known discontinuities, for when the trajectory of the plant crosses a discontinuity, a more appropriate controller can be switched in without the losses incurred during standard adaptation.

Adaptive, learning, and switching controllers have found much application to areas such as aircraft control, process control, and robot manipulation, etc. However their inherent nonlinearity makes their analysis non-trivial, and in some cases even intractable. How then are they to be analysed?

1.2 State-Dependent Systems

State-dependent systems are here defined as nonlinear systems which can be described by the equations:

$$\begin{aligned} \dot{x} &= A(x)x + B(x)u, \quad x(0) = x_0 \\ y &= C(x)x + D(x)u \end{aligned} \tag{1.2.1}$$

Here $A(.), B(.), C(.), D(.)$ are the state-dependent matrix blocks, x is the state, u is the input and y is the output of the system.

Linear time invariant and time varying systems are two well known members of the class of state-dependent systems. Also, many processes not well modelled as linear systems may be more accurately modelled as state-dependent systems. Consider for instance the problem of controlling an aeroplane. Clearly, a full state vector will include such variables as the altitude and velocity. These variables affect the aeroplane's dynamics. Other variables such as temperature and pressure, which directly affect the performance but are only indirectly affected by the controller, may be viewed in this approximation either as uncontrollable states, time-varying parameters, or stochastic disturbances.

Adaptive controllers may be viewed as state-dependent systems, since for these systems the feedback control gain is a function of system output [53]. In a similar way, many learning and switched controllers, such as those developed in this thesis, can be described by (1.2.1). The implication of this viewpoint forms an important stimulus toward to the applications and techniques developed.

1.3 Analysis Techniques

The stability results of this thesis are based on *Matrix Fraction* system descriptions, *Coprime Factorizations* [72], and *Averaging Theory* [57].

Previous work in factorization theory has added much to the knowledge and design of robust linear control systems and permits a very convenient characterisation of the class of all stabilizing controllers for a plant or the dual class of all plants stabilized by a given controller. This work is of particular interest for adaptive and learning control as it provides results guaranteeing robustness of a parametrised controller/plant system. It can be applied so as to restrict the adaptation to a class of stable feedback systems.

Many restrictions, however, must be placed on the systems studied if the theory is a purely linear one. To overcome this, work has been done to extend the linear factorization theory to a nonlinear context, for instance [21, 22, 23, 24, 49, 65].

In some cases, techniques such as linearization about a fixed point and feedback linearization, etc. [59], have been applied to minimise the apparent nonlinearity of a system and hence lead to greater application of linear theory. In general, the more non-linear the system, the less theory there is to help. The result is that many of these methods either only work for certain restricted classes and operating regions, or lose the full power of the linear techniques.

A further analysis technique applied here is that of averaging theory which demonstrates how the trajectories of an intractable system, such as a time-varying system, are bounded with respect to those of an analytically tractable time-averaged system. This powerful analysis technique is finding increasing application to control theory, (see for instance [1] and its references). Here it is applied in reverse, namely to the identification of the trajectories of a simple system with those of a class of higher order systems. The added degree of freedom inherent within this class is utilised to improve computational effort and robustness.

The major objective of the analysis techniques developed here is to aid in the prediction, and consequently the design of stable adaptive, learning and switched systems. Our study restricts to a class of nonlinear systems close to linear in some sense, but with immediate application to feedback control. The aim is not to develop a full theory for the analysis of nonlinear systems, but to explore some new areas which in may in turn enhance existing theory. To this end we investigate factorization and stability theory of two key classes of nonlinear systems, and the asymptotic behaviour of one class of linear time varying systems.

The analysis techniques developed here include:

1. The nonlinear Q, S stabilization results of Chapter 2. These may be applied to generate the class of all (nonlinear) stabilizing controllers for (nonlinear) systems, both expressed as a linear kernel perturbed by a nonlinear system, one form of the so-called Q, S formulism. Many controllers including those developed in Chapters 2, 3 and 6 may be effectively described in this way. In some cases however, the entire complexity will remain within the Q, S subsystem. Thus the theory has general application, but the simplification provided will be dependent on the specific application.

2. The state-dependent factorization theory of Chapter 4 may be used to provide coprime factorization of state dependent controllers. The added restriction of differ-

ential boundedness of the factors permits a characterisation of all plants stabilized by a given controller, and the dual. In comparison with the results of Chapter 2, there is here a more restricted class of systems, but the increased simplification is considerable.

3. The averaging techniques of Chapter 5 allow analysis of switched systems in the case of fast periodic switching. These techniques lead to certain implementation advantages with regard to computational effort. They also give some insight into the asymptotic behaviour of the more complicated state-dependent switching schemes of Chapter 6. As such they are intended as one starting point for a more complete theory of state-dependent switched systems.

1.4 Applications

The first application we investigate is the robustness enhancement of open-loop optimal controllers for nonlinear systems. A major problem with many standard open-loop designs is that they are less robust than alternative closed loop techniques. However, for many nonlinear systems, the calculation or implementation of closed loop optimal controllers may be impractical. A standard method of adding robustness properties to an open-loop optimal control system involves adding feedback to the controlled system. To achieve this, the system is first linearized about the optimal trajectory. Subsequently, a feedback controller is designed to stabilize the linearized system by forcing the actual trajectory closer to the optimal one.

Any system derived from linearization about a non-stationary trajectory will be time-varying. Furthermore, the actual state of the nonlinear system will be affected by exogenous signals. These factors motivate the use of an adaptive controller. Here this is achieved via application of a robust and adaptive Q parametrization control technique. The Q parameter of the proposed scheme is an adaptive filter, and the adaptation task is to adapt the Q filter toward one which encourages close tracking of the optimal trajectory despite disturbances, unmodelled dynamics, etc.

A natural extension to the parameter tuning of the adaptive-Q methods is to what we term *Learning-Q* methods. In this case, the optimal Q filter parameters are identified as functions of the plant's state. Consequently, the tuning procedure involves the learning of these relations. An investigation of such learning-Q systems forms the second application.

The next application investigated is the use of switched controllers to achieve efficient

controller implementation. These controllers may be applied to achieve effective model-order reduction and hybrid control. Theoretical results and simulation studies show that the performance loss, as compared to the standard high-order continuous-time implementations, vanishes as the speed of switching increases.

The final application of this thesis is to resonance suppression via state-dependent switched controllers. Low order switched controllers are shown to effectively control high order uncertain plants in the presence of noise. Although complete analytical results have not been forthcoming, simulation studies and certain theoretically based observations indicate that the switched controller design is indeed a useful one for such control problems.

1.5 Outline of Thesis

The thesis is divided into seven chapters, with Chapters 2 to 6 based on referenced papers. The content of each chapter is largely self contained. Together they present new techniques for the analysis and application of certain state dependent control systems. More specifically, the areas covered by each chapter are :

- In Chapter 2, a general framework to enhance the robustness of an optimal control law is presented with emphasis on the nonlinear case. The framework allows a blending of off-line nonlinear optimal control, on-line linear robust feedback control for regulation about the optimal trajectory, and on-line adaptive techniques to enhance performance / robustness. The adaptive-Q techniques are those developed in previous work based on the Youla-Kucera parametrization for the class of all-stabilizing two-degree-of-freedom controllers. Some general fundamental stability properties are developed which are new, at least for the nonlinear plant and linear robust controller case. Also, performance enhancement results in the presence of unmodelled linear dynamics based on an averaging analysis are reviewed. A convergence analysis based on averaging theory appears possible in principle for any specific nonlinear system, but is beyond the scope of this thesis. Certain model-reference adaptive control algorithms come out as special cases. A nonlinear optimal control problem is studied to illustrate the efficacy of the techniques, and the possibility of further performance enhancement based on functional learning is noted. This work is also reported in [28, 29].

- Chapter 3 describes one approach to the application of functional learning techniques to the problem studied in Chapter 2, namely to assist in achieving near optimal control of nonlinear systems in the presence of disturbances and/or unmodelled dynamics. We still work with the standard approach to achieving robustness of open loop optimal control of nonlinear systems; that of applying feedback control based on plant linearization and application of linear quadratic control methods. In Chapter 2, we show that such methods can be enhanced by augmenting with adaptive loops, achieving what is termed adaptive-Q control. Here, instead of the adaptive-Q filter being a linear system with coefficients adjusted by a least squares law, the filter's coefficients are functionally dependent on a subset of the optimal states associated with a nominal plant. The functional representation is updated by a least squares law in the case that 'measurements' are linear in the function's unknown parameters, as when the function is represented by a sum of bisigmoids in the function input variable space. Such algorithms, and their convergence properties, have been previously studied in an identification context.
  A simulation study of the optimal quadratic regulation of the nonlinear 2-state Van der Pol equations is used to demonstrate improved performance in the presence of disturbances, with both the nominal plant and one perturbed by unmodelled dynamics. The approach could well have application in areas such as aircraft control or robot control where gain schedules are learnt on line. This work is also reported in [33].

- In Chapter 4, we consider the problem of generalizing elements of linear coprime factorization theory, and consequently stability theory, to a nonlinear context. The idea is to work with a suitably wide class of nonlinear systems to cover many adaptive, learning, and switching controllers, yet not cope with so broad a class as to disallow useful generalizations from the linear results. In particular, we work with the class of state-dependent systems (1.2.1). We achieve first right coprime factorizations for idealized situations. To achieve stable left factorizations we specialize to the case where the the matrices are output dependent. Alternatively, we work with systems, perhaps augmented by a direct feedthrough term, where the input is reconstructible from the output. Earlier results for nonlinear feedback control systems, with plant and controller having stable left factorizations, and appropriate regularity-conditions, have allowed the generation of the class of stabilizing controllers for a system in terms

of an arbitrary stable system (parameter). Plant uncertainties, including unknown initial conditions are modelled by means of a Yula-Kucera type parametrization approach developed for nonlinear systems. Certain robust stabilization results are also shown, and simulations demonstrate the regulation of nonlinear plants using the techniques developed. All the results are presented in such a way that specialization to the case of linear systems is immediate. This work is also reported in [43, 44].

- Chapter 5 details the analysis and simulation of the class of switched systems with the switching function a periodic function of time. We first demonstrate via averaging theory, an approach whereby any stable linear system can be approximated by a simple periodic-structure system.

  Next is proposed the control of continuous-time, linear, time-invariant plants via a periodic structure control scheme with a rationale based in averaging analysis. It is established that for continuous-time minimal plants it is possible to design periodic-structure stabilizing first-order controllers which asymptotically approach the performance of an n^{th} order stabilizing time-invariant controller, such as an optimal (LQG) controller, in the limit as the switching rate increases. The proposed controllers suffer only a small loss of performance compared with the n^{th} order controller, are attractive from a computational point of view, and may be implemented in either discrete or continuous time. Simulation results are shown which demonstrate the efficacy of the proposed controllers. This work is also reported in [31, 32].

- Chapter 6 then extends the studies of Chapter 5 to the more general case of the switching being a function of the estimated state of the plant rather than just a periodic function of time. A method of control is proposed whereby a high order plant is controlled at each time instant by one of a set of low order controllers, each designed to control one part of a partial fractions expansion of the plant. The method is motivated toward the control of flexible structures, such as large space structures, and arguments are developed which show that due to certain properties of such, including large model order, model uncertainty, and decentralisation, a switched controller may exhibit benefits not available to a standard controller. Certain switching algorithms are presented, based more on insight than on any optimisation or robustness theory, and simulation results demonstrate the efficacy of such methods. These results perhaps point one way forward for tackling difficult control problems. This work is also reported in [30].

- Chapter 7 contains conclusions, emphasizing what in the author's opinion are the primary theoretical results and algorithms of the work presented. Suggestions for further research are also included.

Chapter 2

Robust Nonlinear Control - Adaptive Q

2.1 Introduction

Optimal nonlinear deterministic control methods are considered very elegant in theory, but lack robustness in practise. In the optimal control approach, a mathematical model of the process is first formulated based on the fundamental laws in operation or via identification techniques. Next, a performance index is derived which reflects the various cost factors associated with the implementation of any control signal. Then, off-line calculations lead to an optimal control law u^* via one of the various methods of optimal control. In theory then, applying such a control law to the physical process should result in optimal performance. However, the process is rarely modelled accurately, and frequently is subject to stochastic disturbances. Consequently, the application of the "optimal" control signal u^* results in poor performance, in that the process output y differs from y^*, the output of the idealized process model.

One approach to achieve improved performance could be to include robustness measures in the cost function, so that for plants "near" the nominal model and "small" disturbances poor performance is avoided. This approach turns out to be difficult to develop in practise.

A standard approach to enhance open-loop optimal control performance is to measure on-line the difference between the ideal optimal process output trajectory y^* and the actual process output y. This difference signal, δy, depends on the difference, δu, between the optimal control u^* for the nominal model and any actual control signal u applied.

For nominal plants with suitably smooth nonlinearities, and small differences δu, δy, a linearization of the process allows an approximate linear dynamic model for relating δy to δu. With this model, optimal linear regulator theory can be applied to calculate δu in terms of δy which is measurable, so as to regulate δy to zero. Indeed, the linearization can extend to yield an associated quadratic performance index consistent with the original nonlinear index so that linear optimal control (LQG) theory can be applied to achieve optimal regulation of δy under the linearization assumptions. Robust regulator designs based on optimal theory, perhaps via loop-transmission recovery (LTR), could be expected to lead to performance improvement over a wider range of perturbations on the nominal plant model.

Even with the application of linearization and feedback regulation to enhance optimal control strategies, there can still be problems with external disturbances and modelling errors. The linearization itself may be a poor approximation when there are large perturbations from the optimal trajectory.

In this chapter, it is proposed to apply robust and adaptive techniques to assist in regulation of the actual plant so that it behaves as closely as possible to the nominal (idealized) model. An adaptive control technique which is designed to enhance performance of a stabilizing regulator for a nominal time-varying linear plant model is presented in an earlier work [63], building on the time-invariant case proposed in [66] and further studied in [67]. Here, this technique is applied in conjunction with an open-loop nonlinear optimal controller and standard linear optimal feedback regulator (LQG) approach, with the view to enhancing performance of the optimal controller when applied to a plant, not the idealized model. Loop recovery (LTR) techniques are also studied to enhance robustness of the optimal regulator designs. Some analysis results are presented giving stability properties of the optimal/adaptive scheme. These generalize known linear system stability plant results to the case of mixed linear system and nonlinear systems as here. Mention is made of performance enhancement properties in the presence of unmodelled dynamics developed for the linear case based on an averaging analysis, although generalizing to a specific nonlinear case appears possible, such an analysis is beyond the scope of this thesis. Simulation results demonstrate the effectiveness of the various control strategies, and the possibility of further performance enhancement based on functional learning is noted. In Section 2, the algorithms of [63] are viewed in the context of non-linear optimal control. In Section 3, some analysis results are developed relevant to the nonlinear control situation, and in Section 4, simulation studies are presented. Conclusions are drawn in Section 5.

2.2 Self-Tuning Optimal Nonlinear Control

Signal Model/Optimal Control *Plant Performance Index and Linearization*

Consider a generalized nominal plant model :

$$\mathrm{G}_0 : \quad \dot{x} = f(x,u), \qquad y = h(x,u), \qquad x(0) = x_0 \tag{2.2.1}$$

and some performance index over the time interval $[0,T]$

$$I = \int_0^T l(x,u)dt \tag{2.2.2}$$

with associated optimal control u^*, state x^*, and output y^*. Consider also a linearized version of the above plant model, denoted $\Delta G_0(x^*)$;

$$\begin{aligned} \Delta G_0(x^*) : d(\delta x)/dt &= A\delta x + B\delta u \\ \delta y &= C\delta x + D\delta u [= \Delta G_0(x^*)\delta u] \end{aligned} \tag{2.2.3}$$

where $\delta x(0) = 0$ and $A, B, C, D = \frac{\partial f}{\partial x}, \frac{\partial f}{\partial u}, \frac{\partial h}{\partial x}, \frac{\partial h}{\partial u}|_{x=x^*}$

The following shorthand notation proves useful subsequently,

$$\Delta G_0(x^*) = \left[\begin{array}{c|c} A & B \\ \hline C & D \end{array}\right]_{x^*} \tag{2.2.4}$$

With ΔG the operator denoting the actual system with input $\delta u = u - u^*$, state $\delta x = x^*$ and output $\delta y = y - y^*$, then ΔG_0 denotes a linearized version of ΔG.

Let us associate with the linearized model a quadratic performance index penalising departures δy and δu away from the optimal trajectory.

$$\Delta I = \frac{1}{T}\int_0^T e'e dt \tag{2.2.5}$$

where,

$$e = L\begin{bmatrix} \delta y \\ \delta u \end{bmatrix}, \; L = \begin{bmatrix} Q_c & S_c \\ S_c' & R_c \end{bmatrix}^{\frac{1}{2}}, \; Q_c \geq 0, \; Q_c - S_c R_c^{-1} S_c \geq 0, \; R_c > 0 \tag{2.2.6}$$

Here e is interpreted as a disturbance response which we seek to minimise in an L_2 sense.

We assume that u^*,x^*,y^* are known a priori, but that when applied to an actual plant G, which includes unmodelled disturbances and/or dynamics, there are departures from the optimal trajectories. With departures $\delta y = y - y^*$ measured on-line, a standard approach is to apply control adjustments $\delta u = u - u^*$ to the optimal control by means of feedback control to minimise (2.2.5). Thus for the augmented plant arrangement, denoted P_A, and depicted in Figure 2-1, let us consider a linear feedback regulator. We base such a design on the linearized situation depicted in Figure 2-2 where the linearized nominal plant, denoted P_0, is given from

$$P_0 = \begin{bmatrix} * & P_{12} \\ * & P_{22} \end{bmatrix} \tag{2.2.7}$$

$$P_{12} = L \begin{bmatrix} \Delta G_0(x^*) \\ I \end{bmatrix}, \quad P_{22} = \Delta G_0(x^*) \tag{2.2.8}$$

The terms P_{11}, P_{21} are not of interest for subsequent analysis.

Feedback Regulator for Performance Enhancement The regulator of the linearized model P_0 is

$$\begin{aligned} K_0(x^*): \; d(\delta\hat{x})/dt &= A\delta\hat{x} + B\delta u - Hr \quad , \delta\hat{x}(0) = 0 \\ r &= \delta y - C\delta\hat{x} - D\delta u \\ \delta u &= F\delta\hat{x} \; [= K_0(x^*)\delta y] \end{aligned} \tag{2.2.9}$$

Here r is the estimator residual, $\delta\hat{x}$ is the estimate of δx and H and F are time-varying matrices formed, perhaps via standard LQG/LTR theory [2], so that under uniform stability of A,B and uniform detectability of A,C the following systems are exponentially stable.

$$\dot{\xi}_F = (A + BF)\xi_f, \qquad \dot{\xi}_H = (A + HC)\xi_H \tag{2.2.10}$$

Actually, the important aspect of the LQG design for our purposes is that under the relevant uniform stabilizability and uniform detectability assumptions, the (time-varying) gains H, F exist, and are given from the solution of two Riccatti equations (with no finite escape time). Moreover, for the limiting case when the time horizon T becomes infinite, the controller K_0 stabilizes ΔG_0. Here stability means that all possible bounded inputs to the closed loop consisting of K_0 feeding back on ΔG_0 result in bounded loop signals (outputs).

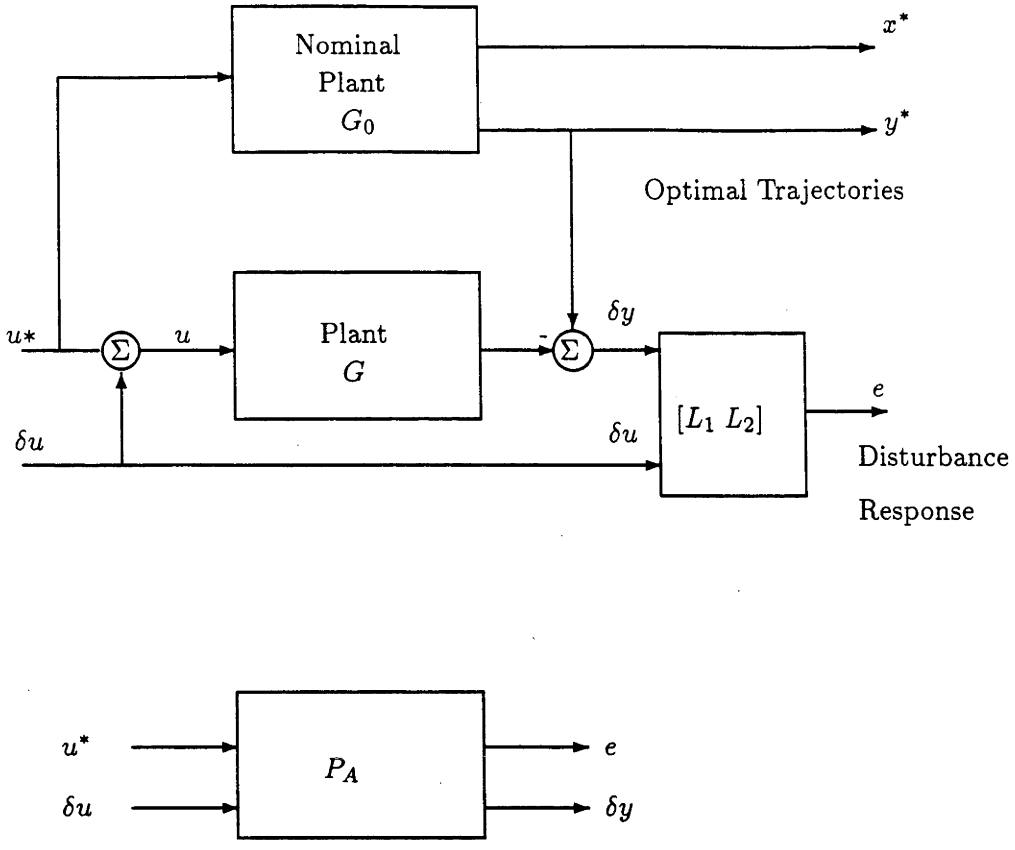

Figure 2-1: The Augmented Plant Arrangement

Robust Feedback Controller It is well known that the LQG controller (2.2.9) for the linearized plants (2.2.3), although optimal for the nominal linear time-varying plant for the assumed noise environment, may be far from optimal in other than the nominal noise environments, or in the presence of structured or unstructured perturbations on (2.2.3). Stability may be lost even for small variations from the nominal plant.

Methods to enhance LQG regulator robustness exist, such as modifying Q_c, S_c, R_c (usually $S_c \equiv 0$) selections, or assumed noise environments, as when loop recovery is used. Such techniques could well serve to strengthen the robustness properties of the optimal/ adaptive schemes studied subsequently. In order to proceed, we here merely assume the existence of a controller (2.2.9) stabilizing ΔG_0, although our objective is to achieve a controller which both stabilizes ΔG, and achieves a low value of index ΔI when applied to ΔG.

Coprime Factorizations It is convenient to introduce normalised coprime factoriza-

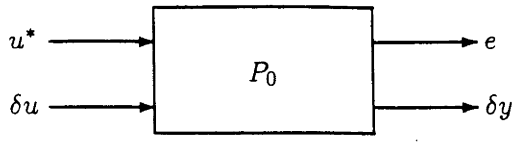

Figure 2-2: The Linearized Augmented Plant

tions for $\triangle G_0(x^*)$ and $K_0(x^*)$, such that

$$\triangle G_0(x^*) = N_0 M_0^{-1} = \tilde{M}_0^{-1}\tilde{N}_0 \tag{2.2.11}$$

$$K_0(x^*) = U_0 V_0^{-1} = \tilde{V}_0^{-1}\tilde{U}_0 \tag{2.2.12}$$

satisfy the double Bezout identity,

$$\begin{bmatrix} \tilde{V}_0 & -\tilde{U}_0 \\ -\tilde{N}_0 & \tilde{M}_0 \end{bmatrix} \begin{bmatrix} M_0 & U_0 \\ N_0 & V_0 \end{bmatrix} = \begin{bmatrix} M_0 & U_0 \\ N_0 & V_0 \end{bmatrix} \begin{bmatrix} \tilde{V}_0 & -\tilde{U}_0 \\ -\tilde{N}_0 & \tilde{M}_0 \end{bmatrix} = \begin{bmatrix} I & 0 \\ 0 & I \end{bmatrix} \tag{2.2.13}$$

where the factors $N_0, M_0, N_0, V_0, \tilde{M}_0, \tilde{N}_0, \tilde{U}_0, \tilde{V}_0$ are stable and causal x^*-dependent operators. Now using the notation of (2.2.4) suitable factorizations are readily verified as in [63], under (2.2.10) as

$$\begin{bmatrix} M_0 & U_0 \\ N_0 & V_0 \end{bmatrix} = \left[\begin{array}{c|cc} A+BF & B & -H \\ \hline F & I & 0 \\ C+DF & -D & I \end{array}\right]_{x^*} \tag{2.2.14}$$

$$\begin{bmatrix} \tilde{V}_0 & -\tilde{U}_0 \\ \tilde{N}_0 & \tilde{M}_0 \end{bmatrix} = \left[\begin{array}{c|cc} A+HC & -(B+HD) & H \\ \hline F & I & 0 \\ C & -D & I \end{array}\right]_{x^*} \tag{2.2.15}$$

The Class of all Stabilizing Controllers As formulated in [28],[63],[66] the class of all linear, causal stabilizing controllers for $\Delta G_0(x^*)$ (the linearized plant model) under (2.2.10) can be generated as depicted in Figure 2-3 using a J subsystem defined below, and a so-called Q parametrization, where the subsystem J_K is readily extracted from Figure 2-4 as

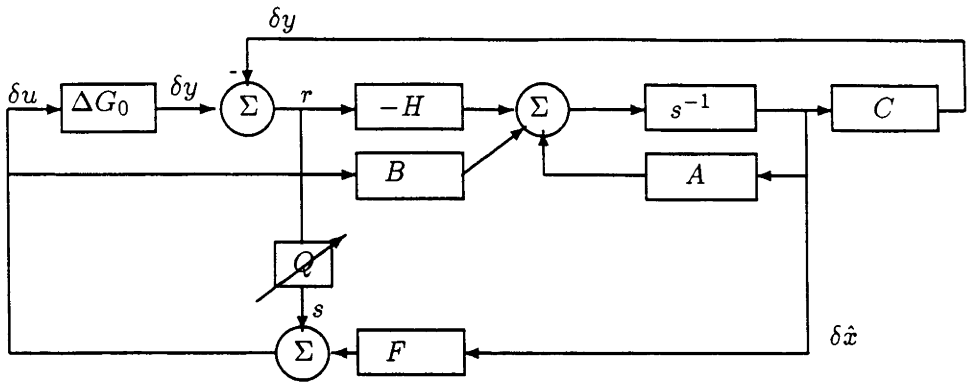

Figure 2-3: Class of all Stabilizing Controllers for ΔG_0

$$\begin{aligned} J_K : \; d\delta\hat{x}/dt &= (A+BF)\delta\hat{x} + Bs - Hr \\ \delta u &= F\delta\hat{x} + s, \quad r = \delta y - C\delta\hat{x} \end{aligned} \tag{2.2.16}$$

Or equivalently

$$J_K = \begin{bmatrix} K_0 & \tilde{V}_0^{-1} \\ V_0^{-1} & -V_0^{-1}N_0 \end{bmatrix} \tag{2.2.17}$$

Q is arbitrary within the class of all causal BIBO stable operators. Thus:

$$K(x^*,Q) = U(Q)V^{-1}(Q) = \tilde{V}^{-1}(Q)\tilde{U}(Q) \tag{2.2.18}$$

$$\begin{aligned} U(Q) &= U_0 + M_0Q \qquad V(Q) = V_0 + N_0Q \\ \tilde{U}(Q) &= \tilde{U}_0 + Q\tilde{M}_0 \qquad \tilde{V}(Q) = \tilde{V}_0 + Q\tilde{N}_0 \end{aligned} \tag{2.2.19}$$

or equivalently, after some manipulations involving (2.2.12,2.2.13)

$$K(x^*,Q) = K_0 + \tilde{V}_0^{-1}Q(I + V_0^{-1}N_0Q)^{-1}V_0^{-1} \tag{2.2.20}$$

Simple manipulations also give an alternative expression for r, as

$$r = \tilde{M}_0\delta y - \tilde{N}_0\delta u \tag{2.2.21}$$

Following [66], we can specialize the results above for an augmented plant $[I \quad \Delta G_0']'$ to yield the corresponding two-degree-of-freedom version with $Q = [Q_1 \quad Q_2]$, where Q_1

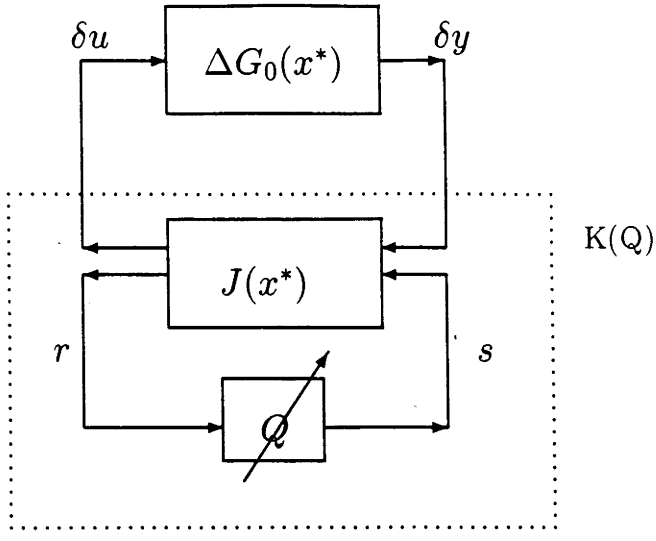

Figure 2-4: Class of all Stabilizing Controllers.

can be interpreted as a feedforward filter, and Q_2 as a feedback filter. It is known that the closed loop transfer functions (operators) of Figure 2-4 are affine in Q, which facilitates either off-line or on-line, optimisation of such Q dependent transfer operators. We proceed with a class of on-line optimisations.

Adaptive Q. Our proposal is to implement a controller $K(Q)$ for some adaptive Q, but applied to ΔG and not ΔG_0. The intention is for Q to be chosen to ensure that $K(Q)$ stabilizes G and achieves good performance in terms of the index ΔI. Thus consider the arrangement of Figure 2-5 where the block P is actually the arrangement depicted in Figures 2-3,2-4 but effectively characterized by ΔG and L operators.

A refinement on this proposal is to consider a two-degree-of-freedom controller scheme based on the work of [66]. This is depicted in Figure 2-6. It can be derived from a one-degree-of-freedom controller arrangement for the augmented plant $\begin{bmatrix} 0 & G^T \end{bmatrix}^T$, re-organized as a two-degree-of-freedom arrangement for G. The objective is to select Q_1, Q_2 causal, bounded-input, bounded-output operators on line so that the response e is minimized in an L_2 sense.

In order to present a least squares algorithm for selection of Q, as in the schemes of [63], some preprocessing of the signals e, $q\delta u$, δy is required.

Prefiltering Using operator notation, we define filtered variables

$$\xi = \begin{bmatrix} P_{12}M_0 u^* \\ P_{12}M_0 r \end{bmatrix}, \quad \zeta = e - P_{12}M_0 s \tag{2.2.22}$$

Least Squares Q Selection Let us define a discrete-time version of Q in Z-transforms as

$$Q_1(z^{-1}) = \frac{\gamma_0+\gamma_1 z^{-1}+\cdots\gamma_p z^{-p}}{1+\alpha_1 z^{-1}+\cdots\alpha_n z^{-n}}, \qquad Q_2(z^{-1}) = \frac{\beta_0+\beta_1 z^{-1}+\cdots\beta_m z^{-m}}{1+\alpha_1 z^{-1}+\cdots\alpha_n z^{-n}}$$
$$Q(z^{-1}) = [Q_1(z^{-1})\ Q_2(z^{-1})], \qquad \theta' = [\alpha_1 \cdots \alpha_n \beta_0 \cdots \beta_m \gamma_0 \cdots \gamma_p] \qquad (2.2.23)$$

The following state (regression) vector in discrete time is

$$\phi'_k = [-s_{k-1} \cdots - s_{k-n}\ r_k \cdots r_{k-m}\ \omega_k \cdots \omega_{k-p}] \qquad (2.2.24)$$

The dimensions n, m, p are set from an implementation convenience/performance trade-off. In the adaptive-Q case, the parameters are time-varying resulting from least squares calculations given below. We assume a unit delay in calculations. Thus θ is replaced by $\hat{\theta}_{k-1}$ and the filter with operator $Q_k = [Q_{1k}\ Q_{2k}]$ is implemented with parameters (time-varying in general) as

$$s_k = \hat{\theta}'_{k-1}\phi_k, \quad \hat{\theta}'_k = [\hat{\alpha}_{1k} \cdots \hat{\alpha}_{nk} \hat{\beta}_{0k} \cdots \hat{\beta}_{mk} \hat{\gamma}_{0k} \cdots \hat{\gamma}_{pk}] \qquad (2.2.25)$$

We seek selections of $\hat{\theta}_k$ so that the adaptive controller minimizes the L_2 norm of the response e_k. Using theory in [66], with suitable initializing we have the adaptive-Q arrangement of Figure 2-6 with equations

$$\begin{aligned}
\hat{\theta}_k &= \hat{\theta}_{k-1} + \hat{P}_k\hat{\phi}_k\hat{e}_{k/k-1}, \ \hat{e}_{k/k-1} = \zeta_k - \hat{\phi}'_k\hat{\theta}_{k-1}, \ e_{k/k} = \xi_k - \hat{\phi}'_k\hat{\phi}_k \\
\hat{P}_k &= (\sum_1^k \hat{\phi}_i\hat{\phi}'_i)^{-1} = \hat{P}_{k-1} - \hat{P}_{k-1}\hat{\phi}_k(I + \hat{\phi}'_k\hat{P}_{k-1}\hat{\phi}_k)^{-1}\hat{\phi}_k\hat{P}_{k-1} \qquad (2.2.26) \\
\hat{\phi}'_k &= [(\hat{e}_{k-1/k-1} - \zeta_{k-1})(\hat{e}_{k-n/k-n} - \zeta_{k-n})\ - \xi_{2,k} \cdots - \xi_{2,k-m} \cdots - \xi_{1,k} \cdots - \xi_{1,k-m}]
\end{aligned}$$

Summary of Proposed Direct Adaptive Scheme. The complete adaptive-Q scheme is a combination of Figures 2-6,2-7 with key equations (2.2.15),(2.2.26).

Remarks

1. The algorithms (2.2.26) should be modified to ensure that $\hat{\theta}_k$ is projected into a restricted domain, such as $||Q_k|| < \epsilon$ for some fixed ϵ. Such projections can be guided by the theory discussed in the next section.

2. To achieve convergence of $\hat{\theta}_k$, then $\hat{P}_k$ must approach zero, or equivalently, $\hat{\phi}_k$ must be

persistently exciting in some sense. However, parameter convergence is not strictly necessary to achieve performance enhancement. With more general algorithms which involve resetting or forgetting, then care must be taken to avoid ill-conditioning of $\hat{P}_k$, perhaps via unstable excitation in the system.

3. It turns out that appropriate scaling can be crucial to achieve the best possible performance enhancement. Scaling gains can be included, to scale r and/or e with no effect on the supporting theory, other than defining projection domains as in Remark 1 above. Likewise, the "scaling" can be generalized to stable dynamic filters for r and/or e with no effect on the supporting theory. In this frequency shaped designs can be effected.

4. Our presentation so far has been for continuous time ΔG and J_K but discrete-time updates of parameters $\hat{\theta}_k$ and then Q_k, based on samplings of r and e. Likewise, our subsequent simulation results are mixed continuous time/discrete time results. Theory, as noted below gives performance enhancement only at the discrete-time sampling instants, so that as in all mixed continuous/discrete system studies, care may be taken to achieve a suitably fast sampling rate. Of course, we could have worked exclusively in discrete-time or continuous time.

5. The scheme described above can be specialized to the cases when Q_1, Q_2 are finite impulse response filters by setting $n = 0$. The Q are stable for all bounded $\hat{\theta}_k$. Also either Q_1 or Q_2 can be set to zero to simplify the processing, although possibly at the expense of performance.

6. In the case that Q_1 is moving average and Q_2 is zero, then our scheme becomes very simple, being a moving average filter Q_1 in series with the closed loop system $\{\Delta G, K_0\}$. In this case then, if Q_1 is stable, guaranteed when the gains $\hat{\theta}_k$ are bounded, and $\{\Delta G, K_0\}$ is stable, then there is obvious stability of the adaptive scheme.

7. When the linearized plant model ΔG_0 is stable, and one selects trivial values $F, H = 0$ so that $K_0 = 0$, then the arrangement of Figure 2-6 simplifies to a familiar model-reference adaptive control arrangement depicted in Figure 2-8.

8. In the case that Q_1 is set to zero, then there is no adaptive feedforward control action.

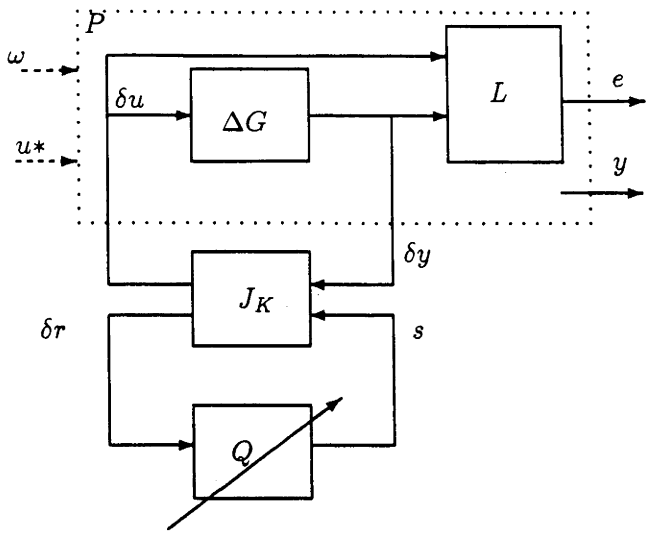

Figure 2-5: Adaptive Q for Disturbance Response Minimization

9. The operators $\Delta G_0, J_K$ are in fact functions of the optimal trajectory x^*, or under suitable generalizations of $x^*, \delta x$. It would make sense to have the operator Q also as a function of x^* (or $x^*, \delta x$). Then this adaptive-Q approach becomes a learning-Q approach as studied in Chapter 3.

2.3 Convergence Properties

In this section we focus on stability results as a first step to achieving convergence results for our system. We first analyze a parametrization of the plant ΔG with input δu and output δy in terms of the co-prime factorizations of the linearized version ΔG_0, and stabilizing linear controller K_0, and establish that this parametrization covers the class of well-posed closed-loop systems under study. Next, stability of the scheme is studied in terms of such parametrizations and then expected convergence properties are noted based on this characterisation and known convergence theories in the linear case.

Nonlinear System Fractional Maps As in the previous section, let us consider the right and left coprime factorizations for the nominal linearized plant and controller of [64] . These operators are expressed as functions of the desired optimal trajectory, x^*, but since x^* is time dependent, then for any specific trajectory $x^*(.)$ the operators are merely linear time-varying operators, and can be treated as such. We define $\Delta G(x^*)$ as the (nonlinear) system with input δu and output δy. Note that $\Delta G_0(x^*)$ is a linearization of $\Delta G(x^*)$. When the notation $\Delta G_0, \Delta G$ is used, the x^* dependence, or equivalently, time

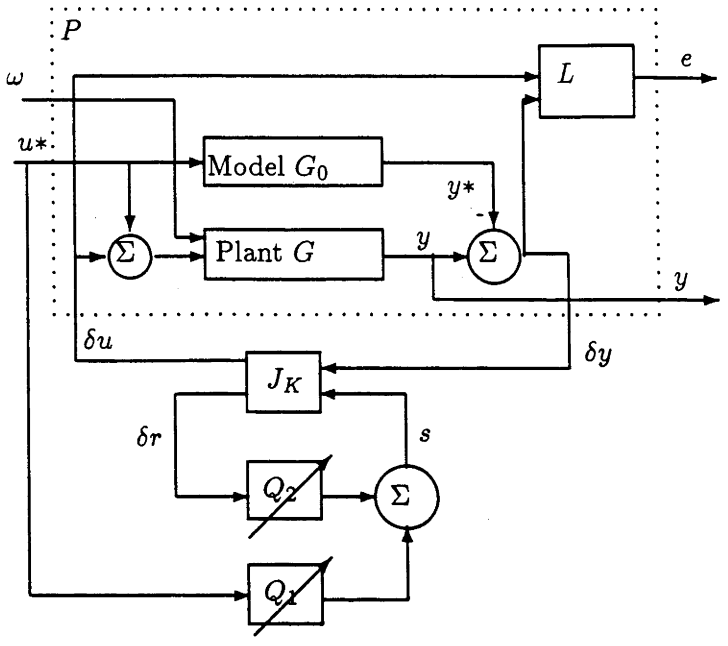

Figure 2-6: Two degree-of-freedom adaptive-Q scheme

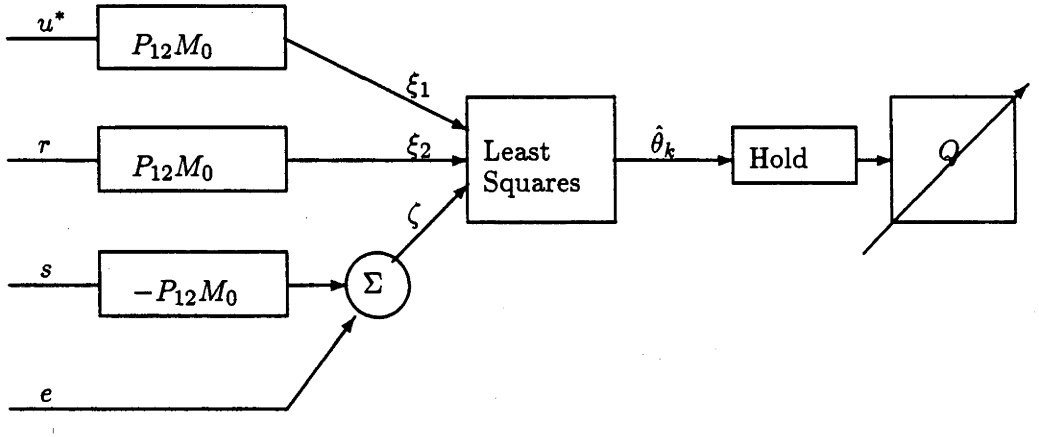

Figure 2-7: The Least Squares Adaptive-Q Arrangement

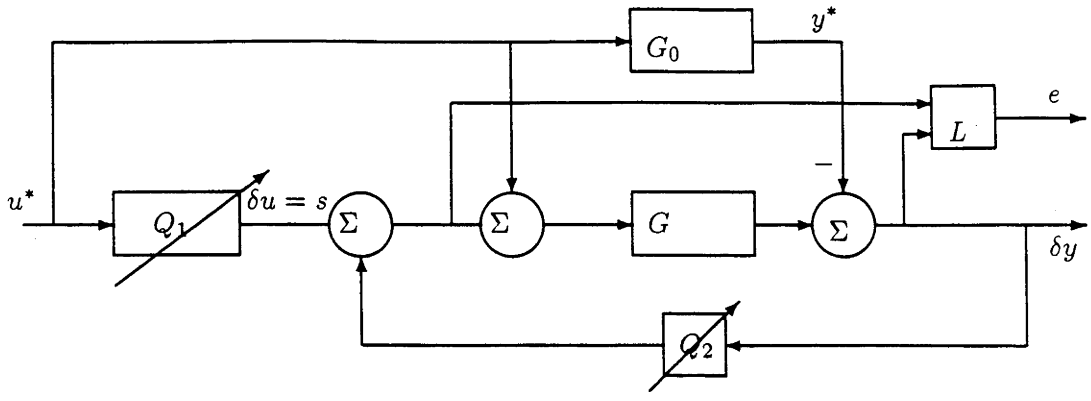

Figure 2-8: Model Reference Adaptive Control Special Case.

dependence is understood. Also, a unity gain feedback loop with open loop operator W_{ol} is said to be well-posed when $(I + W_{ol})^{-1}$ exists. Recall that for a nonlinear operator S, then, in general $S(A + B) \neq SA + SB$, or equivalently superposition does not hold, and care must be taken in the composition of nonlinear operators. Otherwise, manipulation rules for nonlinear operators follow those more familiar ones for linear operators.

Theorem 2.1

(Right fractional map forms) Consider that $\{\Delta G_0, K_0\}$ is well posed and stabilizing with left and right coprime factorizations for $\Delta G_0, K_0$ as in (2.2.11,2.2.12) and the double Bezout (2.2.13) holding. Then any nonlinear plant with ΔG such that $\{\Delta G, K_0\}$ is a well-posed closed-loop system can be expressed in terms of a (nonlinear) operator S in right fractional map forms :

$$\Delta G = N(S)M^{-1}(S);\ \ N(S) = (N_0 + V_0 S),\ M(S) = (M_0 + U_0 S) \tag{2.3.1}$$

$$= \Delta G_0 + \tilde{M}_0^{-1} S (I + M_0^{-1} U_0 S)^{-1} M_0^{-1} \tag{2.3.2}$$

Also, closed-loop system operators are given from

$$\begin{bmatrix} I & -K_0 \\ -\Delta G & I \end{bmatrix}^{-1} = \begin{bmatrix} I & -K_0 \\ -\Delta G_0 & I \end{bmatrix}^{-1} + \begin{bmatrix} U_0 & M_0 \\ V_0 & N_0 \end{bmatrix} \begin{bmatrix} S & 0 \\ 0 & 0 \end{bmatrix} \begin{bmatrix} \tilde{V}_0 & \tilde{U}_0 \\ \tilde{N}_0 & \tilde{M}_0 \end{bmatrix} \tag{2.3.3}$$

Moreover, the maps (2.3.1), (2.3.2) have the block diagram representations of Figures 2-9 (a) and (b) where

$$J_G = \begin{bmatrix} -M_0^{-1} U_0 & M_0^{-1} \\ \tilde{M}_0^{-1} & \Delta G_0 \end{bmatrix} \tag{2.3.4}$$

The solutions of (2.3.1), (2.3.2) are unique , given from the right fractional maps in terms of ΔG, *or* $(\Delta G - \Delta G_0)$ *as*

$$\begin{aligned} S &= (-\tilde{N}_0 + \tilde{M}_0\Delta G)(\tilde{V}_0 - \tilde{U}_0\Delta G)^{-1} && (2.3.5)\\ &= \tilde{M}_0(\Delta G - \Delta G_0)M_0[I - \tilde{U}_0(\Delta G - \Delta G_0)M_0]^{-1} && (2.3.6)\end{aligned}$$

or in terms of the closed-loop system operators as

$$S = \begin{bmatrix} -\tilde{N}_0 & \tilde{M}_0 \end{bmatrix} \left[\begin{bmatrix} I & -K_0 \\ -\Delta G & I \end{bmatrix}^{-1} - \begin{bmatrix} I & -K_0 \\ -\Delta G_0 & I \end{bmatrix}^{-1} \right] \begin{bmatrix} M_0 \\ N_0 \end{bmatrix} \quad (2.3.7)$$

Moreover, $\{N(S), M(S)\}$ *are coprime and obey a Bezout identity*

$$\tilde{V}_0 M(S) - \tilde{U}_0 N(S) = I \quad (2.3.8)$$

Proof. Now simple manipulations allow (2.3.5) to be reorganized under the well-posedness assumption as

$$\begin{bmatrix} I \\ S \end{bmatrix} = \begin{bmatrix} \tilde{V}_0 & -\tilde{U}_0 \\ -\tilde{N}_0 & \tilde{M}_0 \end{bmatrix} \begin{bmatrix} I \\ \Delta G \end{bmatrix} (I - K\Delta G)^{-1}\tilde{V}_0^{-1}$$

and via the Bezout identity, as

$$\begin{bmatrix} M(S) \\ N(S) \end{bmatrix} = \begin{bmatrix} M_0 + U_0 S \\ N_0 + V_0 S \end{bmatrix} = \begin{bmatrix} M_0 & U_0 \\ N_0 & V_0 \end{bmatrix} \begin{bmatrix} I \\ S \end{bmatrix} = \begin{bmatrix} I \\ \Delta G \end{bmatrix} (I - K\Delta G)^{-1}\tilde{V}_0^{-1} \quad (2.3.9)$$

Thus under (2.3.5) then $M^{-1}(S)$ exists and,(2.3.1) holds as follows

$$N(S)M^{-1}(S) = \Delta G(I - K\Delta G)^{-1}\tilde{V}_0^{-1}\left[(I - K\Delta G)^{-1}\tilde{V}_0^{-1}\right]^{-1} = \Delta G$$

To prove the equivalence of (2.3.1) and (2.3.2), simple manipulations give

$$\begin{aligned} \Delta G &= \Delta G_0 + (N_0 + V_0 S)(I + M_0^{-1}U_0 S)^{-1}M_0^{-1} - N_0 M_0^{-1} \\ &= \Delta G_0 + (V_0 - N_0 M_0^{-1}U_0)S(I + M_0^{-1}U_0 S)^{-1}M_0^{-1} \\ &= \Delta G_0 + (V_0 - \tilde{M}_0^{-1}\tilde{N}_0 U_0)S(I + M_0^{-1}U_0 S)^{-1}M_0^{-1} \\ &= \Delta G_0 + \tilde{M}_0^{-1}(\tilde{M}_0 V_0 - \tilde{N}_0 U_0)S(I + M_0^{-1}U_0 S)^{-1}M_0^{-1} \end{aligned}$$

$$= \Delta G_0 + \tilde{M}_0^{-1} S (I + M_0^{-1} U_0 S)^{-1} M_0^{-1}$$

so that under (2.2.13), then (2.3.2) holds. Likewise (2.3.5) is equivalent to (2.3.6) as follows

$$\begin{aligned} S &= \tilde{M}_0(\Delta G - \Delta G_0)(\tilde{V}_0 - \tilde{U}_0 \Delta G)^{-1} \\ &= \tilde{M}_0(\Delta G - \Delta G_0) M_0 (\tilde{V}_0 M_0 - \tilde{U}_0 \Delta G M_0)^{-1} \\ &= \tilde{M}_0(\Delta G - \Delta G_0) M_0 (I + \tilde{U}_0 N_0 M_0^{-1} M_0 - \tilde{U}_0 \Delta G M_0)^{-1} \\ &= \tilde{M}_0(\Delta G - \Delta G_0) M_0 [I - \tilde{U}_0 (\Delta G - \Delta G_0) M_0]^{-1} \end{aligned}$$

To see that the operator of (2.3.1) is equivalent to that depicted in Figure 2-9(a), observe from Figure 2-9(a) that $l = M_0^{-1}(e_1 - U_0 S l)$, or equivalently, $l = (M_0 + U_0 S)^{-1} e$. Also, $(e_2 - w_2) = (N_0 + V_0 S) l = (N_0 + V_0 S)(M_0 + U_0 S)^{-1} e_1$ which is equivalent to (2.3.1).

Now suppose there is some other $(S + \Delta S)$ which also satisfies (2.3.1), then

$$\begin{aligned} \begin{bmatrix} I \\ \Delta G \end{bmatrix} &= \begin{bmatrix} M_0 & U_0 \\ N_0 & V_0 \end{bmatrix} \begin{bmatrix} I \\ S \end{bmatrix} (M_0 + U_0 S)^{-1} \\ &= \begin{bmatrix} M_0 & U_0 \\ N_0 & V_0 \end{bmatrix} \begin{bmatrix} I \\ S + \Delta S \end{bmatrix} (M_0 + U_0 S + U_0 \Delta S)^{-1} \end{aligned}$$

for some ΔS. Then, using (2.2.13),

$$\begin{aligned} \begin{bmatrix} \tilde{V}_0 & -\tilde{U}_0 \\ -\tilde{N}_0 & \tilde{M}_0 \end{bmatrix} \begin{bmatrix} I \\ \Delta G \end{bmatrix} &= \begin{bmatrix} I \\ S \end{bmatrix} (M_0 + U_0 S)^{-1} \\ &= \begin{bmatrix} I \\ S + \Delta S \end{bmatrix} (M_0 + U_0 S + U_0 \Delta S)^{-1} \end{aligned} \qquad (2.3.10)$$

Premultiplication by $[I \quad 0]$ gives $M_0 + U_0 S = M_0 + U_0 S + U_0 \Delta S$, and premultiplication by $[0 \quad I]$ gives then in turn that $\Delta S = 0$.

To verify (2.3.7), first observe that

$$\begin{bmatrix} I & -K_0 \\ -\Delta G & I \end{bmatrix} = \begin{bmatrix} M_0 & -U_0 \\ -N_0 & V_0 \end{bmatrix} \begin{bmatrix} I & 0 \\ -S & I \end{bmatrix} \begin{bmatrix} M_0 + U_0 S & 0 \\ 0 & V_0 \end{bmatrix}^{-1} \tag{2.3.11}$$

Thus

$$\begin{bmatrix} I & -K_0 \\ -\Delta G & I \end{bmatrix}^{-1} - \begin{bmatrix} I & -K_0 \\ -\Delta G_0 & I \end{bmatrix}^{-1} =$$
$$\left[\begin{bmatrix} M_0 + U_0 S & 0 \\ 0 & V_0 \end{bmatrix} \begin{bmatrix} I & 0 \\ -S & I \end{bmatrix}^{-1} - \begin{bmatrix} M_0 & 0 \\ 0 & V_0 \end{bmatrix} \right] \begin{bmatrix} M_0 & -U_0 \\ -N_0 & V_0 \end{bmatrix}^{-1} =$$
$$\begin{bmatrix} M_0 & U_0 \\ N_0 & V_0 \end{bmatrix} \begin{bmatrix} 0 & 0 \\ S & 0 \end{bmatrix} \begin{bmatrix} M_0 & -U_0 \\ -N_0 & V_0 \end{bmatrix}^{-1}$$

and applying the double Bezout (2.2.13)gives

$$\begin{bmatrix} \tilde{V}_0 & -\tilde{U}_0 \\ -\tilde{N}_0 & \tilde{M}_0 \end{bmatrix} \left[\begin{bmatrix} I & -K_0 \\ -\Delta G & I \end{bmatrix}^{-1} - \begin{bmatrix} I & -K_0 \\ -\Delta G_0 & I \end{bmatrix}^{-1} \right] \begin{bmatrix} M_0 & -U_0 \\ -N_0 & V_0 \end{bmatrix} = \begin{bmatrix} 0 & 0 \\ S & 0 \end{bmatrix}$$

,or equivalently (2.3.3) holds, and (2.3.7). (This result is generalized in Theorem 2.2)

Simple manipulations from Figure 2-9(b) give the transfer function of the G block to be $J_{21}S(1 - J_{11}S)^{-1}J_{12} + J_{22}$, and substitution of (2.3.4) gives ΔG by (2.3.2).

To establish coprimeness of $N(S), M(S)$ observe that under the double bezout (2.2.13)

$$\tilde{V}_0 M(S) - \tilde{U}_0 N(S) = \tilde{V}_0 M - \tilde{U}_0 N + (\tilde{V}_0 U_0 - \tilde{U}_0 V_0)S = I$$

which is unimodular, Thus from [47] Lemma 2.1, $N(S)M(S)^{-1}$ is a right co-prime factorization.

∎

Remarks

1. When ΔG is linear, the above results specialize to known results in [64], although the details of the theorem proof appears quite different so as to avoid using superposition when nonlinear operators $\Delta G, S$ are involved.

2. The fact that $\tilde{M}_0, \tilde{N}_0, M_0, N_0, \tilde{U}_0, \tilde{V}_0, U_0, V_0$ are linear has allowed derivations to take place without differential boundedness or other such assumptions as in a full non-linear theory as developed in [46], [47] using left coprime factorizations.

3. Dual left coprime factorization results , apart from those in [46], [47] involving differential boundedness, are elusive at this time. Certainly dualizing certain of the above proof steps requires superposition and thus linearity of $\Delta G, S$.

4. Dual results apply for fractional mappings of $K = K(Q)$, as in (2.3.12),(2.3.13) along with duals of the other results. Thus $K(Q)$ can be expressed as a linear controller K_0 augmented with a non-linear Q.Also, by duality, Figure 2-9(a) depicts a block diagram arrangement for

$$K \triangleq K(Q) = U(Q)V^{-1}(Q); \;\; U(Q) = (U_0 + M_0Q), V(Q) = (V_0 + N_0Q) \quad (2.3.12)$$

where

$$Q = (-\tilde{U}_0 + \tilde{V}_0K)(\tilde{M}_0 - \tilde{N}_0K)^{-1} \quad (2.3.13)$$

Stabilization Results

We define a system $\{G, K\}$ to be *internally stable* iff for all bounded inputs, the outputs are bounded.

Theorem 2.2

Consider the well-posed feedback system $\{\Delta G, K\}$ under the conditions of Theorem 2.1, with ΔG and K parameterised by S, Q as in (2.3.1), (2.3.12) and as depicted in Figures 2-9 (a) and (b). Then $\{\Delta G(S), K(Q)\}$ is well posed and stable if and only if the feedback system $\{Q, S\}$ depicted in Figure 2-10 is well posed and internally stable. Moreover, referring to Figure 2-9(c), the $J_k/\Delta G$ block with input/output operator T satisfies

$$T = S \quad (2.3.14)$$

Proof. Observe that from (2.3.1),(2.3.12)

$$\begin{bmatrix} I & -K(Q) \\ -\Delta G(S) & I \end{bmatrix} = \begin{bmatrix} M_0 & -U_0 \\ -N_0 & V_0 \end{bmatrix} \begin{bmatrix} I & -Q \\ -S & I \end{bmatrix} \begin{bmatrix} M_0 + U_0S & 0 \\ 0 & V_0 + N_0Q \end{bmatrix}^{-1} \quad (2.3.15)$$

Clearly, under the double Bezout identity (2.2.13), or equivalently under $\{\Delta G_0, K_0\}$ well posed and internally stable,

$$\begin{bmatrix} I & -K(Q) \\ -\Delta G(S) & I \end{bmatrix}^{-1} \text{ exists} \iff \begin{bmatrix} I & -Q \\ -S & I \end{bmatrix}^{-1} \text{ exists.}$$

Equivalently, $\{G(S), K(Q)\}$ is well posed if and only if $\{Q, S\}$ is well posed. Thus under well posedness assumptions, taking inverses in, and exploiting (2.3.15) then simple manipulations yield

$$\begin{bmatrix} I & -K(Q) \\ -\Delta G(S) & I \end{bmatrix}^{-1}$$

$$= \left[\begin{bmatrix} M_0 & 0 \\ 0 & V_0 \end{bmatrix} + \begin{bmatrix} U_0 & 0 \\ 0 & N_0 \end{bmatrix}\begin{bmatrix} S & 0 \\ 0 & Q \end{bmatrix}\right]\begin{bmatrix} I & -Q \\ -S & I \end{bmatrix}^{-1}\begin{bmatrix} \tilde{V}_0 & \tilde{U}_0 \\ \tilde{N}_0 & \tilde{M}_0 \end{bmatrix} \quad (2.3.16)$$

$$= \begin{bmatrix} I & -K_0 \\ -\Delta G_0 & I \end{bmatrix}^{-1} + \begin{bmatrix} U_0 & M_0 \\ V_0 & N_0 \end{bmatrix}\begin{bmatrix} S & 0 \\ 0 & Q \end{bmatrix}\begin{bmatrix} I & -Q \\ -S & I \end{bmatrix}^{-1}\begin{bmatrix} \tilde{V}_0 & \tilde{U}_0 \\ \tilde{N}_0 & \tilde{M}_0 \end{bmatrix} \quad (2.3.17)$$

Now internal stability of $\{\Delta G_0, K_0\}$, $\{S, Q\}$, and stability of $N_0, \tilde{N}_0$ etc leads to internal stability of the right hand side and thus of $\{\Delta G(S), K(Q)\}$ as claimed. Moreover from (2.3.17),(2.2.13)

$$\begin{bmatrix} S & 0 \\ 0 & Q \end{bmatrix}\begin{bmatrix} I & -Q \\ -S & I \end{bmatrix}^{-1} =$$

$$\begin{bmatrix} -\tilde{N}_0 & \tilde{M}_0 \\ \tilde{V}_0 & -\tilde{U}_0 \end{bmatrix}\left[\begin{bmatrix} I & -K(Q) \\ -\Delta G(S) & I \end{bmatrix}^{-1} - \begin{bmatrix} I & -K_0 \\ -\Delta G_0 & I \end{bmatrix}^{-1}\right]\begin{bmatrix} M_0 & -U_0 \\ -N_0 & V_0 \end{bmatrix}$$

Thus well posedness and internal stability of $\{\Delta G(S), K(Q)\}$ and $\{\Delta G_0, K_0\}$ gives well posedness and internal stability of $\{Q, S\}$ to complete the first part of the proof.
Now with J_K defined as in (2.2.17) then the operator T in Figure 2-9(c) can be represented as

$$\begin{aligned} T &= V_0^{-1}\Delta G(I - \tilde{V}_0^{-1}\tilde{U}_0\Delta G)^{-1}\tilde{V}_0^{-1} - \tilde{N}_0\tilde{V}_0^{-1} \quad (2.3.18)\\ &= V_0^{-1}\Delta G(\tilde{V}_0 - \tilde{U}_0\Delta G)^{-1} - \tilde{N}_0\tilde{V}_0^{-1} \\ &= [V_0^{-1}\Delta G - \tilde{N}_0 + \tilde{N}_0\tilde{V}_0^{-1}\tilde{U}_0\Delta G](\tilde{V}_0 - \tilde{U}_0\Delta G)^{-1} \\ &= \tilde{M}_0[\tilde{M}_0^{-1}(V_0^{-1} + \tilde{N}_0\tilde{V}_0^{-1}\tilde{U}_0)\Delta G - \Delta G_0](\tilde{V}_0 - \tilde{U}_0\Delta G)^{-1} \end{aligned}$$

$$= \tilde{M}_0[\Delta G - \Delta G_0](\tilde{V}_0 - \tilde{U}_0\Delta G)^{-1}$$
$$= S$$

∎

Remarks

1. Note that this proof does not use superposition associated with operators S, Q, but does in regard to M_0, N_0 etc. The results following Theorem 2.1 also apply for Theorem 2.2. Thus the proof approach differs (of necessity) from the proof approach given in [64] for the linear S, Q case based on work with the left factorizations , since when working with left factorizations, superposition is used associated with the operators Q, S.More general versions of this approach where G_0, K_0 are nonlinear will be explored in subsequent work.

2. If $|S| < \epsilon$ then by the small gain theorem for closed feedback loops, if $|Q| < 1/\epsilon$ then Q stabilizes the loop. From this, and Theorem 2.2 with $(\Delta G - \Delta G_0)$ suitably small in norm, then there exists some Q which will guarantee stability.

3. In the case where $\Delta G = \Delta G_0$ then trivially $S = 0$, and any Q selection based on identification of S will be trivially $Q = 0$. This contrasts the awkwardness of one alternative design approach which would seek to identify the closed-loop system as a basis for a controller augmentation design.

4. Observations on examples in the linear ΔG case have shown that if K_0 is robust for G, then S can be approximated by a low order system [67], so making any Q selection more straightforward than might be otherwise expected.

5. In [76] stability results are studied for nested linear systems based on the Q/S parametrization approach. The authors demonstrate how an $(n+1)$ loop control diagram can be specialised to an equivalent $n-$loop diagram, and shows that internal stability of an $(n+1)$ control loop is equivalent to that of the controller in the last loop stabilizing the n-th frequency-shaped plant-model error. It is clear that our results could also likewise extend, at least in the case when all approximations but the last were linear.

Averaging Convergence Analysis The adaptive scheme has the property that when $\Delta G = \Delta G_0$, then Q_k converges to zero, so that when K_0 is the nominal optimal

regulator, then the adaptive regulator $K(Q_k)$ converges to $K_0 = K(0)$, the optimal one. Such details are studied in [63]. More general results are given in [74] for the case of linear ΔG, based on an averaging analysis. One result concerns the case for when $\{\Delta G, K_0\}$ is a stabilizing pair, as well as $\{\Delta G_0, K_0\}$. There is guaranteed performance enhancement when $\{\Delta G, K_0\}$ is not stabilizing, but is small in that $\{\Delta G, K(Q)\}$ is stabilizing for some Q with $||Q|| < \epsilon$ with ϵ known, then with Q_K projected into the domain $\{||Q|| < \epsilon\}$, there is guaranteed performance enhancement. For the more general case where ΔG is nonlinear, then new results are needed. One approach is the averaging analysis as used in [74] but for nonlinear systems as in [38], but clearly any results obtained will be problem specific and beyond the scope of this thesis. A first step in such an analysis is to derive appropriate stability results. Stability results for the proposed scheme in the nonlinear ΔG, but linear $K_0, \Delta G_0$ case are studied in the next section. These are more developed than those for the nonlinear $K_0, \Delta G_0, \Delta G$ studied in references [46],[47]. Convergence results for a learning-Q approach for linear systems as in Remark 8 in Section 2, would follow similar lines to the adaptive-Q approach, at least when $\Delta G_0, J_k$ and Q are functions only of x^*. But in the more general case when the operators are functions of x, or δx, a stabilization theory coping with nonlinear ΔG_0,J_K is developed in Chapter 4.

2.4 Simulations

In this section, we demonstrate the efficacy of our approach through simulation studies. Consider an optimal control problem based on the van der Pol equation

$$\dot{x}_1 = (1 - x_2^2)x_1 - x_2 + u, \;\; \dot{x}_2 = x_1, \;\; y = x_1 \tag{2.4.1}$$

with $x_1(0) = 0, \; x_2(0) = 1$ and the performance index defined by

$$I = \frac{1}{2}\int_0^5 (x_1^2 + x_2^2 + u^2)dt \tag{2.4.2}$$

A second-order algorithm [27], using 400 integration steps, was adopted for the numerical solution of the open-loop optimal control signal u^*. An arbitrary initial nominal control $u \equiv 0, t \in [0, 5]$, was chosen. The value of the performance index was reduced to the optimal one in 4 iterations in updating $u(\cdot)$ over the range $[0, 5]$.

Four situations have been studied in simulations. For each case we add a stochastic

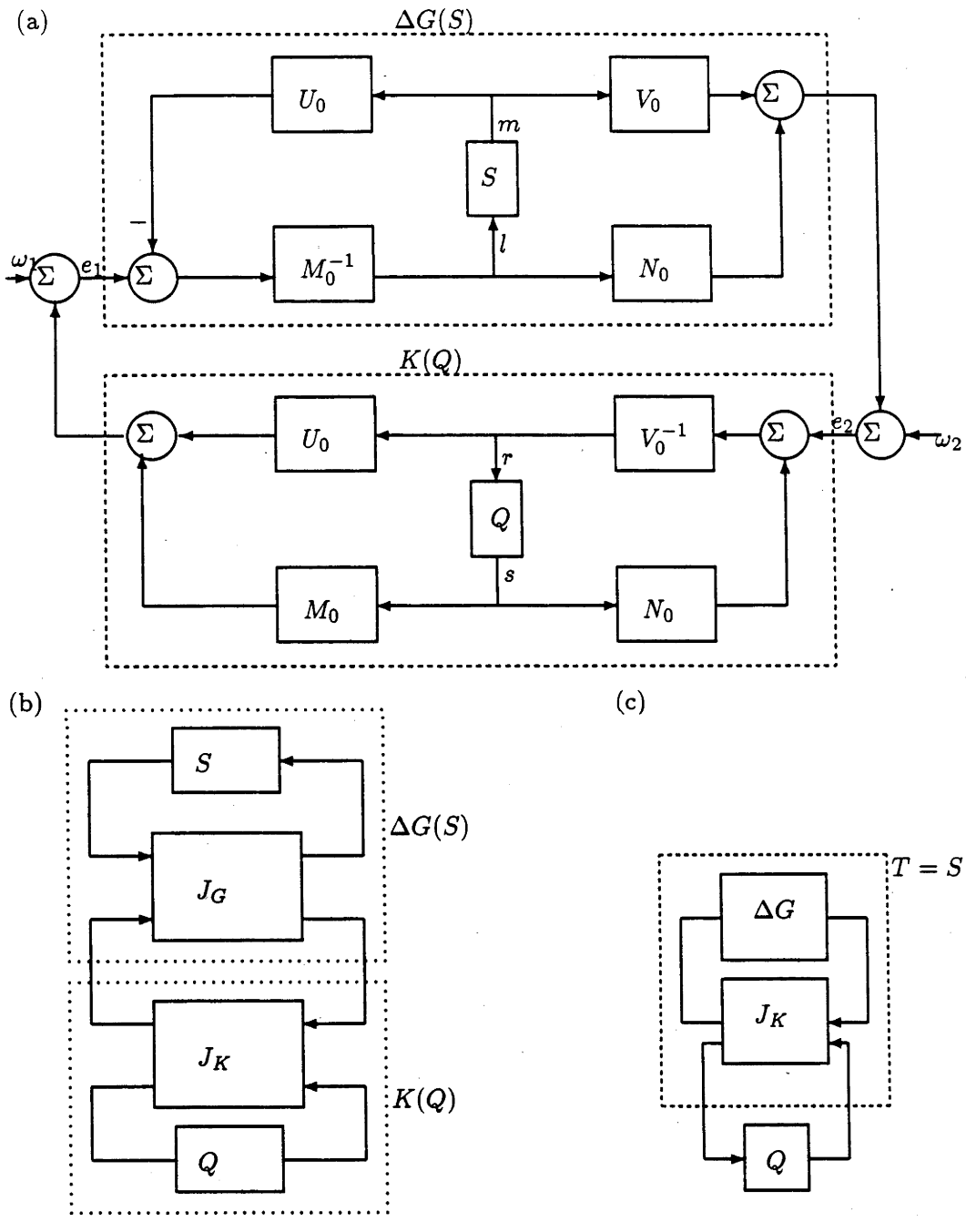

Figure 2-9: The feedback system $\{\Delta G(S), K(Q)\}$.

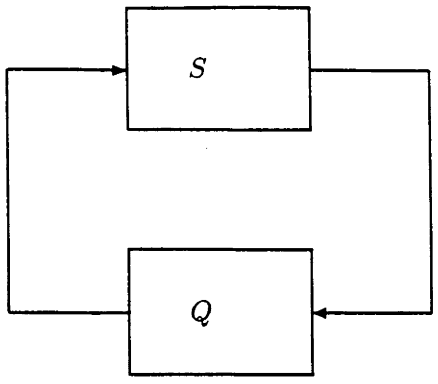

Figure 2-10: The feedback system $\{Q, S\}$.

or a deterministic disturbance which disturbs the optimal input signal. Also, in some of the simulations we apply a plant with unmodelled dynamics. The objective is to regulate perturbations from the optimal by means of the index $\triangle I = \int_0^5 (\delta x_1^2 + \delta x_2^2 + \delta u^2) dt$ which is expressed in terms of perturbations $\delta x, \delta u$. For each of the disturbances added, and for the unmodelled dynamics case, we compare five controller strategies, and demonstrate the robustness and performance properties of the adaptive-Q methodology.

Case 1: Open-loop design.

Here we adopt the optimal control signal u^* as an input signal of the nonlinear system with added disturbance. Figure 2.11 shows that the open-loop design is quite sensitive to such disturbances in that x_1, x_2 differ significantly from x_1^*, x_2^*.

Case 2: LQG's design.

In order to construct feedback controllers, we adopt the standard LQG theory based on the linearized plant model of (2.4.1) about the optimal trajectories and the performance index (2.4.2). Of course, the input signals $u^* + \delta u$ are no longer 'optimal' for the nominal plant. The LQG controller's design yields better performance than the open-loop case in that the errors $x_1 - x_1^*, x_2 - x_2^*$ are mildly smaller than in the previous figure for the open-loop case. See Table 2.4.1. It is well known, however, that the LQG controller, although optimal for the nominal plant model under the assumed noise environment, may lose performance and perhaps its stability even for small variations from the nominal plant model.

Case 3: LQG/LTR design

In order to enhance the robustness properties of LQG controllers, we adopt well known loop transfer recovery (LTR) techniques [14]. Thus the system noise covariance Q_f in a state estimator design, is parametrized by a scaler $q > 0$, and a loop recovery property is achieved

as q becomes large. In our scheme the state estimator 'design system and measurement noise covariances', $Q_f(q)$ and R_f, are given by $Q_f(q) = I + q^2 \begin{bmatrix} 1 \\ 0 \end{bmatrix} [1\ 0], \qquad R_f = I$ with $q = 50$. There is a more dramatic reduction of errors $x_1 - x_1^*, x_2 - x_2^*$ over that for the LQG design of the previous case as indicated in Table 2.4.1. Of course, the Case 3 is identical to the Case 2 when $q = 0$. Also, simulations not reported here show that the LQG/LTR design performs virtually identically to an LQ design where states δx are assumed available for feedback.

Case 4: Adaptive Q design

The adaptive Q, two-degree-of-freedom, controller design for optimal control problem is studied, with the LQG or LQG/LTR controller K_0 and the adaptive $Q = [Q_1,\ Q_2]$ using least square techniques. Third-order FIR models are chosen for the forward $Q_1(z)$ and the backward $Q_2(z)$. Simulations, summarized in Table 2.4.1 show that adaptive-Q controller design strengthens the robustness/performance properties of both the LQG and LQG/LTR design without the need for any high gains in the controller. See also Figure 2-11. The intention in this first design example has not been to demonstrate that an adaptive-Q approach works dramatically better than all others, although one example is shown where such is the case. Rather, we have sought to stress that the adaptive-Q method is perhaps best used only after a careful robust fixed controller design, and then only to achieve fine turning. Actually, for the design study here, the robust LQG/LTR design performed better than the LQG adaptive-Q design. The values of $\triangle I$ for all five cases are summarized in Table2.4.1 for a deterministic disturbance $d = .2$, and then two stochastic disturbances, with, in the first instance d uniformly distributed between .1 and .3, and in the second d uniformly distributed between 0 and 1.

Table 2.4.1: Trajectory 1. I.C. = [0 1]

	Open loop	LQG	LQG/LTR	LQG/Ad-Q	LQG/LTR/Ad-Q	disturbance
$\triangle I$	3.0712	0.7486	0.2295	0.3478	0.1600	$d = .2$
	3.0556	0.7435	0.2278	0.3449	0.1592	$d \in U(.1, .3)$
	6.2587	3.2557	1.3483	1.9925	1.0010	$d \in U(0, 1)$

To demonstrate the robustness of the adaptive-Q control strategy, the simulations were repeated with unmodelled dynamics in the actual plant. The state equations of the actual plant in this case are $\dot{x}_1 = (1 - x_2^2)x_1 - x_2 + x_3 + u,\ \dot{x}_2 = x_1,\ \ddot{x}_3 = -\dot{x}_3 - 4x_3 + u,\ y = x_1$ with initial state vector [0 1 0].

The simulations in Tables 2.4.1 and 2.4.2 are repeated for different initial conditions,

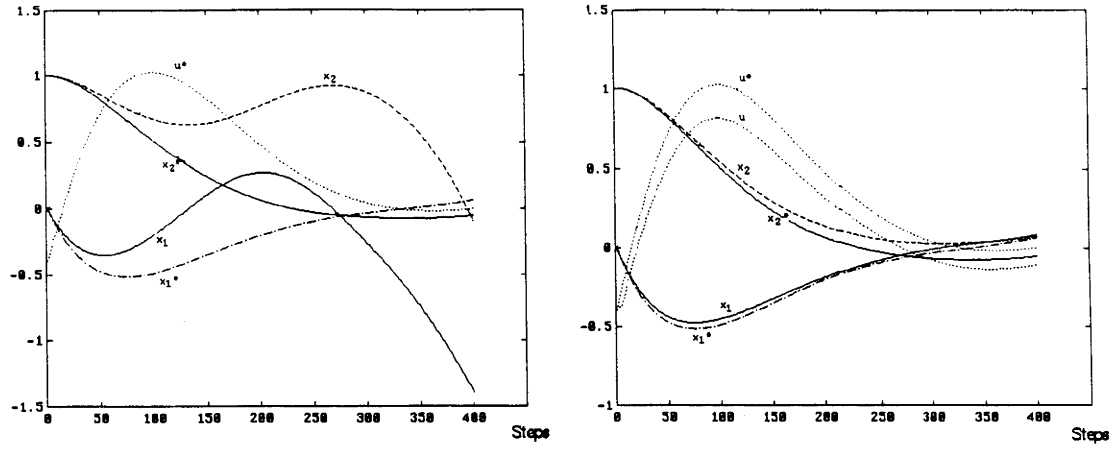

Figure 2-11: Open Loop and LQG/LTR/Adaptive-Q Trajectories

and thus a different optimal trajectory. The results are included in Tables 2.4.3 and 2.4.4.

This trajectory also had the same unmodelled dynamics added to demonstrate robustness.

Remarks

1. In our simulation for the adaptive Q controller, two passes are needed for "warming up" of the controller. Subsequently, the coefficients in Q_1 and Q_2, in the notation of (2.12), "converge" to slowly varying values in the vicinity of $\gamma_0 = 0.0976, \gamma_1 = -0.0002, \gamma_2 = -0.1016, \beta_0 = -11.18, \beta_1 = -9.247, \beta_2 = -7.891$, with $\alpha_i \equiv 0$.

2. The prefilters $P_{12}M_0$ used in our study are as follows.

$$\dot{x}_{ps} = (A + BF)x_{ps} + Bu^*, \quad \xi_1 = \begin{pmatrix} F \\ I \end{pmatrix} x_{ps} + \begin{pmatrix} I \\ 0 \end{pmatrix} u^*$$

with input u^* and output ξ_1. Likewise for the prefilters driven by δr and s.

3. Our simulations not reported here show significant improvements when scaling adjustments are made to r and e. Also, other simulations not reported here show that there is insignificant benefit with increasing the dimensions $p = 3, m = 3, n = 0$ in Q, although the cost of reducing p or m is significant.

2.5 Conclusions

A method to combine off-line (open-loop) optimal control approaches with robust feedback control and on-line (closed-loop) adaptive control techniques is presented, with emphasis on nonlinear cases. Stability properties for the nonlinear case are discussed. Simulation results show that our proposed method can enhance robustness/performance properties, in the presence of unmodelled dynamics, and deterministic or stochastic disturbances. The method can be generalized to a learning-Q approach where the Q feedback operator is a function of the optimal state trajectory x^*, or of x itself, and this will be discussed in Chapter 3.

Table 2.4.2: Trajectory 1 with Unmodelled Dynamics. I.C. = [0 1 0]

	Open loop	LQG	LQG/LTR	LQG/Ad-Q	LQG/LTR/Ad-Q	disturbance
$\triangle I$	5.9077	1.9438	0.6623	0.984	0.4251	$d = .2$

Table 2.4.3: Trajectory 2. I.C. = [1 .5]

	Open loop	LQG	LQG/LTR	LQG/Ad-Q	LQG/LTR/Ad-Q	disturbance
$\triangle I$	3.6646	0.7524	0.2165	0.3447	0.1505	$d = .2$
	3.6478	0.7476	0.2148	0.3415	0.1495	$d \in U(.1, .3)$
	7.4502	3.3817	1.2766	1.9734	0.9278	$d \in U(0, 1)$

Table 2.4.4: Trajectory 2 with Unmodelled Dynamics. I.C. = [1 0.5 0]

	Open loop	LQG	LQG/LTR	LQG/Ad-Q	LQG/LTR/Ad-Q	disturbance
$\triangle I$	4.7301	1.2805	0.5162	0.6313	0.2981	$d = .2$

Chapter 3

Robust Nonlinear Control - State Dependent Q

3.1 Introduction

Some work has been done in the area of linear robust control, and adaptive control, by optimising over the set of all proper stabilizing controllers for a given plant parametrised by a stable filter denoted Q, and more generally where appropriate, with Q permitted to be unstable. For off-line robust controller design, the Q filter is optimised off line and incorporated into the controller. In adaptive-Q design, the Q filter is implemented in a separate loop and its parameters are updated via an on-line least squares algorithm for performance enhancement. For robust nonlinear optimal control, it makes sense to explore the adaptive-Q enhancement approach addressed in Chapter 2, but with the algorithm modified such that Q is state (or state estimate) dependent. Such an approach is termed here learning-Q control.

Well studied frequency shaped H_2 and H_∞ robust controller designs for linear systems depend on an off-line optimisation of the stable filter Q. Where there are no additional constraints, the optimal theory of [13, 19] leads to elegant algorithms. When there are constraints on the controller structure then numerical optimisation techniques must be applied as in [8, 15]. Certainly such techniques can be applied to achieve robustness in optimisation control working with a linearized state-dependent plant model.

Recall that in Chapter 2, building on the linear system design approach of [66], nonlinear open-loop optimal control is fine tuned, not only by a robust feedback controller based on linearization about the optimal trajectory, but also by an adaptive-Q filter which

implements both feedforward and feedback controller augmentations. The performance in the presence of an unknown constant disturbance is studied. Simulations show improvement with the introduction of the time-varying linear feedback controller, as expected, and further improvement is achieved with the addition of an adaptive-Q filter to minimise a quadratic index which penalises departures from the optimal state and control trajectories. The approach of Chapter 2 is in essence one based on linearization. The Q filter is not plant state dependent, or state estimate dependent as are the plant and linearized controller. It seems reasonable to explore further enhancements of the scheme of Chapter 2 by working with a nonlinear Q filter with parameters being functionally dependent on the state estimates, or desired optimal states of the nominal plant.

In generalizing the least squares based adaptive-Q filter coefficients update scheme of [66], applied in the nonlinear control of Chapter 2, the essence of our task is to replace a parameter least squares algorithm by one involving functional learning. To optimise the Q-filter when its parameters are state dependent, the key strategy we propose here is to apply functional learning algorithms as in [50]. The least squares based functional learning of [50] suggests bisigmoid sum representations of the parameters over the state space, or for practical reasons, over only the significant components of the state space. The parameters of this representation are tuned on line by a least squares scheme. Bisigmoids, such as gaussians or truncated gaussians, B-splines, or radial basis functions have the dual roles of interpolating between parameter estimates at grid points in the state space, and of spreading learning on either side of a trajectory in the state space. Polynomials or sigmoids cannot play such a dual role, and indeed are likely to cause unacceptably poor performance outside the region of most excitation. The new schemes proposed are termed here learning-Q schemes.

One of the motivations for our work has been to build on the functional learning control techniques developed earlier for control of robots with uncertain dynamics [67]. In this work, the approach is in essence a model reference adaptive control approach generalized to incorporate functional learning. It is dependent for its success on very specific robot passivity properties, and the work is essentially a continuous-time integral operator approach. Here, we seek a more general technique based on adaptive-Q methods and one which is developed in a discrete time setting from the start.

In Section [2], we review the relevant least squares based functional learning theory, Section [3] defines the plant model class, reviews the adaptive Q controller algorithms and generalizes these by application of the least squares based functional learning approach

to this context. Section [4] presents theoretical analysis results , Section [5] presents the results of the simulation studies for controller designs applied to the Van der Pol equations to illustrate the power of the proposed techniques, and Section [6] has the conclusion.

3.2 Least Squares Functional Learning

In adaptive control, the controller for the plant adapts to optimise some performance specification. Should the plant be time varying, then the adaptive controller tracks in some sense an optimal controller. There is built into the controller a forgetting factor so that distant past experiences are totally forgotten. If the plant dynamics are nonlinear being a function of a slowly changing variable , such as the slow states of the plant, then it makes sense to remember the past in such a way that the controller can recall appropriately from past experience and give better performance than it would with built-in forgetting. To facilitate such control action, enhanced with memory, functional learning algorithms appear attractive.

Functional learning here refers to a method by which the values of a function $y = f(x)$ can be estimated at all points in the input variable space Γ_x from data pairs (x_i, y_i), or noisy measurements of these. Given an estimate $f(.)$ at time k, denoted $\hat{f}$, then with a new measurement x_k, a prediction of y_k is $\hat{y}_k = \hat{f}(x_k)$. The error $(y - \hat{y}_k)$ can then be used to update $\hat{f}(.)$ for time $k+1$ based on assumed smoothness properties of $f(.)$. The function is here represented as a sum of simply parametrised functions which could be basis functions such as polynomials or gaussians. We define the error between a representation of a given function $\hat{f}(.)$ and the actual function $f(.)$ in terms of some error norm. Thus, here, the learning involves adapting the parameters of the basis functions to achieve lower error norms. We look to approximate arbitrary continuous functions within a class of such.
A key representation theorem for our approach is in [12]. This theorem tells us that sums of sigmoids, or more general bisigmoids such as gaussians or truncated gaussians, suitably parametrised are dense, and can represent functionals over finite domains.

Given a function, $f(.)$, an approximation to that function could be represented by a superposition of a finite number of the simply parametrised functions $f_i(.)$, such as sigmoids or bisigmoids, each centered at different points , γ_i ,within the input variable Γ_x space. The representation must be chosen with regard to required accuracy, convergence properties, and computability. For example, to approximate a two input variable scalar function with a bounded first derivative by a grid of simply parametrised functions being

piecewise constant functions on a grid, the following result is easily established.

Lemma 3.1 *Suppose there is given a two input variable scalar function $f(x,y)$ with a first derivative bounded by C, and a square region $R = \{(x,y) : |x|, |y| < r\}$ over which it is to be approximated. Furthermore, suppose there is an approximation to the function by a piecewise constant function on a rectangular N by N grid covering the region R. Then the l_2 error bound e between $f(x,y)$ and the approximation $\hat{f}(x,y)$ is*

$$e = O(\frac{C^2}{N^2}) \tag{3.2.1}$$

Proof. See Appendix ∎

In selecting the simply parametrized functions $f_i(.)$ for learning in the control environment of interest, we take into account the need for 'fast' learning, reasonable interpolation and extrapolation approximation properties, and the ability to spread learning in the Γ_x space. For 'fast' learning, we require here that the measurements are linear in the parameters of $f_i(.)$ so that the least squares techniques can apply. This contrasts the case of neural networks where backward propagation gradient algorithms are inevitably 'slow' in convergence.

For reasonable interpolation capabilities, any of a number of selections such as polynomials, splines, sigmoids, or bisigmoids can be used, but to avoid poor extrapolation outside the domains of most excitation of x_k in Γ_x, we select bisigmoids. Likewise, only the bisigmoids allow learning along the trajectories in Γ_x to be spread acceptably to neighbourhoods of such trajectories. This approach is taken in [50] for an open loop identification task, which we now adapt for our control task. First let us review the least squares learning taken in [50], and related results.

Consider the signal model usually derived from an ARMAX representation,

$$y_k = \Phi_k' \Theta(x_k) + \omega_k \tag{3.2.2}$$

where y_k are the measurements, Φ_k is a known regression vector of the model inputs and outputs, and $\Theta(.)$ are the unknown functionals with input variables x_k, representing the perhaps nonlinear 'parameters' of an ARMAX model. Here ω_k is taken to the zero mean white noise.

Let us investigate finite representations estimating $\Theta(x)$ of the form

$$\hat{\Theta}(x) = \sum_{i=1}^{n} K_I'(x, \gamma_i)\hat{\theta}(\gamma_i) = K_I'(x)\hat{\Theta}(\Gamma_I) \tag{3.2.3}$$

with $\hat{\Theta}'(\Gamma_I) = [\hat{\theta}'(\gamma_1) \cdots \hat{\theta}'(\gamma_n)]$, and $K_I'(x) = [K_I'(x, \gamma_1) \cdots K_I'(x, \gamma_n)]$. Here $\theta(\gamma_i)$ are the parameters and $K_I(x, \gamma_i)$ the interpolation function representation (3.2.3). For simplicity we work with $K_I(x, \gamma_i)$ which acts as both a scalar interpolating function and learning spread function between the points $x \in \Gamma_x$ and $x \in \Gamma_I$. Here $\Gamma_I = \{\gamma_1, \gamma_2, \ldots, \gamma_n\}$ is a preselected set of points in Γ_x. In our simulations, we use gaussians or truncated gaussians for the vectors indicated above. Now (3.2.2) can be represented as

$$y_k = \Phi(x_k)'\Theta(\Gamma_I) + \hat{\omega}_k \tag{3.2.4}$$

where

$$\Phi(x_k) = K_I(x_k)\Phi_k, \quad \Theta(x_k) = K_I(x_k)\Theta(\Gamma_I) \tag{3.2.5}$$

and $\hat{\omega}_k$ approximates ω_k.

Consider an error measure for the representation :

$$d_2^{(r)}(\hat{\Theta}) = \frac{1}{r}[\sum_{k=1}^{r} \|\Theta(x_k) - \hat{\Theta}(x_k)\|^2]^{\frac{1}{2}} \tag{3.2.6}$$

As shown in [50], under strong persistence of excitation conditions on x_k minimisation of this index is equivalent to minimisation of the d_2 index :

$$d_2(\hat{\Theta}) = [\int_{\Gamma_x} \|\Theta(x) - \hat{\Theta}(x)\|^2 dx]^{\frac{1}{2}} \tag{3.2.7}$$

A key result associated with this latter minimisation task is as follows

Theorem 3.1

The minimisation task of the index $d_2(\hat{\Theta})$ has a unique critical point , denoted $\hat{\Theta}^*$ if and only if the elements of $K_I(x)$ are allowable, in that

$$\infty > [\int_{\Gamma_x} K_I(x)K_I'(x)dx] > 0 \tag{3.2.8}$$

This optimal $\hat{\Theta}$ is given from

$$\hat{\Theta}^* = (\int_{\Gamma_x} K_I(x)K_I'(x)dx)^{-1} \int_{\Gamma_x} y(x)K_I'(x)dx \tag{3.2.9}$$

Moreover, when $\Theta(x)$ is reconstructible with respect to the class of functions $\hat{\Theta}(x)$ of (3.2.3), then $\Theta(x)$ is uniquely parametrized as in (3.2.3) with $\Theta = \hat{\Theta}^*$ given in (3.2.9).

Proof. The proof of this can be found in [50] ∎

In order to minimise $d_2^{(r)}$ of (3.2.6) for $r = 1, 2, \ldots$, given a sequence $\{x_k, y_k\}$, standard least squares derivations applied to (3.2.6,3.2.7) lead to a recursive estimate of $\Theta(x_k)$, denoted $\hat{\Theta}_k(x_k)$, as

$$\hat{\Theta}_k(x_k) = K_I'(x_k)\hat{\Theta}_k(\Gamma_I) \tag{3.2.10}$$

$$\hat{\Theta}_k(\Gamma_I) = \hat{\Theta}_{k-1}(\Gamma_I) + P_k(\Gamma_I)\Phi_I(x_k)[y_k - \Phi_I'(x_k)\hat{\Theta}_{k-1}(\Gamma_I)] \tag{3.2.11}$$

where

$$P_k^{-1}(\Gamma_I) = P_{k-1}^{-1}(\Gamma_I) + \Phi_I(x_k)\Phi_I'(x_k), \quad \Phi(x_k) = K_I(x_k)\Phi_k \tag{3.2.12}$$

with suitable initial conditions $\hat{\Theta}_0$, P_0. Under appropriate conditions [50], P_k^{-1} approaches a diagonal matrix. With truncated K_I then P_k^{-1} is block diagonal with only one block updated at each iteration and only one corresponding segment of $\hat{\Theta}_k$ updated. In selecting a truncation, there is clearly a trade off between function estimation accuracy and computational effort.

3.3 Learning-Q Controller Scheme

In this section, we extend the adaptive-Q methodology of Chapter 2 to one based on a Learning-Q subsystem implemented via the application of Least Squares Functional Learning. The learning-Q methods are developed to provide performance enhancement by building in memory of past experiences.

The feedback control approach based on linearization is expected to perform well when the actual plant differs only marginally from the nominal optimal plant so that the difference between the actual, and optimal output trajectories, $\delta y = y - y^*$ is small and consequently δu is small. What fall back position can we use if this is not the case? We proceed to develop our so called learning-Q approach, which generalizes the work on adaptive-Q systems of Chapter 2 where additional adaptive controllers in a two-degree-of-freedom configuration are applied based on the approach of [64], [66].

Least Squares (Scalar variable case) Now with the definitions of Chapter 2 holding, and as shown in [64] for the case of scalar variables $\delta u_k, \delta y_k, r_k, b_k$ (for simplicity), with $s_k = Q_1 u_k^* + Q_2 r_k$, (2.2.22) can be re-organized using readily derived relationships so that ζ_k is linear in Θ, as

$$\xi_k = \Phi_k' \Theta + e_k \tag{3.3.1}$$

$$\Phi_k' = [(\hat{e}_{k-1/k-1} - \zeta_{k-1}) \cdots (\hat{e}_{k-n/k-n} - \zeta_{k-n}) \ - \xi_k \cdots - \xi_{k-m}] \tag{3.3.2}$$

These equations allow a least squares recursive update for Θ, denoted $\hat{\Theta}_k$, to minimise the index $\Sigma_{i=1}^k ||e_{i|\Theta}||^2$ as spelt out in Chapter 2 for the adaptive-Q scheme. Here $e_{i|\Theta}$ denotes $e_{i|\hat{\Theta}_1 \ldots \hat{\Theta}_{k-1}\Theta}$ in obvious notation. In fact the details are a special case of those now derived for the proposed learning-Q scheme, and indeed the adaptive-Q scheme is that of Figure 3-1 specialized to the case when $\hat{\Theta}_k(x^*)$ is independent of x^*, so that $\hat{Q}_k(x_k^*)$ is replaced by $\hat{Q}_k$.

Learning-Q Scheme based on x^* We build upon the work of Chapter 2 by extending the adaptive-Q scheme to what could be viewed as an adaptive-$Q(x^*)$ scheme, but which we call a learning-Q scheme. The Q filter with which we work has coefficients which are functions of the state space. Denoting $\hat{Q}_k(x), \hat{\alpha}_{ik}(x), \hat{\beta}_{ik}(x)$, the key idea of the learning-Q algorithm is to update estimates $\hat{Q}_k(.)$, for all x in some domain Γ_x in which x_k^* lies. The Q filter is implemented as $\hat{Q}_k(x_k^*)$. The arrangement is depicted in Figure 3-1. The least squares functional learning block yields estimates $\hat{\Theta}(x_k^*)$ for implementation of the filter $\hat{Q}_k(x_k^*)$, being driven from ζ_k, ξ_k, e_k and x_k^*. The parameter estimates $\hat{\Theta}_k(x_k^*)$ are derived via the approach of Section 2. Thus , corresponding to (3.2.4) of section 2, we have the formulation (3.3.1) , and corresponding to (3.2.10)-(3.2.12) we have

$$\hat{\Theta}_k(x_k^*) = K_I'(x_k^*)\hat{\Theta}_k(\Gamma_I) \tag{3.3.3}$$

$$\hat{\Theta}_k(\Gamma_I) = \hat{\Theta}_{k-1}(\Gamma_I) + P_k(\Gamma_I)\Phi_I(x_k^*)[\xi_k(x^*) - \Phi_k'\hat{\Theta}(\Gamma_I)] \tag{3.3.4}$$

$$P_k^{-1} = P_{k-1}^{-1}(\Gamma_I) + \Phi_I(x_k^*)\Phi_I'(x_k^*) \tag{3.3.5}$$

Learning-Q Scheme based on $\hat{x}_k$. The Q filter can be implemented as $\hat{Q}_k(\hat{x}_k)$, where $\hat{x}_k = x_k^* + \delta\hat{x}_k$, as an alternative to implementing $\hat{Q}_k(x_k^*)$. This suggests also that the nominal

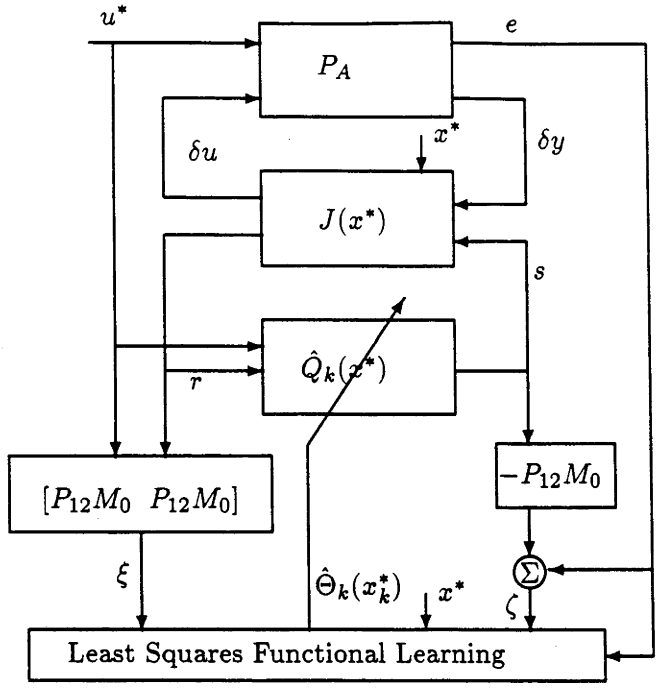

Figure 3-1: Two-degree-of-freedom learning-Q scheme (A-D converters not shown)

plant ΔG_0, controller K_0 and indeed J be functions of $\hat{x}_t$, rather than x_t^*. For this case then, any $\Delta G_0(\hat{x}_t), K_0(\hat{x}_t), J(\hat{x}_t)$ are inevitably nonlinear and a nonlinear factorization theory is required. For details see Chapter 2.

Of course when δx is small, one expects that x_t^* could be just as good an estimate of x_t as $\hat{x}_t$. In this case, there would be an advantage in working in a full nonlinear context. However, we would expect δx to be small only when the plant is nearly linear, and to avoid dealing with a full nonlinear context is really to avoid tackling systems that are in essence nonlinear.

3.4 Simulation Results

The Signal Model and Performance Index Consider the specific nominal plant model (Van der Pol equation):

$$\mathrm{G}_0 : \dot{x}_1 = (1 - x_2)x_1 - x_2 + u + b, \;\; \dot{x}_2 = x_1, \;\; y = x_1 \tag{3.4.1}$$

with scalar input u, scalar output y, and state vector $x = [x_1, x_2]'$.Consider also a regulator performance index defined by

$$I = \frac{1}{2}\int_0^5 (x_1^2 + x_2^2 + u^2)dt \tag{3.4.2}$$

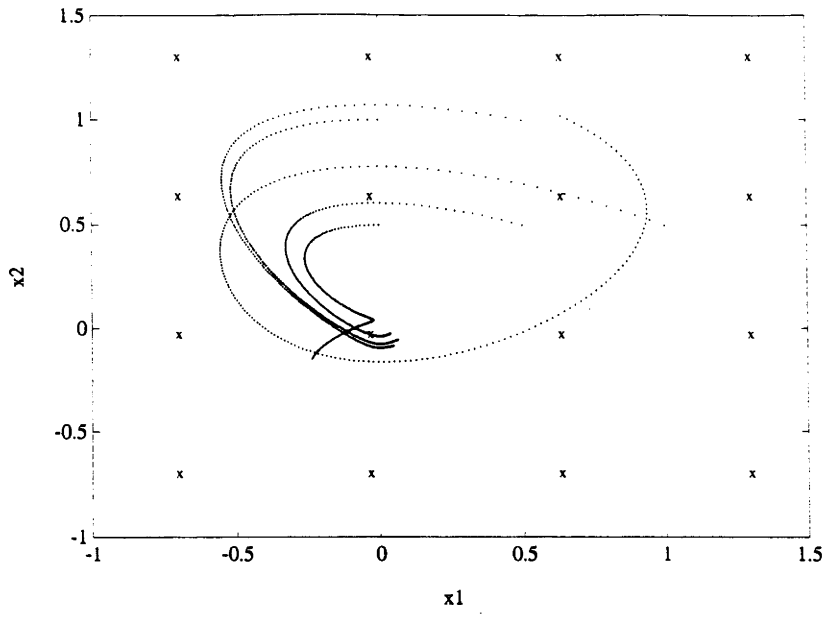

Figure 3-2: Five Optimal Regulation Trajectories in Γ_{x_1,x_2} space.

Of course for such a simple example, one could use a trivial linearization, by taking $u = \hat{x}_1\hat{x}_2 + u_1$ and then optimise $U_1 = K\hat{x}$ via LQG control, and thereby achieve an attractive nonlinear controller. Also, for more general nonlinear systems one could similarly exploit the linearization approach of [34]. However, here we wish to illustrate the design approach of the previous sections and use this plant as an example. Here, for each initial condition investigated, an optimal trajectory is calculated, as in Chapter 2. Next, the closed loop feedback controller schemes of the previous section are studied in the presence of constant and stochastic disturbances added to the plant input, and some of the simulations include unmodelled dynamics. The actual plant with unmodelled dynamics is

$$\dot{x}_1 = (1 - x_2)x_1 - x_2 + x_3 + u + b, \quad \dot{x}_2 = x_1, \dot{x}_3 = -\dot{x}_3 - 4x_3 + u, \quad y = x_1 \qquad (3.4.3)$$

where x_3 is the state of the unmodelled dynamics and b is the disturbance.

Learning Objective The major objective of the learning-Q method is to learn from one trajectory, or set of trajectories information which will enhance the control performance for a new trajectory.

Implementation of Learning For the simulations, functions $\Theta(x) = \Theta(x_1, x_2)$ are represented as the sum of equal covariance gaussians centred on a sparse two-dimensional

grid in Γ_{x_1,x_2} space. In the learning-Q scheme; the weighting of the gaussians is updated to best fit the given data via least squares functional learning. The tailing off of the gaussians will ensure that trajectory information effectively spreads only to the neighbouring grid points with more weighting on the near neighbours.

3.4.1 Selection of Algorithm Parameters

The algorithm is given the positions and spread of the interpolation functions, as well as the shapes of the functions themselves. It then learns the weightings. Simulations are run to give baseline estimates of these variables.

Selection of Grid Points The state space of interest is selected to include the space spanned by the optimal trajectories. The gaussians are fixed initially at a four by four grid $of \gamma_i$ over a unit "box" region covering well the trajectory region to avoid distortions due to edge effects. A scaling method facilitates quick changes of the apparent denseness and compactness of the grid. Optimal placing of the grid points for one particular trajectory is not usually optimal for other trajectories, and the chosen grid points can be seen in Figure 3-2.

The spread of the interpolating function The interpolating function is of the form $W_0 e^{-n^2 d_i^2 k}$; where: n is the number of gaussians in each dimension, d is $||x - \gamma_i||^2$, W_0 is the initial weighting, and k is a constant used to tune the learning (in our simulations $W_0 = 10^{-10}, k = 4$). The "optimal" spread of the gaussian is a function of the shape of the function being learned, and the denseness of the gaussians in the grid.

Trajectory Selection The data must be "persistently" spanning the grid space in order to learn all the gaussian weights. As the estimates are functions of stochastic outputs, greater excitation of a mode allows for a more accurate estimate of the weighting of that mode. Five initial conditions have been chosen to illustrate performance enhancement due to the learning-Q approach. The initial conditions of x are : $(.5, 1)$, $(.5, .5)$, $(1, .5)$, $(0, .5)$, $(0, 1)$. The optimal regulation state trajectories calculated from these initial conditions are shown in Figure 3-2, to indicate the extent to which the state space Γ_x is covered in the learning process.

Run Number	Global Learning	Local Learning
5	0.3373	0.3422
10	0.3296	0.3355

Table 3.4.1: Error index for Global and Local Learning

3.4.2 Results

For the trajectories and algorithm parameters of the previous subsection, robustness and performance properties are examined.

1. Persistence of Excitation.

   In order to test the learning, two simulations were compared. In the first, denoted *Global Learning* Trajectories 1 through 5 were executed and then repeated, each time enhancing the learning with the knowledge previously learned. In the second , denoted *Local Learning* Trajectory 5 was repeated 10 times, to achieve enhanced learning. In the example of Table (1) below, the disturbance was $d = 0.2$.

   As can be seen in Table (1), the global learning actually gives marginally better results than the specialized local learning by virtue of its satisfying persistence of excitation requirements. These are typical of other simulations not reported here.

2. Deterministic Disturbances There are three types of disturbances simulated. First a zero disturbance is used, and since the plant then follows the optimal trajectory, as expected the values of δx and δu are zero. The other disturbances used are: a constant $\omega = .2$, stochastic disturbances, uniformly distributed , and disturbances where the disturbance is a function of position in state space.
   Since the error index is a function of the total level of input disturbances, the constant disturbance is the one used to compare various parameters and methods, with the stochastic and functional disturbances being then used to test the selected parameters under more realistic conditions.

3. Stochastic Disturbance

   The simulation is run for each trajectory with $d = RAND(-.5, .5)$, i.e. the disturbance is uniformly distributed with an upper bound of .5, and a lower bound of $-.5$. In the case of 'global learning ', where Trajectories 1 through 5 were run, then repeated for all of the trajectories, the algorithm gives an improvement in the error

Trajectory	Run 1	Run 2	% improvement
1	0.0157	0.0086	45%
2	0.0160	0.0070	56%
3	0.0637	0.0213	66%
4	0.0708	0.0123	83%
5	0.0113	0.0199	-5%

Table 3.4.2: Improvement after learning

index, except Trajectory 5. Details are summarized in Table 3.

4. Unmodelled Dynamics

The simulations were run with the disturbances as before, as well as with the inclusion of the unmodelled dynamics as in (3.4.3). The system achieved good control, with for example the error indices of Trajectories 1 through 5, then repeated in a stochastic disturbance case being $2.8, 0.9, 1.5, 1.1, 1.6$ and the second run giving $1.7, 1.0, 1.5, 1.1, 1.7$.

5. Nearest Neighbour Approximation and Grid Size

The standard algorithm requires $O(n^2)$ iterations for calculation of the values of an n by n grid. An approximation can be made where only the weights of the closest gaussians are updated at each step. This approximation significantly speeds the algorithm, but loses accuracy. As is shown in Table 5, for the case with a stochastic disturbance d = RAND(-.5,.5) as above, and with no unmodelled dynamics, however going to a finer grid of 5 by 5 gaussians, with the nearest neighbour approximation/truncation improves upon the 4 by 4 full calculation/untruncated case.

As expected, the finer grid improves in comparison to the others during the second run, as it is better able to fit to the information given. The Θ_1 surfaces generated in this simulation for the 2 by 2, 3 by 3, 4 by 4 and 5 by 5 cases for the constant disturbance $d = 0.2$ are shown in Figure 3-3. The error index averaged over the second run for these cases are respectively, .3204,.3252,.3465,.3230. The 4by4 case gave the worst result, possibly due to the artifact on the surface not displayed by

Average	4x4 truncated	4x4	5x5 truncated
Run 1	0.3970	0.3844	0.3828
Run 2	0.3458	0.3451	0.3304

Table 3.4.3: Comparison of grid sizes and approximations

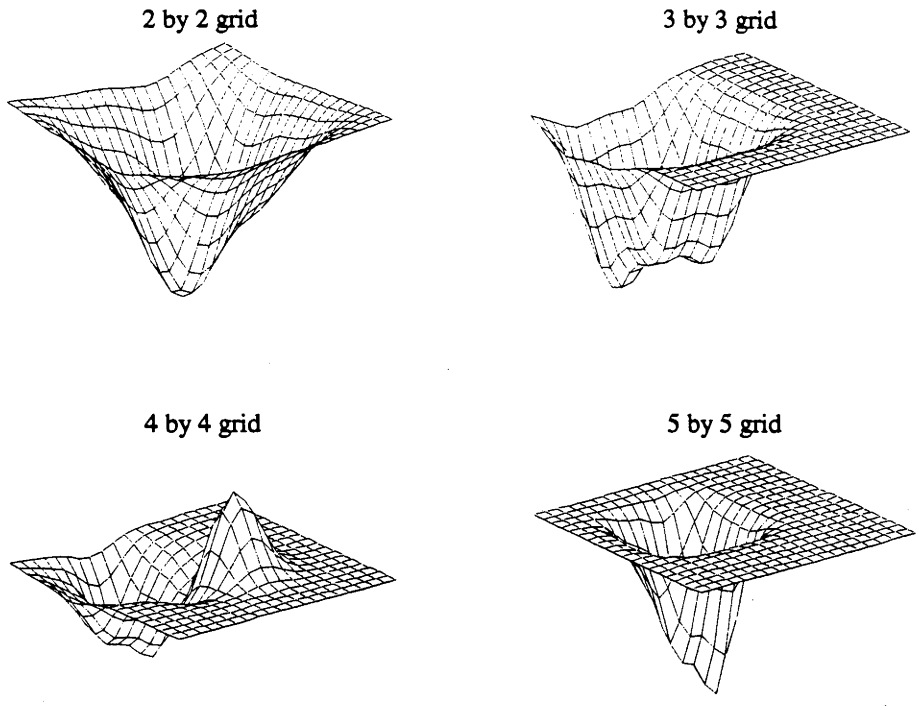

Figure 3-3: Comparison of Error surfaces learnt for various grid cases.

the others. These results show that a finer grid spacing may not always improve the control.

6. Comparison with Adaptive case

We compare the results of our learning controller with those of the straight adaptive controller as in Chapter 2. In the first instance, when running a trajectory for the first time, the adaptive algorithm gives better results than the learning algorithm. Allowing the learning algorithm previous experience on other trajectories however, lets it in most cases "beat" the adaptive one. For instance, in the non zero mean stochastic disturbance case $\{\omega \in .2 \pm .1\}$, with no unmodelled dynamics, for Trajectory 1, the adaptive case gave .4907, with the learning case giving .3671 after learning on some trajectories.

However, the adaptive case can also be enhanced to give better performance than the learning scheme by exploiting previous information, as born out by the following subsection. Simulations are performed comparing the extended adaptive to the learning scheme with a variety of disturbances and with/without unmodelled dynamics. The constant, stochastic, and non-constant deterministic disturbances were $d = .2$; $d \in 0.2 \pm .05$; $d = x_1^2 + x_2^2$. The results are summarised in Tables 3.4.4,3.4.5.

Disturbance	Learn	Adapt	% Improvement
constant	0.3651	0.2885	21%
stochastic	0.3684	0.2839	28%
deterministic	1.8846	1.1248	40%

Table 3.4.4: Error index averages without unmodelled dynamics

3.5 Conclusion

We have demonstrated that least squares functional learning can be successfully applied to the control of non linear plants when augmented with a plant linearization, in the case of stochastic or functional disturbances, and with unmodelled dynamics. However, as expected, the adaptive-Q scheme is more responsive to effects that are not state dependent. The learning-Q method with the interpolation functions on a 4 by 4 grid robustly controls our plant, but as expected, is surpassed by an adaptive scheme of Chapter 2, with "learning" enhancements. Work is currently being undertaken to improve the algorithm via truncation of the adaptation to those interpolation functions closest to the current region of interest to allow much finer grid spacings leading to further improvements in the control. The proposed learning algorithm has some computational advantages. The adaptive method must continually adapt on-line the parameters for good control. Here, once we have learned the "optimal" $Q(x)$ filter on a finite set of trajectories, we no longer need to adapt $Q(x)$, of course the on-line adaptive Q scheme of Chapter 2 can be applied in addition for further gains. The control is dependent on the accuracy of the of the functional learning, although there are clearly diminishing returns for increased resolution in the functional learning.

Disturbance	Learn	Adapt	% Improvement
constant	1.5044	0.9891	34%
stochastic	1.4925	0.9825	34%
deterministic	2.4608	2.0293	18%

Table 3.4.5: Error index averages with unmodelled dynamics

Chapter 4

Coprime Factorizations of State Dependent Systems

4.1 Introduction

Coprime factorization results for linear systems have proved powerful tools for characterizing the class of all stabilizing controllers for linear systems. Such characterizations have led to robust stabilization results and has set the stage for (robust) optimal controller design for linear systems [72], [17]. The challenge is to develop coprime factorization tools to cope with nonlinear systems.

The class of all stabilizing controllers for linear, continuous-time , time invariant systems have been characterized in terms of polynomial matrix function descriptions [77] and for discrete time using stable transfer function matrix fraction descriptions [40]. State space form matrix fraction (transfer function) descriptions were first developed in [45], so opening the way for working with time varying stable linear operators instead of transfer functions, see [63] and its references.

For nonlinear systems, a number of generalizations are available, building on the work of [22]. See also [47, 65, 71].

The less restrictive the assumptions on the nonlinearities, the less closely one can echo the linear results. Thus, at this stage there is incentive to work with restricted classes of nonlinear systems which commonly arise in practise, and yet allow a factorization theory to develop which goes some of the way to match in elegance and power the well established linear results.

It is desirable that nonlinear factorization and stabilization results are developed which

transparently specialize to the familiar results associated with state space descriptions for a linear system G as follows. Let us denote such linear systems

$$G: \begin{array}{rcl} \dot{x} &=& Ax + Bu \\ y &=& Cx + Du \end{array} : \left[\begin{array}{c|c} A & B \\ \hline C & D \end{array}\right] \tag{4.1.1}$$

where $x(t)$ is the state vector, $u(t)$ the input vector, and $y(t)$ the output vector. A useful class of such nonlinear generalizations are denoted

$$G(x_0): \begin{array}{rcl} \dot{x} &=& A(x)x + B(x)u \\ y &=& C(x)x + D(x)u \end{array} : \left[\begin{array}{c|c} A(x) & B(x) \\ \hline C(x) & D(x) \end{array}\right]_{x(0)} \tag{4.1.2}$$

initialized by $x(0) = x_0$.

Such systems can arise, for example, from linearization of more general nonlinear systems

$$\dot{x} = f(x,u); \quad y = h(x,u) \tag{4.1.3}$$

in the vicinity of a known trajectory x^*. Thus with $\delta x = x - x^*$

$$\delta\dot{x} = \frac{\partial f}{\partial x}|_x \delta x + \frac{\partial f}{\partial u}|_x \delta u + \cdots \tag{4.1.4}$$

$$\delta y = \frac{\partial h}{\partial x}|_x \delta x + \frac{\partial h}{\partial u}|_x \delta u + \cdots \tag{4.1.5}$$

Neglecting higher order terms, and setting $x = \delta x + x^*$, gives a nonlinear system of the form (4.1.2) with state δx, $A(\delta x) = \frac{\partial f}{\partial x}|_{x^*+\delta x}$, etc.

Work has been done to generate coprime factorizations of a class of systems which includes (4.1.2), the class

$$\dot{x} = f(x) + G(x)u \tag{4.1.6}$$

The existence of coprime right factorizations for systems in (4.1.6) is shown in [60] for the case when the smooth feedback stabilization problem is solvable for the system, and it follows that feedback linearizable systems admit such factorizations. Under the assumptions of stabilizability and detectability, [61] gives right coprime factorizations, and under the assumption of existence of controller and observer forms, [39] gives both right and left coprime factorizations.

In this chapter, working with nonlinear systems of the form of (4.1.2) under appropriate regularity conditions, we achieve matrix fraction descriptions in terms of an arbitrary stable system (parameter) . Then certain robust stabilization results from [47] are shown to be applicable to this case. All the results are presented in such a way that specialization for the case of linear systems is immediate. We generalize certain key linear results pertaining to cascading and inverting linear plants to this class and then use these results to create sets of right coprime and stable left factorizations for this sub-class which are pertinent in idealized nominal plant, stabilizing controller arrangements. For some of this work we need certain augmentation techniques. When used in conjunction with existing nonlinear theory, the resulting factorizations allow us to generate the class of all stabilizing (augmented) controllers for a given (augmented) nonlinear plant. Of course, it is trivial to dualize to the class of all (augmented) plants stabilized by a given (augmented) controller. We relate these back to our original unaugmented plant/controller systems, and explore some bounds of possible nonlinear stabilization/factorization theories of this type.

Section 2 generalizes the linear cascade and inverse operations, and also introduces right coprime factorizations for systems (4.1.2). It also sets up a general theorem proof methodology used in the rest of the Chapter. Section 3 specializes to the case where the state dependence is reconstructible from the output of the plant alone, giving right coprime and stable left factorizations as well as certain Bezout identities, at least for idealized nominal plant/controller arrangements. Section 4 includes the augmentation method to obtain further results for the stable left factorizations, and justifies this approach by proving that stability results for the augmented plant carry over to certain arrangements including the nominal plant. Then results from [47] and [48] are reviewed, and coupled with these factorizations lead to the controller class K_Q which stabilizes a given nominal plant. Also, stabilization results are quoted for an Yula-Kucera type parametrization of nonlinear plants, and this is used to extend the theory to the case of unequal initial conditions between the plant and controller. Section 5 presents simulation studies for the control of certain nonlinear plants. Conclusions are drawn in Section 6.

4.2 Nonlinear Factorizations

Nonlinear System Class The nominal plants, and controllers and derivative systems studied in this chapter, belong to a class of non-linear systems (operators)

$$G(\gamma, x_0): \begin{array}{rcl} \dot{x} &=& A(\gamma)x + B(\gamma)u, \quad x(0) = x_0 \\ y &=& C(\gamma)x + D(\gamma)u \end{array} : \left[\begin{array}{c|c} A(\gamma) & B(\gamma) \\ \hline C(\gamma) & D(\gamma) \end{array}\right]_{x(0)=x_0} \tag{4.2.1}$$

where, either γ = constant, $\gamma = t$, $\gamma = x(t)$, or indeed $\gamma = (x(t), t)$, although a number of our results exclude this latter time-varying case. Variations such as $\gamma = u(t)$ or $y(t)$, or more generally $\gamma = (u(t), x(t))$,or indeed causally filtered $x(t)$ or strictly causally filtered $y(t)$, denoted $x_w(t), y_w(t)$ can be handled in our technical approach, although for simplicity of presentation we work primarily with the cases $\gamma = x(t)$ and $\gamma = x_w(t)$. The partitioned matrix notation with an initial state subscript is a mild generalization of the common notation for the γ = constant case. The following assumption is crucial to certain results to follow:

Assumption The matrices $A(\gamma), B(\gamma)$,etc. are assumed to exist, and are bounded, for all finite γ, and are such that $x(.), y(.)$ of (4.2.1) exist for all $x(0)$, $t \geq 0$, and are unique. (4.2.2)

There exists a complete factorization stability theory for the cases γ = constant and $\gamma = t$ leading to a description of the class of all stabilizing controllers for the plant. Here we show that the nonlinear (time-varying) case when $\gamma = x(t)$, so that $G(\gamma, x_0)$ is G of (4.1.2), likewise, yields a "partial" theory along similar lines. We proceed by first considering in turn, the cascade of nonlinear systems as in (4.1.2) and the inverse, for the case when $D^{-1}(x)$ exists.

Cascade First consider the cascade of systems P_1, P_2 as in Figure 4-1 where each is of the form of (4.1.2). The state equations of the cascade P_2P_1 with input $u = u_1$ and output $y = y_2$ and state $x' = [x_1' \; x_2']$ are

$$\begin{array}{rcll} \dot{x}_1 = & A_1(x_1)x_1 + B_1(x_1)u_1 & , x_1(0) \\ \dot{x}_2 = & A_2(x_2)x_2 + B_2(x_2)y_1 & , x_2(0) \\ u_2 = y_1 = & C_1(x_1)x_1 + D_1(x_1)u_1 & \\ y_2 = & C_2(x_2)x_2 + D_2(x_2)y_1 & \end{array} \tag{4.2.3}$$

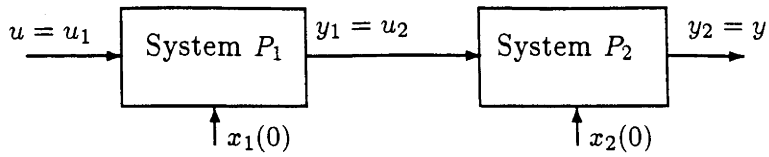

Figure 4-1: Cascade of System P_2 and System P_1

That is, in the partitioned matrix operator notation of (4.1.2), the following cascade relationship is established

$$\begin{aligned} P_2P_1 &= \left[\begin{array}{c|c} A_2(x_2) & B_2(x_2) \\ \hline C_2(x_2) & D_2(x_2) \end{array}\right]_{x_2(0)} \left[\begin{array}{c|c} A_1(x_1) & B_1(x_1) \\ \hline C_1(x_1) & D_1(x_1) \end{array}\right]_{x_1(0)} \\ &= \left[\begin{array}{cc|c} A_1(x_1) & 0 & B_1(x_1) \\ B_2(x_2)C_1(x_1) & A_2(x_2) & B_2(x_2)D_1(x_1) \\ \hline D_2(x_2)C_1(x_1) & C_2(x_2) & D_2(x_2)D_1(x_1) \end{array}\right]_{\substack{x_1(0) \\ x_2(0)}} \end{aligned} \tag{4.2.4}$$

Inverse Let us consider the following system $R(x_0)$ defined in terms of the system matrices (4.1.2) where $D^{-1}(x)$ exists for all x.

$$R(x_0) = \left[\begin{array}{c|c} A(x_R) - B(x_R)D^{-1}(x_R)C(x_R) & B(x_R)D^{-1}(x_R) \\ \hline -D^{-1}(x_R)C(x_R) & D^{-1}(x_R) \end{array}\right]_{x_R(0)=x_0} \tag{4.2.5}$$

Lemma 4.1 *Consider the system $G(x_0)$ of (4.1.2), where $D^{-1}(x)$ exists for all x and the associated system $R(x_0)$ of (4.2.5). Then for the cascade $G(x_0)R(x_0)$ and $R(x_0)G(x_0)$,*

$$x_R(t) = x(t) \quad \text{for all } t > 0 \tag{4.2.6}$$

where x_R denotes the state of the system $R(x_0)$ in each of the cascades. Moreover $R(x_0)$ is the inverse operator $G^{-1}(x_0)$ satisfying $G^{-1}(x_0)G(x_0) = G(x_0)G^{-1}(x_0) = I$, that is

$$R(x_0) = G^{-1}(x_0) \tag{4.2.7}$$

Proof. In the right inverse case, the state equations of the cascaded system $G(x_0)R(x_0)$ are derived from the cascade form (4.2.4) as,

$$G(x_0)R(x_0) = \left[\begin{array}{cc|c} A(x_R) - B(x_R)D^{-1}(x_R)C(x_R) & 0 & B(x_R)D^{-1}(x_R) \\ -B(x)D^{-1}(x_R)C(x_R) & A(x) & B(x)D^{-1}(x_R) \\ \hline -D(x)D^{-1}(x_R)C(x_R) & C(x) & D(x)D^{-1}(x_R) \end{array}\right]_{\substack{x_R(0)=x_0 \\ x(0)=x_0}} \tag{4.2.8}$$

Let us denote the input to the system as u, the output as y, and also define the output from $R(x_0)$ as y_R. Now, from (4.2.5) $y_R = D^{-1}(x_R)[u - C(x_R)x_R]$, then from (4.2.8),

$$\begin{aligned} \dot{x} &= A(x)x + B(x)y_R, \quad x_0 \\ \dot{x}_R &= A(x_R)x_R + B(x_R)y_R, \quad x_0 \\ y &= D(x_R)D^{-1}(x_R)[u - C(x_R)x_R] + C(x)x \end{aligned} \tag{4.2.9}$$

Thus in (4.2.9), x and x_R obey the same differential equation. Now under the solution uniqueness assumption (4.2.2) on the class of systems (4.1.2) of this section, and with $x(0) = x_R(0)$, then $x(t) = x_R(t)$ for all $t \geq 0$, and consequently, $A(x_R) \equiv A(x)$, etc. From (4.2.9) we then have $y = u$, giving $G(x_0)R(x_0) = I$ as required.

Another proof of this latter result is instructive. From (4.2.8) consider a co-ordinate basis change from state $[x'_R \; x']'$ to state $[x'_R \;\; (x' - x'_R)]'$, achieved by elementary row and column operators on the partitioned matrix (column two is added to column one, then the first row is subtracted from the second).

$$G(x_0)R(x_0) = \left[\begin{array}{ccc|c} A(x) - B(x)D^{-1}(x)C(x) & 0 & & B(x)D^{-1}(x) \\ 0 & A(x) & & 0 \\ \hline 0 & C(x) & & I \end{array}\right]_{\substack{x_R(0)=x_0 \\ [x(0)-x_R(0)]=0}} = I \tag{4.2.10}$$

The second equality follows from deletion of the unobservable mode x_R and the uncontrollable mode with zero initial condition $[x_R(t) - x(t)]$.

To demonstrate the left inverse case, first note from application of (4.2.4)

$$R(x_R(0))G(x_0) =$$

$$\left[\begin{array}{cc|c} A(x) & 0 & B(x) \\ B(x_R)D^{-1}(x_R)C(x) & A(x_R) - B(x_R)D^{-1}(x_R)C(x_R) & B(x_R)D^{-1}(x_R)D(x) \\ \hline D^{-1}(x_R)C(x) & -D^{-1}(x_R)C(x_R) & D^{-1}(x_R)D(x) \end{array}\right]_{\substack{x(0)=x_0 \\ x_R(0)=x_0}}$$

Also, defining $y_R \equiv C(x)x + D(x)u$, gives

$$\begin{aligned} \dot{x} &= [A(x) - B(x)D^{-1}(x)C(x)]x + [B(x)D^{-1}(x)]y_R \quad , x_0 \\ \dot{x}_R &= [A(x_R) - B(x_R)D^{-1}(x_R)C(x_R)]x_R + [B(x_R)D^{-1}(x_R)]y_R \quad , x_0 \end{aligned}$$

$$y = D^{-1}(x_R)[C(x)x - C(x_R)x_R] + D^{-1}(x_R)D(x) \tag{4.2.11}$$

Thus $x_R(t)$ and $x(t)$ obey the same differential equation and so by the uniqueness assumption (4.2.2), when $x_R(0) = x(0)$, then $x_R(t) = x(t)$ and $y = u$ for $t \geq 0$. Note also

$$R(x_0)G(x_0) = \left[\begin{array}{cc|c} A(x) & 0 & B(x) \\ 0 & A(x) & 0 \\ \hline 0 & -D^{-1}(x)C(x) & I \end{array}\right]_{\substack{x(0) \\ [x(0)-x_R(0)]=0}} = I \tag{4.2.12}$$

∎

Remarks :

1. The results of this lemma are critically dependent on the initial condition constraints $x_R(0) = x(0)$. It does not appear straightforward to give robustness conditions which would also achieve the limit $\lim_{t\to\infty}[x_R(t) - x(t)] = 0$ for unequal initial conditions, as in the well understood linear system case when $G(x), R(x_R)$ are both linear and asymptotically stable. Our approach will be to deal with initial condition mismatching along with unmodelled dynamics and external inputs/disturbances in subsequent sections.

2. In manipulations it is important to notice that for cascading P_1 and $(P_2 + P_3)$ then $P_1(P_2 + P_3) \neq P_1P_2 + P_1P_3$, in general, whereas of course for matrix multiplication $A(x)[B(x) + C(x)] = A(x)B(x) + A(x)C(x)$.

Nominal Plant and Stabilizing Controller For plants $G(x_0)$ Let us consider first a familiar state estimate feedback controller arrangement $K(\hat{x}_0)$ as, see also Figure 4-2(a), .

$$K(\hat{x}_0) = \left[\begin{array}{c|c} A(\hat{x}) + B(\hat{x})F(\hat{x}) + H(\hat{x})[C(\hat{x}) + D(\hat{x})F(\hat{x})] & -H(\hat{x}) \\ \hline F(\hat{x}) & 0 \end{array}\right]_{\hat{x}(0)=\hat{x}_0} \tag{4.2.13}$$

where $F(\hat{x})$ is the nonlinear state feedback gain, and $-H(\hat{x})$ is the nonlinear output injection in the estimator.

Of course, in the linear case, when $A(.), B(.), F(.)$ etc. are not state dependent, then $K(\hat{x}_0)$ stabilizes $G(\hat{x}_0)$ for arbitrary $\hat{x}_0, x_0$ when $\dot{\xi} = (A + BF)\xi$ and $\dot{\zeta} = (A + HC)\zeta$

are asymptotically stable. Moreover, the effects of initial conditions $\hat{x}_0 \neq x_0$ decay exponentially. Stabilizing F, H are readily found given the conditions $[A, B]$ completely controllable and $[A, C]$ completely observable.

In the nonlinear case studied here, let us first consider the nominal plant/controller pair $\{G(x_0)|_{x_0=\hat{x}_0}, K(\hat{x}_0)\}$. Also, in order to proceed with a theory that transparently specializes to familiar linear system results, let us restrict attention to the time invariant (nonlinear) system case and assume the following

Assumption The state estimate feedback gain $F(\xi)$, is constructed such that

$$\dot{\xi} = [A(\xi) + B(\xi)F(\xi)]\xi, \quad \xi(0) = \xi_0 \tag{4.2.14}$$

is exponentially stable for arbritary initial conditions ξ_0.

Of course, it is necessary that the pair $[A(.), B(.)]$ be appropriately controllable. Also, it should be noted that in the time-invariant case exponential stability is equivalent to bounded-input, bounded-output (BIBO) stability. Under assumption (4.2.14), it is clear that the feedback pair $\{G(x_0)|_{x_0=\hat{x}_0}, K(\hat{x}_0)\}$ has certain exponential stability properties by virtue of the following lemma.

Lemma 4.2 *Referring to (4.1.2), (4.2.13), consider the plant $G(x_0)|_{x_0=\hat{x}_0}$ with states $x(t)$, and a feedback controller $K(\hat{x}_0)$ with states $\hat{x}(t)$ as in Figure 4-2 (b). Then*

$$x(t) = \hat{x}(t) \text{ for all } t \geq 0 \tag{4.2.15}$$

Moreover, the states $x(t)$, of both plant and controller satisfy

$$\dot{x} = [A(x) + B(x)F(x)]x, \quad x(0) = x_0 \tag{4.2.16}$$

which is exponentially stable under (4.2.14)

Proof. Defining $u^* = -H(\hat{x})C(x)x - H(\hat{x})D(x)F(\hat{x})\hat{x}$, the relevant equations can be organized as

$$\begin{aligned} \dot{x} &= [A(x) + H(\hat{x})C(x)]x + B(x)u + u^* + H(\hat{x})D(x)F(\hat{x})\hat{x}, \quad x(0) = x_0 \\ \dot{\hat{x}} &= [A(\hat{x}) + H(\hat{x})C(\hat{x})]\hat{x} + B(\hat{x})u + u^* + H(\hat{x})D(\hat{x})F(\hat{x})\hat{x}, \quad \hat{x}(0) = x_0 \end{aligned} \tag{4.2.17}$$

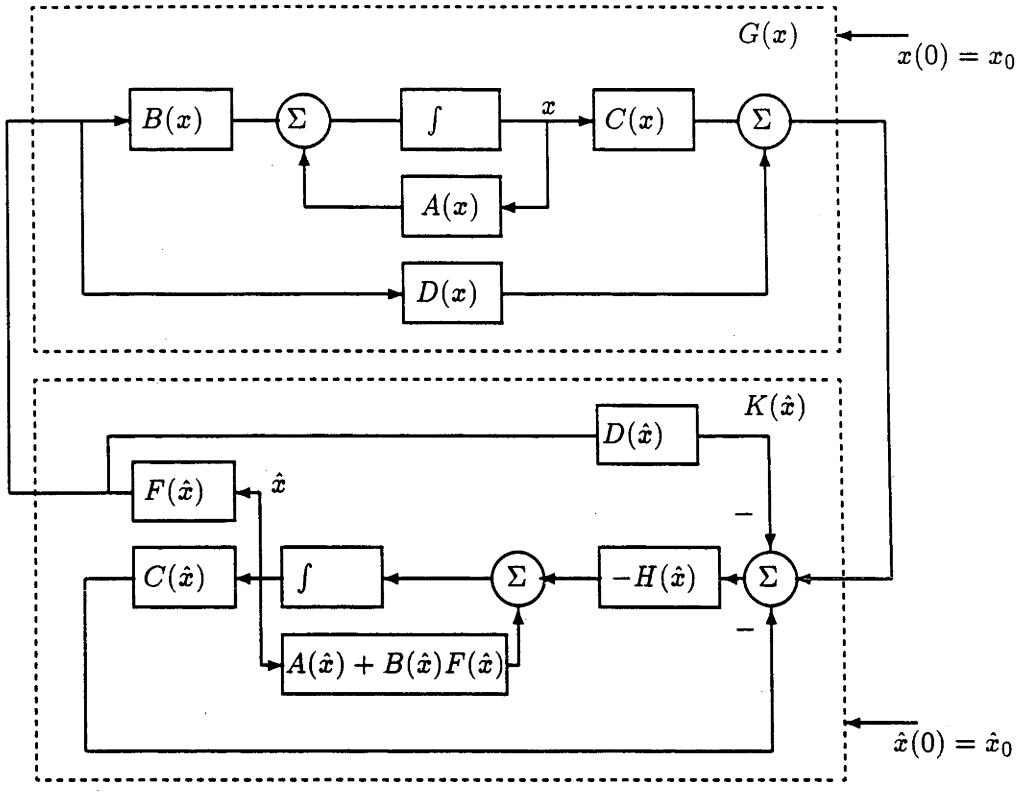

(a) Usual state estimate feedback arrangement.

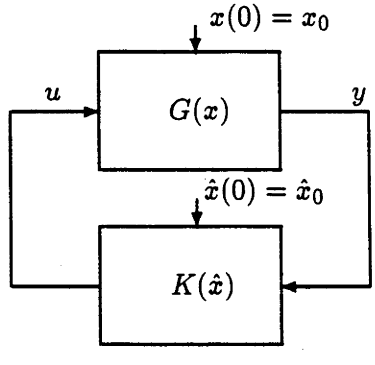

(b) Nominal plant $G(x_0)$ with controller $K(\hat{x}_0)$

Figure 4-2: Equivalent loops for the pair $\{G(\hat{x}), K(\hat{x})\}$.

Apply Assumption (4.2.2), then (4.2.15) holds as required. Also, given that $x(t) = \hat{x}(t)$, and since $u = F(\hat{x})\hat{x}$ then (4.2.17) becomes equivalent to (4.2.16) ∎

Remark The equations for $\delta x = x - \hat{x}$ appear instructive only in special cases, such as the linear case, when $\delta\dot{x} = (A + HC)\delta x$. Yet it is the stability of the δx equations, fed from the x state equation, along with the stability of (4.2.16), that determines the internal stability of the feedback system $\{G(x_0), K(\hat{x}_0)\}$, when $\hat{x}_0 \neq x_0$.

Right Coprime Factorization

Lemma 4.3 *Consider the nominal plant/controller arrangement of Figure 4-2 (b) with the definitions (4.1.2), (4.2.13), and stability Assumption (4.2.14). Define also the system with state* $\hat{x}(t)$

$$\begin{bmatrix} M(x_1(0)) & U(x_2(0)) \\ N(x_1(0)) & V(x_2(0)) \end{bmatrix} \equiv$$

$$\left[\begin{array}{cc|cc} A(x_1)+B(x_1)F(x_1) & 0 & B(x_1) & 0 \\ 0 & A(x_2)+B(x_2)F(x_2) & 0 & -H(x_2) \\ \hline F(x_1) & F(x_2) & I & 0 \\ C(x_1)+D(x_1)F(x_1) & C(x_2)+D(x_2)F(x_2) & D(x_1) & I \end{array}\right]_{\substack{x_1(0) \\ x_2(0)}} \tag{4.2.18}$$

Then stable right factorizations of the nominal plant $G(x_0)$ *and controller* $K(\hat{x}_0)$ *are given from*

$$G(x_0) = N(x_0)M^{-1}(x_0), \quad K(\hat{x}_0) = U(\hat{x}_0)V^{-1}(\hat{x}_0) \tag{4.2.19}$$

Moreover, internal stability of $\{G(x_0), K(\hat{x}_0)\}$ *is equivalent to the BIBO stability condition,*

$$\begin{bmatrix} I & -K(\hat{x}_0) \\ -G(x_0) & I \end{bmatrix}^{-1} \text{ BIBO stable} \Leftarrow \begin{bmatrix} M(x_0) & -U(\hat{x}_0) \\ -N(x_0) & V(\hat{x}_0) \end{bmatrix}^{-1} \text{ BIBO stable}$$

$$\begin{bmatrix} M(x_0) & -U(\hat{x}_0) \\ -N(x_0) & V(\hat{x}_0) \end{bmatrix}^{-1} \text{ BIBO stable} \Rightarrow \text{ the factorizations in (4.2.19) are right coprime}$$

Notation and Definitions: The definition (4.2.18) should be interpreted as

$$M(x_0) = \left[\begin{array}{c|c} A(x)+B(x)F(x) & B(x) \\ \hline F(x) & I \end{array}\right]_{x(0)}, \text{ and } U(\hat{x}_0) = \left[\begin{array}{c|c} A(\hat{x})+B(\hat{x})F(\hat{x}) & -H(\hat{x}) \\ \hline F(\hat{x}) & 0 \end{array}\right]_{\hat{x}(0)},$$

etc.

Given M, N, a right factorization of $G = NM^{-1}$, then M, N is a *right coprime* factorization of G iff for all unbounded inputs u, Mu or Nu is unbounded. (In the linear case this is the standard definition that N,M have no common zero in the right half plane). The pair $\{G, K\}$ here denotes the feedback system consisting of plant G and controller K as shown in Figure 4-2 (b). *Internal stability* of a feedback pair is defined as being BIBO stability for all possible additional inputs to the loop with outputs being the outputs of the systems in the feedback loop.

Proof. Defining x_M and x as the states of M and G respectively, then cascade $G(x_0)$ with $M(x_0)$,

$$G(x_0)M(x_0) = \left[\begin{array}{cc|c} A(x_M)+B(x_M)F(x_M) & 0 & B(x_M) \\ B(x)F(x_M) & A(x) & B(x) \\ \hline D(x)F(x_M) & C(x) & D(x) \end{array}\right]_{\substack{x_M(0)=x_0 \\ x(0)}} \tag{4.2.20}$$

From (4.2.20), and defining the output of the block M driven by u as $y_M \equiv u + F(x_M)x_M$, then

$$\begin{array}{rcll} \dot{x}_M & = & A(x_M)x_M + B(x_M)y_M; & x_M(0) = x_0 \\ \dot{x} & = & A(x)x + B(x)y_M; & x(0) = x_0 \end{array} \tag{4.2.21}$$

Now from (4.2.21) and under the uniqueness Assumption (4.2.2), we have $x_M(t) = x(t)$, $t \geq 0$, so that

$$G(x_0)M(x_0) = \left[\begin{array}{cc|c} A(x)+B(x)F(x) & 0 & B(x) \\ 0 & A(x)+B(x)F(x) & 0 \\ \hline C(x)+D(x)F(x) & C(x) & D(x) \end{array}\right]_{\substack{x(0) \\ x(0)-x(0)=0}} = N(x_0) \tag{4.2.22}$$

where the last equation follows from a co-ordinate basis change, and removal of uncontrollable and unobservable modes. Then right multiplication by $M^{-1}(x_0)$ gives $G(x_0) = N(x_0)M^{-1}(x_0)$ as required. Likewise the dual case for the controller factorization is established, and stability is given by the assumption (4.2.14). The coprimeness and stability conditions are Theorem 2.1 and Lemma 2.2 of [48]. ∎

Remarks

1. The second inverse in (4.2.20) can be written down from (4.2.18) via Lemma (4.1),but appears instructive only in special cases, such as the linear case when its stability is guaranteed by a H selection such that $\dot{\zeta} = (A + HC)\zeta$ is asymptotically stable. However this inverse cannot, in general, be factored as $\begin{bmatrix} \tilde{V}(x_v(0)) & \tilde{U}(x_u(0)) \\ \tilde{N}(x_n(0)) & \tilde{M}(x_m(0)) \end{bmatrix}$ where

$$G = \tilde{M}^{-1}(x_m(0))\tilde{N}(x_n(0)), \quad K = \tilde{V}^{-1}(x_v(0))\tilde{U}(x_u(0)) \tag{4.2.23}$$

as in the linear case since superposition does not hold for nonlinear systems. To see the difficulties, note that, omitting the initial conditions, then for all u_1, u_2

$$\begin{bmatrix} \tilde{V} & -\tilde{U} \\ -\tilde{N} & \tilde{M} \end{bmatrix} \begin{bmatrix} M & U \\ N & V \end{bmatrix} \begin{bmatrix} u_1 \\ u_2 \end{bmatrix} = \begin{bmatrix} \tilde{V}(Mu_1 + Uu_2) - \tilde{U}(Nu_1 + Vu_2) \\ -\tilde{N}(Mu_1 + Uu_2) + \tilde{M}(Nu_1 + Vu_2) \end{bmatrix} \begin{bmatrix} u_1 \\ u_2 \end{bmatrix}$$

$$\neq \begin{bmatrix} (\tilde{V}M - \tilde{U}N)u_1 + (\tilde{V}U - \tilde{U}V)u_2 \\ (\tilde{M}N - \tilde{N}M)u_1 + (\tilde{M}V - \tilde{N}U)u_2 \end{bmatrix} \Leftrightarrow \begin{bmatrix} \tilde{V}M - \tilde{U}N = I; & \tilde{V}U - \tilde{U}V = 0 \\ \tilde{M}N - \tilde{N}M = 0; & \tilde{M}V - \tilde{N}U = I \end{bmatrix}$$

Consequently, since $\tilde{M}N = \tilde{N}M, \tilde{V}U = \tilde{U}V$ by assumption, then both $\tilde{V}M - \tilde{U}N = I$ and $\tilde{M}V - \tilde{N}U = I$ can not be simultaneously satisfied in general.

2. To demonstrate why we cannot achieve the left factorizations (4.2.23) for our class of systems, in general, consider the cascade $K = \tilde{V}^{-1}\tilde{U}$, omitting the initial conditions. Now, in general, the state space matrices of $\tilde{U}$ are a function of the input to $\tilde{U}$. When this input can not be recovered (without differentiation) from the output of $\tilde{U}$, the generic case, then in the cascade $\tilde{V}^{-1}\tilde{U}$, the state space matrices of $\tilde{V}^{-1}$ do not have access to this input, and thus cannot, in general, equal those of the state space formulation of $\tilde{U}$. Consequently, there is not the possibility of the state space matrices of $\tilde{V}^{-1}$ tracking those of $\tilde{U}$. This situation is avoided in the next sections by guaranteeing via restrictions and or augmentations that the information needed to reconstruct the state dependence is always available to both members of a cascade.

Robustness Properties Thus far, the work in this section has dealt with the special case of equal initial conditions in the nominal plant and controller and no external disturbances. Such disturbances are dealt with in a later section by introducing certain dif-

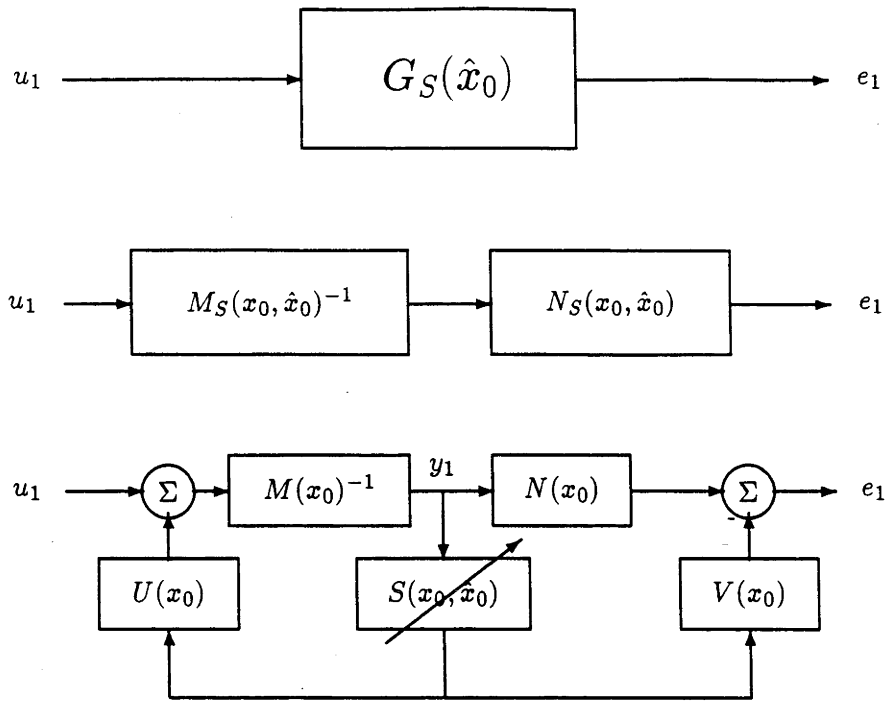

Figure 4-3: The system $G_S(x_0)$

ferential boundedness constraints. Let us now recall a lemma from [48] which we specialize and mildly extend to the class of systems (4.1.2), obeying assumptions (4.2.2),(4.2.14).

Theorem 4.1

[48] Consider a well-posed and stable system $\{G(x_0),K(x_0)\}$, *where* $G(x_0), K(x_0)$ *fall within the class (4.1.2), and the functions obey assumptions (4.2.2),(4.2.14). Then*

$$\begin{bmatrix} M(x_0) & -U(x_0) \\ -N(x_0) & V(x_0) \end{bmatrix}^{-1} \text{ exists and is internally stable.} \tag{4.2.24}$$

Consider also an arbitrary map, $S(x_0,\hat{x}_0)$ *within the class of systems (4.1.2). Then* $S(x_0,\hat{x}_0)$ *has a right factorization*

$$S(x_0,\hat{x}_0) = P_G(x_0,\hat{x}_0)D_G(x_0,\hat{x}_0)^{-1} \tag{4.2.25}$$

where the inverse is guaranteed to exist, and

$$\begin{bmatrix} D_G(x_0,\hat{x}_0) \\ P_G(x_0,\hat{x}_0) \end{bmatrix} = \begin{bmatrix} I \\ S(x_0,\hat{x}_0) \end{bmatrix} (M(x_0) - U(x_0)S(x_0,\hat{x}_0))^{-1} \tag{4.2.26}$$

$$M(x_0)D_G(x_0,\hat{x}_0) - U(x_0)P_G(x_0,\hat{x}_0) = I \tag{4.2.27}$$

Further there exists a plant $G_S(\hat{x}_0)$ as depicted in Figure 4-3 such that

$$\begin{aligned} G_S(\hat{x}_0) &= N(x_0)D_G(x_0,\hat{x}_0) - V(x_0)P_G(x_0,\hat{x}_0) \\ &= N_S(x_0,\hat{x}_0)M_S(x_0,\hat{x}_0)^{-1} \end{aligned} \tag{4.2.28}$$

where

$$N_S(x_0,\hat{x}_0) = N(x_0) - V(x_0)S(x_0,\hat{x}_0); \quad M_S(x_0,\hat{x}_0) = M(x_0) - U(x_0)S(x_0,\hat{x}_0) \tag{4.2.29}$$

Also, given an arbitrary plant $G_S(\hat{x}_0)$ in the class (4.1.2), then it can be parameterised in terms of $S(.)$ given by (4.2.25) where

$$\begin{bmatrix} D_G(x_0,\hat{x}_0) \\ P_G(x_0,\hat{x}_0) \end{bmatrix} = \begin{bmatrix} M(x_0) & -U(x_0) \\ -N(x_0) & V(x_0) \end{bmatrix}^{-1} \begin{bmatrix} I \\ -G_S(\hat{x}_0) \end{bmatrix} \tag{4.2.30}$$

$G_S(\hat{x}_0)$ has a right factorization (4.2.28), and again (4.2.25),(4.2.26),(4.2.27) hold.

Proof. Most of the proof follows as in [48]. It remains only to observe that with the definitions of the theorem holding, then the factor $(M(x_0) - U(x_0)S(x_0,\hat{x}_0))^{-1}$ will exist for any $S(x_0,\hat{x}_0)$, and to show that Figure 4-3 represents $G_S(x_0)$.

From the definitions in (4.2.18) and denoting by $*$ functions not relevant to the argument,

$$M(x_0) = \left[\begin{array}{c|c} * & * \\ \hline * & I \end{array}\right]; \quad U(x_0) = \left[\begin{array}{c|c} * & * \\ \hline * & 0 \end{array}\right]; \quad S(x_0,\hat{x}_0) = \left[\begin{array}{c|c} * & * \\ \hline * & * \end{array}\right]$$

Then by (4.2.4) we have

$$U(\hat{x}_0)S(x_0,\hat{x}_0) = \left[\begin{array}{c|c} * & * \\ \hline * & 0 \end{array}\right] \tag{4.2.31}$$

thus we can express

$$M(x_0) - U(x_0)S(x_0,\hat{x}_0) = \left[\begin{array}{c|c} * & * \\ \hline * & I \end{array}\right] \tag{4.2.32}$$

The equation (4.2.32) can be inverted by Lemma 4.1, since the 'D' function is the identity, which is trivially invertible.

From Figure 4-3 we have

$$y_1 = M(x_0)^{-1}(U(x_0)S(x_0,\hat{x}_0)y_1 + u_1) \tag{4.2.33}$$

$$e_1 = (N(x_0) - V(x_0)S(x_0,\hat{x}_0))y_1 \tag{4.2.34}$$

Then since it has been established that $M(x_0) - U(x_0)S(x_0,\hat{x}_0)$ is invertible, (4.2.33) can be reformulated in the form

$$y_1 = (M(x_0) - U(x_0)S(x_0,\hat{x}_0))^{-1}u_1 \tag{4.2.35}$$

Then combining (4.2.35) with (4.2.34) gives (4.2.28) as required. ∎

Corollary 4.1 *With the conditions of Theorem 4.1 holding then*

$$S(x_0,\hat{x}_0)\ \textit{BIBO stable} \Leftrightarrow N_S(x_0,\hat{x}_0), M_S(x_0,\hat{x}_0)\textit{coprime} \tag{4.2.36}$$

Proof. We can express $N_S(x_0,\hat{x}_0), M_S(x_0,\hat{x}_0)$ in the form

$$\begin{bmatrix} I \\ S(x_0,\hat{x}_0) \end{bmatrix} = \begin{bmatrix} M(x_0) & -U(x_0) \\ -N(x_0) & V(x_0) \end{bmatrix}^{-1} \begin{bmatrix} M_S(x_0,\hat{x}_0) \\ -N_S(x_0,\hat{x}_0) \end{bmatrix} \tag{4.2.37}$$

($\Rightarrow$)

The stability property (4.2.24), and the above equation (4.2.37) give $N_S(x_0,\hat{x}_0), M_S(x_0,\hat{x}_0)$ BIBO stable. From above, and pre-multiplying by [1 0] we have the Bezout

$$I = \begin{bmatrix} I & 0 \end{bmatrix} \begin{bmatrix} M(x_0) & -U(x_0) \\ -N(x_0) & V(x_0) \end{bmatrix}^{-1} \begin{bmatrix} M_s(x_0) \\ N_s(x_0) \end{bmatrix} \tag{4.2.38}$$

The stability property (4.2.24) also guarantees stability of the matrix $\begin{bmatrix} I & 0 \end{bmatrix} \begin{bmatrix} M(x_0) & -U(x_0) \\ -N(x_0) & V(x_0) \end{bmatrix}^{-1}$, and consequently we have $M_s(x_0,\hat{x}_0), N_S(x_0,\hat{x}_0)$ coprime by Lemma 2.1 of [48].

($\Leftarrow$)

If $N_s(x_0,\hat{x}_0), M_s(x_0,\hat{x}_0)$ are coprime then they are stable, and (4.2.37) gives $S(x_0,\hat{x}_0)$ BIBO stable. ∎

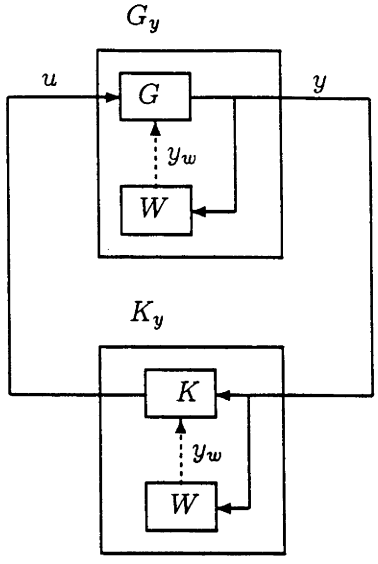

Figure 4-4: The Feedback System $\{G_y, K_y\}$

Remarks:

1. We have reached a major objective of this section, namely to achieve a right factorization for the feedback pair $\{G_S(\hat{x}_0), K(x_0)\}$ in terms of a factorization of the pairs $\{G(x_0), K(x_0)\}$. An interesting special case is when $G_S(\hat{x}_0) = G(\hat{x}_0)$. This case represents a nominal plant, but with initial conditions not necessarily equal to those of the controller.

2. It is not possible to generate a complete robustness theory based only on the material in this section. To facilitate the robustness theory , in the following sections we restrict the class of plant and controller or work with augmentations forms, then achieve stabilization results for these situations. For the case of augmentations, results are generated which relate back to the standard plants and controllers.

4.3 Systems with output dependent nonlinearities

In the previous section, the systems considered had *state* dependent nonlinearities. Of course, a mild generalization would have permitted filtered state dependent nonlinearities. Here we specialize to *output* dependent nonlinearities to achieve a more complete factorization theory, including stable left factorizations, and Bezout identities. To avoid any algebraic loop that might arise in an implementation of $y = C(y)x + D(y)u$, and to widen the class of systems, we introduce a strictly causal filter on y giving y_w, so that $y = C(y_w)x + D(y_w)u$. We foreshadow that to achieve our objectives of stable left fac-

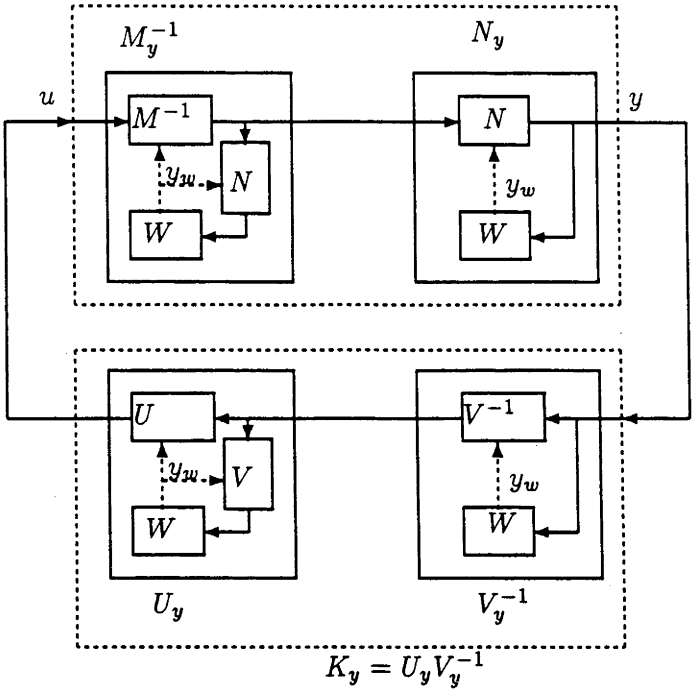

Figure 4-5: The Feedback System $\{N_y M_y^{-1}, U_y V_y^{-1}\}$

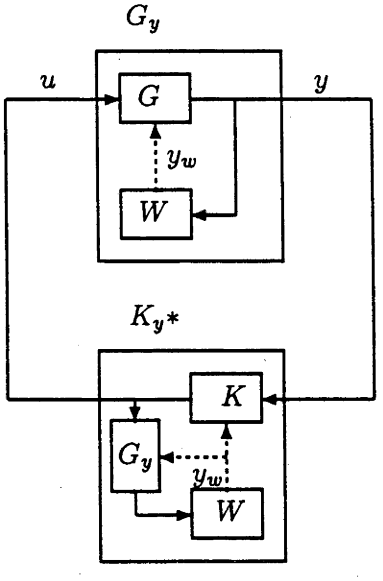

Figure 4-6: The Feedback System $\{G_y, K_y^*\}$

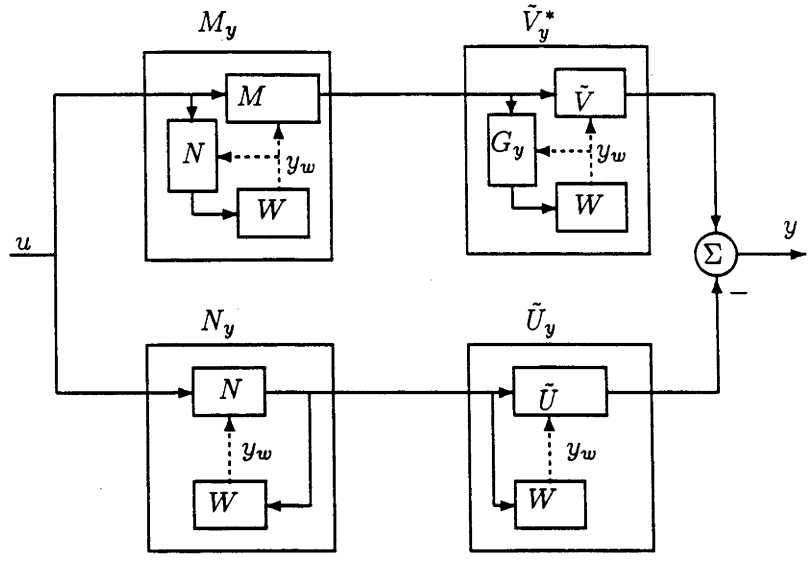

Figure 4-7: The Bezout $\tilde{V}_y^* M_y - \tilde{U}_y N_y = I$

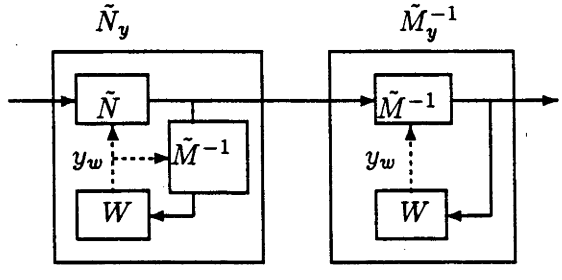

Figure 4-8: $G_y = \tilde{M}_y^{-1} \tilde{N}_y$

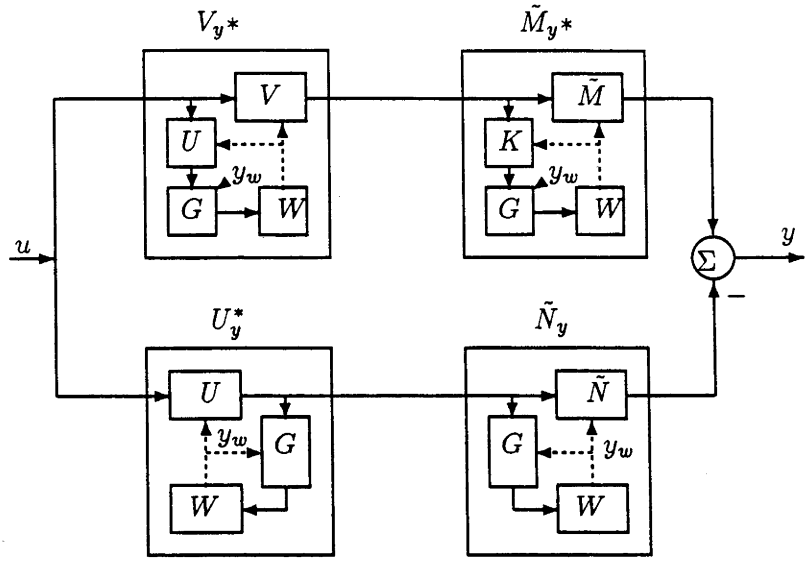

Figure 4-9: The Bezout $\tilde{M}_y^* V_y^* - \tilde{N}_y U_y^* = I$

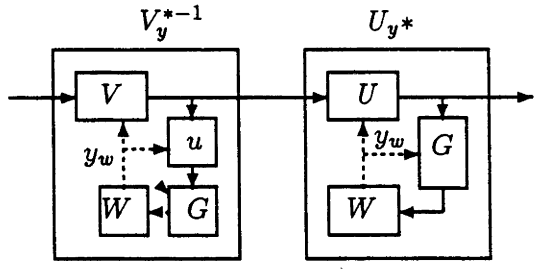

Figure 4-10: $K_y^* = U_y^* V_y^{*-1}$

torization, not only do we need the restrictions introduced so far on initial conditions and output nonlinearities, but also we need to work with plant/controller nominal models that only make sense in a feedback arrangement.

We proceed by considering the plant/controller arrangement as depicted in Figure 4-4. More precisely, let us define a plant as follows.

$$G_y(x_0): \begin{array}{lcll} \dot{x} & = & A(y_w)x + B(y_w)u; & x(0) = x_0 \\ \dot{x}_w & = & A_w x_w + B_w y; & x_w(0) \\ y & = & C(y_w)x + D(y_w)u & \\ y_w & = & C_w x_w & \end{array} \quad : \quad \left[\begin{array}{c|c} A(y_w) & B(y_w) \\ \hline C(y_w) & D(y_w) \end{array}\right]_{x(0)}^{W(y)} \tag{4.3.1}$$

Here y_w is the output of a filter W driven by y where

$$W: \quad \left[\begin{array}{c|c} A_w & B_w \\ \hline C_w & 0 \end{array}\right]_{x_w(0)} \tag{4.3.2}$$

Of course, any member of (4.3.1) with states $[x' \;\; x_w']'$ is a specialization of the more general class of nonlinear systems (4.2.1).

Note also that when the inverse of the nonlinear system exists, as when $D^{-1}(x)$ exists, then W can be taken to have the state tracking properties of this inverse (requiring generalization of A_w to $A_w(y_w)$ and B_w to $B_w(y_w)$). Now setting $C_w = I$ makes y_w equivalent to the state of the inverse system which is x itself.

The feedback controller $K_y : u \rightarrow y$ is likewise more precisely defined as

$$K_y(x_0) \quad : \quad \left[\begin{array}{c|c} A(y_w) + B(y_w)F(y_w) + H(y_w)[C(y_w) + D(y_w)F(y_w)] & -H(y_w) \\ \hline F(y_w) & 0 \end{array}\right]_{\hat{x}(0)=\hat{x}_0}^{W(u)} \tag{4.3.3}$$

We claim below right factorizations of G_y, K_y, as depicted in Figures 4-5, 4-7,4-8,4-9,4-10 , where the operator notation can be interpreted in state space terms in the following example for N_y.

$$N_y \quad : \quad \left[\begin{array}{cc|c} A(y_w) + B(y_w)F(y_w) & 0 & B(y_w) \\ B_w(y_w)[C(y_w) + D(y_w)F(y_w)] & A_w(y_w) & B_w(y_w)D(y_w) \\ \hline C(y_w) + D(y_w)F(y_w) & 0 & D(y_w) \end{array}\right]_{\substack{x(0)=x_0 \\ x_w(0)}}$$

$$y_w \quad = \quad \text{Causal Filtered version of } C_w(y_w)x_w \tag{4.3.4}$$

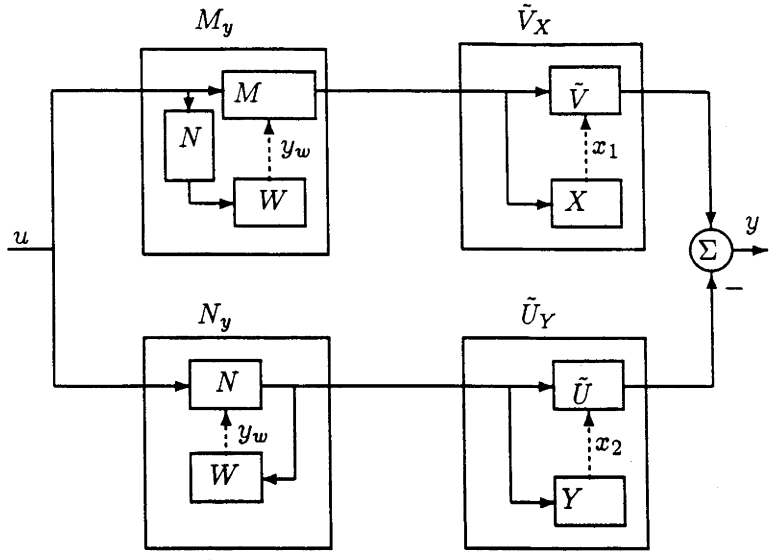

Figure 4-11: The Bezout $\tilde{V}_X M_y - \tilde{U}_Y N_y = I$

Likewise, the definitions allow state space definitions for other operators V_y, U_y, M_y etc depicted in Figures 4-5 - 4-10 can be formulated, and the left fractional descriptions for $\tilde{M}_y^*, \tilde{M}_y, \tilde{N}_y, \tilde{V}_y^*, \tilde{U}_y$ can be generated from the linear versions as in [63] with the appropriate state dependence added as in Figures 4-5 - 4-10. Note that the pair $\{G_y, K_y\}$ here denotes the feedback system consisting of plant G_y and controller K_y as shown in Figure 4-4.

An important lemma connecting right coprimeness and a Bezout identity is

Lemma 4.4 *[47] Consider a right factorization of the plant G, as in (4.4.4). Then if there exists a BIBO stable pair $\tilde{V}$ and $\tilde{U}$ such that*

$$\tilde{V}M - \tilde{U}N = Z, \ \textit{unimodular} \tag{4.3.5}$$

then NM^{-1} is a right coprime factorization for G.

With this lemma in mind, we proceed.

Lemma 4.5 *Consider the system G_y, K_y, K_y^* and assorted factors $M_y, N_y, \tilde{M}_y^*, \tilde{M}_y, \tilde{N}_y, \tilde{V}_y^*$, U_y^*, V_y^*, U_y, V_y as depicted in Figures 4-5 - 4-12, and define $G_y^* = \tilde{M}_y^{*-1}\tilde{N}_y$. Then the following factorizations and Bezout equations hold, as illustrated in the Figures 4-5 - 4-12.*

$$G_y = N_y M_y^{-1}; \quad K_y^* = U_y^* V_y^{*-1}; \quad K_y = U_y V_y^{-1} \tag{4.3.6}$$

$$\tilde{V}_y^* M_y - \tilde{U}_y N_y = I, \quad \tilde{M}_y^* V_y^* - \tilde{N}_y U_y^* = I \tag{4.3.7}$$

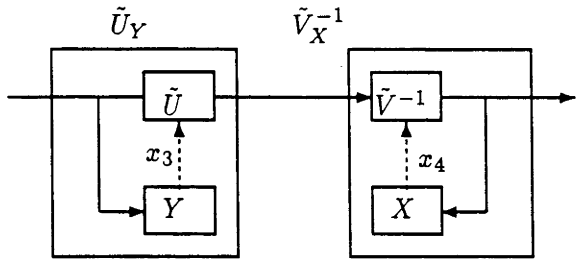

Figure 4-12: The system $\tilde{V}_X^{-1}\tilde{U}_Y = K$

Moreover the feedback systems in (4.3.8) will have identical state and input/output responses given identical initial conditions.

$$\text{The trajectories of } \{G_y(x_0), K_y(\hat{x}_0)\}, \{G_y(x_0), K_y^*(\hat{x}_0)\}, \{G_y^*(x_0), K_y(\hat{x}_0)\},$$
$$\{G_y^*(x_0), K_y^*(\hat{x}_0)\} \text{ are identical, when } \hat{x}(0) = x(0). \tag{4.3.8}$$

Moreover, with BIBO stability of the factors in the Bezout identities (4.3.7),the factorizations $G_y = N_y M_y^{-1}$ and $K_y^* = U_y^* V_y^{*-1}$ are coprime.

Proof. First note that each of these equations collapses in the linear case when all the state space matrices are invariant of y_w to the well known linear equations as in [63]. The equations of (4.3.7) are represented in Figures 4-9, 4-11. Note that for each of the systems W, the input is identically Nu. Thus, given equal initial conditions, the outputs of the W blocks ,y_w, which are fed into the other systems are also identical, and consequently the matrix blocks $A(y_w), B(y_w), \ldots$ are identical for all the systems. This behaviours of the nonlinear systems along a y_w trajectory is identical to that of linear time-varying systems with $A(y_w)$ etc. replaced by $A(t) = A(y_w(t))$. Then the result simply follows from a direct application of the linear time-varying theory as in [63]. The proof of the other relationships are all similar, each hinging on the fact that the outputs y_w are identical under the conditions of the lemma, along with application of the linear theory.

The coprimeness result follows directly from Lemma (4.4). Of course, more complete line-by-line proofs along the lines of that of Lemma (4.7) can also be generated. ∎

Remarks

1. In the linear case, $K_y = K_y^* = \tilde{V}_y^{*-1}\tilde{U}_y^*$ and $G_y = G_y^* = \tilde{M}_y^{*-1}\tilde{N}_y$. The starred factors are here introduced only to facilitate the Bezout identities (4.3.7) and thereby

to establish the coprimeness properties. Of interest in its own right is the property (4.3.8). It is possible to directly establish coprimeness of the factorization $G_y = \tilde{M}_y^{-1}\tilde{N}_y$, but this does not give rise to a Bezout identity, in general. Also in the linear case, the BIBO stability of factors is guaranteed with $\dot{\zeta} = (A+BF)\zeta$ asymptotically stable.

2. To ensure BIBO stability of the factors in the nonlinear case, it makes sense to examine the following assumption:

Assumption The state estimate feedback gain $F(y_w)$, and the state output injection $H(y_w)$ are constructed such that

$\dot{\xi} = [A(y_w) + B(y_w)F(y_w)]\xi, \quad \xi(0)$

$\dot{\zeta} = [A(y_w) + H(y_w)C(y_w)]\zeta, \quad \zeta(0)$

are exponentially stable for arbitrary initital conditions $\xi(0), \zeta(0)$, for any admissible trajectory y_w. (4.3.9)

We don't claim here that such an assumption can be satisfied, except possibly for a limited set of trajectories y_w,or even that a complete theory can be based on this assumption.

3. Factors such as $\tilde{V}_y^*$ are introduced in the lemma since it is not possible ,in general, to find a $\tilde{V}_y$ such that $K_y = \tilde{V}_y^{-1}\tilde{U}_y$ and also $\tilde{V}_y M_y - \tilde{U}_y N_y = I$, at least with the factors being obvious generalizations of the linear ones where the matrices $A(.), B(.)$, etc. are all functions of the one variable, viz. y_w.

4. A further limitation of the nonlinear theory is evident from Figure 4-11,4-12, as now explained. Let us express $K = \tilde{V}_X^{-1}\tilde{U}_Y$ as in Figure 4-12, where X and Y are filters generating the variables x_i for $i = 1,2,3,4$ which feed into the relevant state space matrices $A(.), B(.)$, etc. In order for $\tilde{V}_X^{-1}\tilde{U}_Y$ of Figure 4-12 to generalize the linear results using the methodology of this chapter, we require $x_3 = x_4$. But, from Figure 4-12,

$$Y = X\tilde{V}_X^{-1}\tilde{U}_Y = XK \Leftrightarrow \{x_3 = x_4\} \tag{4.3.10}$$

Similarly, for the Bezout $\tilde{V}_X M_y - \tilde{U}_Y N_y = I$ to hold as required in Figure 4-11, using

our methodology we require $x_1 = x_2$. But from Figure 4-11

$$XM_y = YN_y \Leftrightarrow X = YG \Leftrightarrow \{x_1 = x_2\} \tag{4.3.11}$$

Combining (4.3.10) and (4.3.11) we have

$$\{x_1 = x_2\} \text{ and } \{x_3 = x_4\} \Rightarrow X = XKG \tag{4.3.12}$$

and since in a well posed system $KG \neq I$, then in the nonlinear case where $X \neq 0$ we cannot achieve simultaneously, $\tilde{V}_X M_y - \tilde{U}_Y N_y = I, \tilde{V}_X^{-1}\tilde{U}_Y = K$ for any $X, Y \neq 0$, at least in our "linear" approach. Dual arguments can be constructed to justify the need for working with other starred versions $K^* = U_y^* V_y^{*-1}$, etc.

4.4 Augmented Systems Factorizations

As shown in the previous section, it appears difficult to construct left factorizations associated with the nominal plant/controller pair $\{G(\hat{x}_0), K(\hat{x}_0)\}$ without certain modifications and restrictions. In order to proceed in this section, we propose an alternative "trick" of first obtaining factorizations and stability results for an augmented feedback pair $\{\mathcal{G}(\hat{x}_0), \mathcal{K}(\hat{x}_0)\}$, and thereby achieve stability results of a related pair $\{G(x_0), \overline{\mathcal{K}}(\hat{x}_0)\}$ trivially different from the original feedback pair $\{G(x_0), K(\hat{x}_0)\}$. Thus in the first instance, consider the feedback pair $\{G(x_0), K(x_0)\}$ of Figure 4-2, re-organised as the pair $\{G(x_0), \overline{\mathcal{K}}(\hat{x}_0)\}$. Where

$$G(x_0) = \left[\begin{array}{c|c} A(x) & B(x) \\ \hline C(x) & D(x) \end{array}\right]_{x(0)=x_0} \quad ; \quad \overline{\mathcal{K}}(\hat{x}_0) =$$

$$\left[\begin{array}{cc|c} A(x_g) + B(x_g)F(x_g) + H(x_g)(C(x_g) + D(x_g)F(x_g)) & 0 & -H(x_g) \\ B(x_g)F(x_g) & A(x_g) & 0 \\ \hline F(x_g) & 0 & 0 \end{array}\right]_{\begin{bmatrix} \hat{x}(0)=\hat{x}_0 \\ x_g(0)=\hat{x}_0 \end{bmatrix}} \tag{4.4.1}$$

The situation is depicted in shorthand notation in Figure 4-13. Clearly, without external inputs and with $x_0 = \hat{x}_0$, then the pair $\{G(\hat{x}_0), \overline{\mathcal{K}}(\hat{x}_0)\}$ behaves as $\{G(\hat{x}_0), K(\hat{x}_0)\}$ in terms of states and system inputs and outputs. Consider now the further re-organization

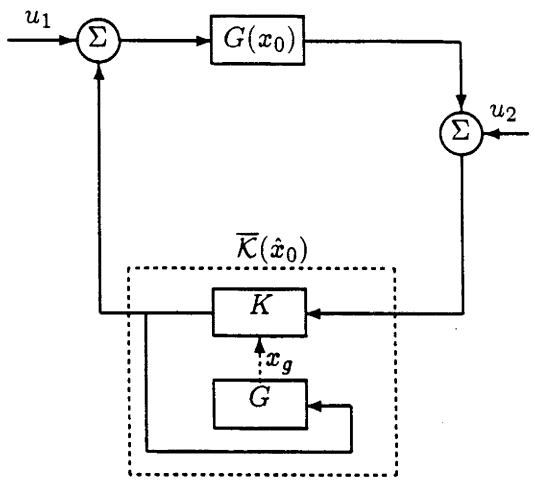

Figure 4-13: The system $\{G(x_0), \overline{\mathcal{K}}(\hat{x}_0)\}$

of $\{G(x_0), \overline{\mathcal{K}}(\hat{x}_0)\}$ as an augmented pair $\{\mathcal{G}(x_0), \mathcal{K}(x_0)\}$, depicted in Figure 4-14 where

$$\mathcal{G}(x_0) = \begin{bmatrix} G(x_0) \\ I \end{bmatrix}; \quad \mathcal{K}(\hat{x}_0) =$$

$$\left[\begin{array}{cc|cc} A(x_g)+B(x_g)F(x_g)+H(x_g)(C(x_g)+D(x_g)F(x_g)) & 0 & -H(x_g) & 0 \\ 0 & A(x_g) & 0 & B(x_g) \\ \hline F(x_g) & 0 & 0 & 0 \end{array}\right]_{\begin{bmatrix} \hat{x}(0)=\hat{x}_0 \\ x_g(0)=\hat{x}_0 \end{bmatrix}} \tag{4.4.2}$$

Again, in the absence of external inputs the states of the pair $\{G(x_0), \overline{\mathcal{K}}(\hat{x}_0)\}$ are identical to those of $\{\mathcal{G}(x_0), \mathcal{K}(\hat{x}_0)\}$. In order to proceed, we recall a stability definition

Definition The system $\{G(x_0), K(\hat{x}_0)\}$ is said to be ϵ_1, ϵ_2 bounded-input stable, iff for all inputs u_1, u_2 such that $|u_1| \leq \epsilon_1, |u_2| \leq \epsilon_2$ the outputs y_1, y_2 and e_1, e_2 are bounded.

Lemma 4.6 *With $\mathcal{G}(x_0), \mathcal{K}(\hat{x}_0), \overline{\mathcal{K}}(\hat{x}_0)$ defined in (4.4.1),(4.4.2) , and given positive constants $\epsilon_1, \epsilon_2, \epsilon_3$ then*

$$\{\mathcal{G}(x_0), \mathcal{K}(\hat{x}_0)\} \text{ is } \epsilon_1, \begin{bmatrix} \epsilon_2 \\ \epsilon_3 \end{bmatrix} \text{ bounded-input stable} \quad \Rightarrow \quad \{G(x_0), \overline{\mathcal{K}}(\hat{x}_0)\} \text{ is } \min(\epsilon_1, \epsilon_3), \epsilon_2 \text{ bounded-input stable} \tag{4.4.3}$$

Proof. From Figures 4-13,4-14 it is immediate that the feedback loop of $\{G(x_0), \overline{\mathcal{K}}(\hat{x}_0)\}$ of Figure 4-13 is simply a specialization of the feedback loop $\{\mathcal{G}(x_0), \mathcal{K}(\hat{x}_0)\}$ shown in Figure 4-14 taking $u_3 = -u_1$. Now define ϵ_{min} as $\min(\epsilon_1, \epsilon_3)$, then we have that $\{\mathcal{G}(x_0), \mathcal{K}(\hat{x}_0)\}$ is

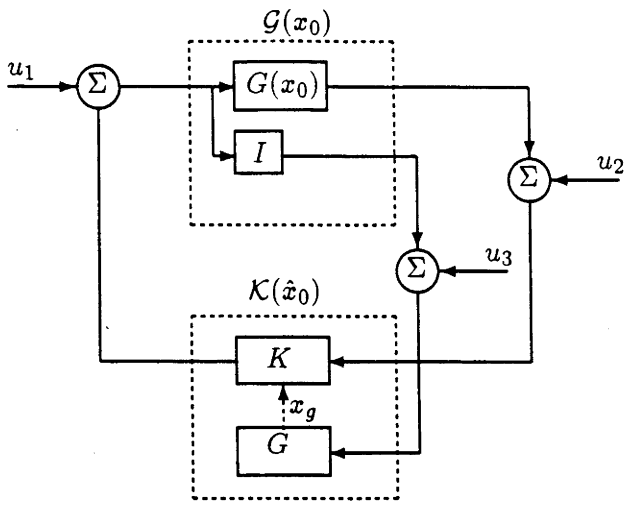

Figure 4-14: The system $\{\mathcal{G}(x_0), \mathcal{K}(\hat{x}_0)\}$

$\epsilon_{min}, \begin{bmatrix} \epsilon_2 \\ \epsilon_{min} \end{bmatrix}$ bounded-input stable. Thus it is stable for any input signals $\epsilon_a, \begin{bmatrix} \epsilon_b \\ -\epsilon_a \end{bmatrix}$ where $\epsilon_a \leq \epsilon_{min}; \epsilon_b \leq \epsilon_2$. The system $\mathcal{G}(x_0), \mathcal{K}(\hat{x}_0)$ with input $\epsilon_a, \begin{bmatrix} \epsilon_b \\ -\epsilon_a \end{bmatrix}$ is trivially equivalent to the system $G(x_0), \overline{\mathcal{K}}(\hat{x}_0)$ with input ϵ_a, ϵ_b, thus the stability property carries over to this case giving (4.4.3). ∎

Remark: This lemma tells us that developing a factorization and robust stability theory associated with $\{\mathcal{G}(x_0), \mathcal{K}(\hat{x}_0)\}$ gives corresponding stability properties for $\{G(x_0), \overline{\mathcal{K}}(\hat{x}_0)\}$ which in turn can be considered as an idealized nominal version of the pair $\{G(x_0), K(\hat{x}_0)\}$. Any differences between the nominal and actual controller can be taken into account in the same way as differences between the nominal plant and actual plant.

We propose factorizations as follows:

$$\mathcal{G}(x_0) = \tilde{\mathcal{M}}^{-1}(x_0)\tilde{\mathcal{N}}(x_0) \quad = \mathcal{N}(x_0)\mathcal{M}^{-1}(x_0); \qquad \mathcal{K}(x_0) = \tilde{\mathcal{V}}^{-1}(x_0)\tilde{\mathcal{U}}(x_0) \tag{4.4.4}$$

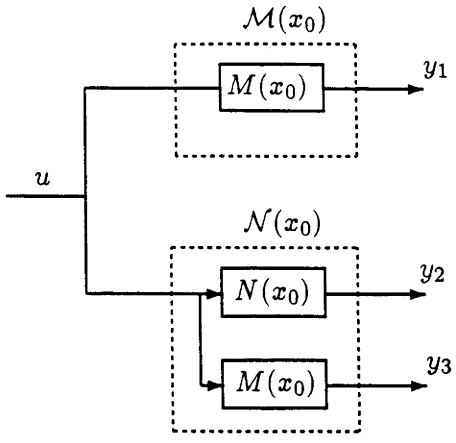

Figure 4-15: The block $[\mathcal{M}'(x_0)\ \mathcal{N}'(x_0)]'$

where

$$\begin{bmatrix} \mathcal{M}(x_0) \\ \mathcal{N}(x_0) \end{bmatrix} = \left[\begin{array}{c|c} A(x)+B(x)F(x) & B(x) \\ \hline F(x) & I \\ \begin{bmatrix} C(x)+D(x)F(x) \\ F(x) \end{bmatrix} & \begin{bmatrix} D(x) \\ I \end{bmatrix} \end{array}\right]_{[x(0)=x_0]} \tag{4.4.5}$$

This situation is depicted in the sub blocks $\mathcal{N}(x_0), \mathcal{M}(x_0)$ of Figure 4-15 where $N(x_0)$, $M(x_0)$ are defined in (4.2.18). Likewise, we propose

$$\begin{bmatrix} \tilde{\mathcal{V}}(x_0) \\ \tilde{\mathcal{N}}(x_0) \end{bmatrix} = \left[\begin{array}{cc|c} A(x) & 0 & B(x) \\ 0 & A(x)+H(x)C(x) & B(x)+H(x)D(x) \\ \hline 0 & -F(x) & I \\ \begin{bmatrix} 0 & C(x) \\ 0 & 0 \end{bmatrix} & & \begin{bmatrix} D(x) \\ I \end{bmatrix} \end{array}\right]_{\begin{bmatrix} x(0)=x_0 \\ x_2(0)=x_0/2 \end{bmatrix}} \tag{4.4.6}$$

and

$$\begin{bmatrix} \tilde{\mathcal{U}}(x_0) \\ \tilde{\mathcal{M}}(x_0) \end{bmatrix} = \left[\begin{array}{cc|cc} A(x) & 0 & 0 & B(x) \\ 0 & A(x)+H(x)C(x) & -H(x) & 0 \\ \hline 0 & F(x) & 0 & 0 \\ \begin{bmatrix} 0 & -C(x) \\ 0 & 0 \end{bmatrix} & & \begin{bmatrix} I & 0 \\ 0 & I \end{bmatrix} & \end{array}\right]_{\begin{bmatrix} x(0)=x_0 \\ x_2(0)=x_0/2 \end{bmatrix}} \tag{4.4.7}$$

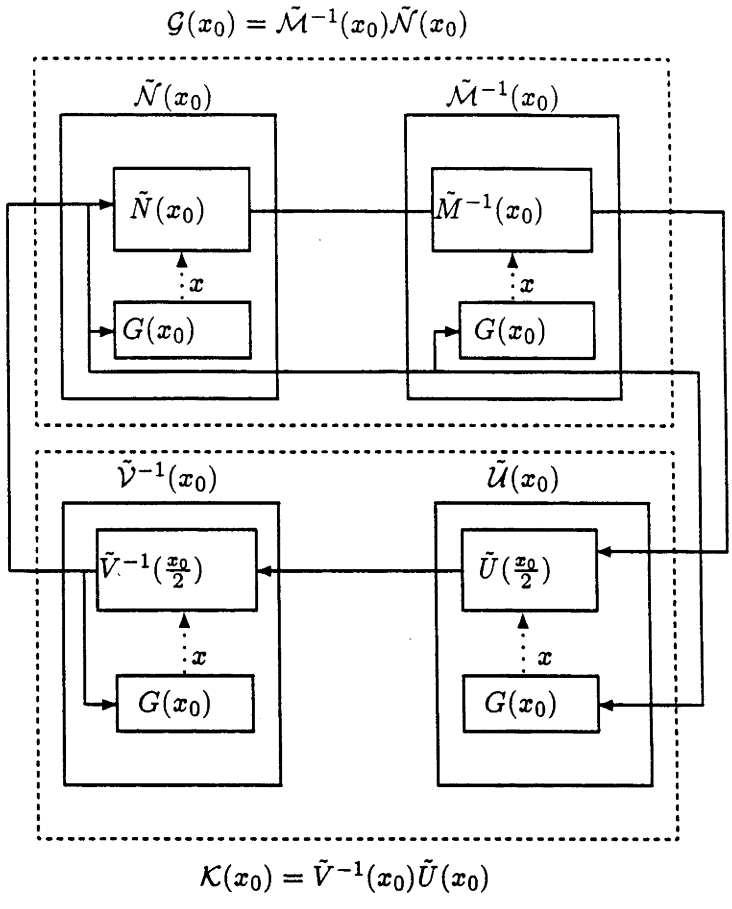

Figure 4-16: The feedback system $\{\mathcal{G}(x_0), \mathcal{K}(x_0)\}$ in factor form.

The feedback system $\{\mathcal{G}(x_0), \mathcal{K}(x_0)\}$, with the above left factorizations is shown in Figures 4-16,4-17. To ensure (BIBO) stability of these left factorizations, we impose (4.2.14) and its "dual", viz.

Assumption The state output injection $H(\xi)$, is constructed such that the system

$$\dot{\xi} = A(\xi)\xi; \qquad \xi(0) = \xi_0$$

$$\dot{\zeta} = [A(\xi) + H(\xi)C(\xi)]\zeta; \quad \zeta(0) = \zeta_0$$

has an exponentially decaying partial state ζ (4.4.8)

Remark:

Note that in the systems $\tilde{\mathcal{N}}, \tilde{\mathcal{V}}, \tilde{\mathcal{M}}, \tilde{\mathcal{U}}, \mathcal{M}, \mathcal{N}$, the matrices $A(.), B(.), \ldots$ are all functions of x which is the state of the nominal plant $G(x_0)$ driven by the inputs to $\mathcal{N}, \tilde{\mathcal{V}}$ etc, respectively. In the systems $\tilde{\mathcal{M}}, \tilde{\mathcal{U}}$ the matrices are functions of the state of a nominal

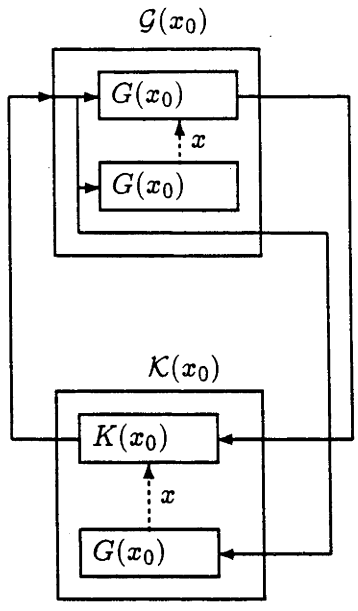

Figure 4-17: The feedback system $\{\mathcal{G}(x_0), \mathcal{K}(x_0)\}$ in simplified form.

plant $G(x_0)$ driven by the "augmented" input to $\tilde{M}, \tilde{U}$, respectively. This can be seen from Figures 4-16,4-17.

Lemma 4.7 *Consider the system $\mathcal{G}(x_0), \mathcal{K}(x_0)$ as defined in (4.4.2). Then, (4.4.4) holds with the definitions (4.4.5)-(4.4.7). Moreover, under the assumptions (4.2.2),(4.2.14), (4.4.8), the factors are BIBO stable and $\mathcal{M}, \mathcal{N}$ are right coprime satisfying the Bezout identity*

$$\tilde{\mathcal{V}}(x_0)\mathcal{M}(x_0) - \tilde{\mathcal{U}}(x_0)\mathcal{N}(x_0) = I \tag{4.4.9}$$

Proof.

$$\begin{aligned}
\mathcal{G}(x_0)\mathcal{M}(x_0) &= \left[\begin{array}{c|c} A(x) & B(x) \\ \hline C(x) & D(x) \\ 0 & I \end{array}\right]_{[x(0)=x_0]} \left[\begin{array}{c|c} A(x_1)+B(x_1)F(x_1) & B(x_1) \\ \hline F(x_1) & I \end{array}\right]_{[x_1(0)=x(0)]} \\
&= \left[\begin{array}{cc|c} A(x_1)+B(x_1)F(x_1) & 0 & B(x_1) \\ B(x)F(x_1) & A(x) & B(x) \\ \hline D(x)F(x_1) & C(x) & D(x) \\ F(x_1) & 0 & I \end{array}\right]_{\left[\begin{smallmatrix} x_1(0)=x_0 \\ x(0)=x_0 \end{smallmatrix}\right]} \\
&= \mathcal{N}(x_0)
\end{aligned} \tag{4.4.10}$$

The equalities follow since by the uniqueness Assumption (4.2.2), with initial conditions

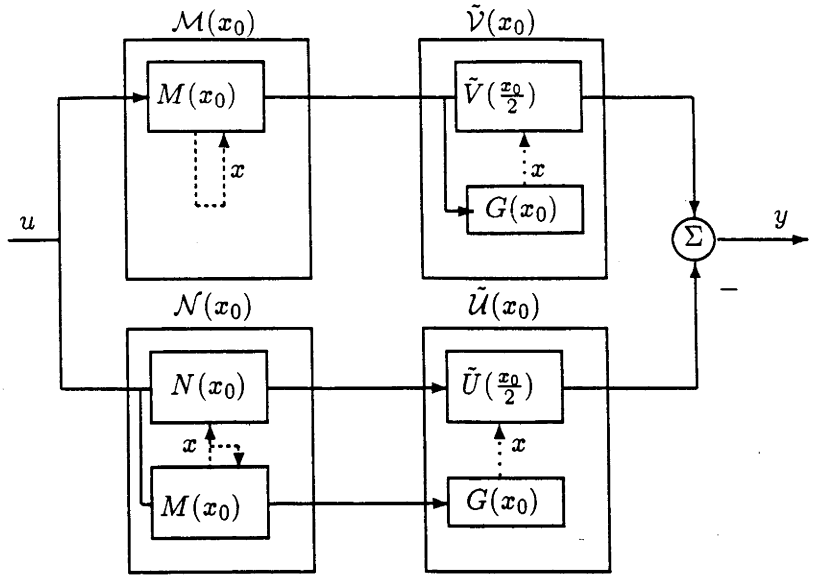

Figure 4-18: The Bezout $\tilde{\mathcal{V}}(x_0)\mathcal{M}(x_0) - \tilde{\mathcal{U}}(x_0)\mathcal{N}(x_0) = I$

$x_1(0) = x_0$, then $x_1(t) = x(t) \forall t \geq 0$. The second equality is simply the removal of an unobservable mode. Since $\mathcal{M}^{-1}(x_0)$ exists via Lemma (4.1), then $\mathcal{G}(x_0) = \mathcal{N}(x_0)\mathcal{M}^{-1}(x_0)$ as in (4.4.4) The proofs of the remaining factorizations of (4.4.4) are similar.

To prove the coprimeness of $M(x_0), N(x_0)$ we first verify (4.4.9). Now

$$\tilde{\mathcal{V}}(x_0)\mathcal{M}(x_0) - \tilde{\mathcal{U}}(x_0)\mathcal{N}(x_0)$$

$$= \left[\begin{array}{ccc|c} A(x_2)+B(x_2)F(x_2) & 0 & 0 & B(x_2) \\ B(x)F(x_2) & A(x) & 0 & B(x) \\ B(x)F(x_2)+H(x)D(x)F(x_2) & 0 & A(x)+H(x)C(x) & B(x)+H(x)D(x) \\ \hline F(x) & 0 & -F(x) & I \end{array}\right] \left[\begin{array}{c} x_2(0)=x_0 \\ x(0)=x_0 \\ x_1(0)=\frac{x_0}{2} \end{array}\right]$$

$$- \left[\begin{array}{ccc|c} A(x_3)+B(x_3)F(x_3) & 0 & 0 & B(x_3) \\ B(x_4)F(x_4) & A(x_4) & 0 & B(x_4) \\ -H(x_4)C(x_3)-H(x_4)D(x_3)F(x_3) & 0 & A(x_4)+H(x_4)C(x_4) & -H(x_4)D(x_4) \\ \hline 0 & 0 & F(x_2) & 0 \end{array}\right] \left[\begin{array}{c} x_3(0)=x_0 \\ x_4(0)=x_0 \\ x_5(0)=\frac{x_0}{2} \end{array}\right]$$

where x, x_1 are the states of $\tilde{\mathcal{V}}$, x_2 of $\mathcal{M}$, x_3 of $\mathcal{N}$, and x_4, x_5 of $\tilde{\mathcal{U}}$. Now, both systems operators on the R.H.S. of the above equation will have the same inputs. Thus applying the uniqueness Assumption (4.2.2) (as in the Lemma 4.2 proof) we have that the partial

states satisfy $\begin{bmatrix} x_2(t) \\ x(t) \end{bmatrix} = \begin{bmatrix} x_3(t) \\ x_4(t) \end{bmatrix} \forall t \geq 0$ and thus $A(x_2) \equiv A(x_3)$, etc. Moreover, by applying the uniqueness Assumption (4.2.2) to the state equations for x_2 and x, then it is clear that $x_2(t) = x(t) \forall t \geq 0$, so that $x(t) = x_2(t) = x_3(t) = x_4(t)$. So denoting $A \equiv A(x) \equiv ...$, then after a co-ordinate basis change and deletion of unobservable and uncontrollable modes, we have

$$\tilde{\mathcal{V}}(x_0)\mathcal{M}(x_0) - \tilde{\mathcal{U}}(x_0)\mathcal{N}(x_0) = \left[\begin{array}{cc|c} A+BF & 0 & B \\ BF+HDF & A+HC & B+HD \\ \hline F & -F & I \end{array}\right]_{\begin{bmatrix} x(0)=x_0 \\ x_1(0)=x_0/2 \end{bmatrix}}$$

$$- \left[\begin{array}{cc|c} A+BF & 0 & B \\ -(HC+HDF) & A+HC & -HD \\ \hline 0 & F & 0 \end{array}\right]_{\begin{bmatrix} x(0)=x_0 \\ x_5(0)=x_0/2 \end{bmatrix}} \tag{4.4.11}$$

Then a co-ordinate basis change $\begin{bmatrix} x \\ x_5 \end{bmatrix} \rightarrow \begin{bmatrix} x \\ x - x_5 \end{bmatrix}$ and the resulting subtractions gives the required result (4.4.9).

In fact, a study of Figure 4-18 and knowledge of linear system results allows a shortcut to the proofs. The key is to realize first that the subblocks $N(x_0), M(x_0), G(x_0)$ with their inputs depicted in the figure all have the same state $x(t)$ by virtue of Assumption (4.2.2) and manipulations such as in the proof of Lemma 4.2, and consequently that the coefficients $A(.)$, etc. in N, M, U, V are all functions of the same state x. The initial state requirements on the various subblocks are identical to those for linear systems to avoid any transients in achieving $y = u$.

From (4.4.10),(4.4.11), Assumption (4.4.8) and Lemma (4.4), we have that $\mathcal{M}(x_0)$, $\mathcal{N}(x_0)$ are co-prime giving the coprime factorization of $\mathcal{G}(x_0) = \mathcal{N}(x_0)\mathcal{M}^{-1}(x_0)$ of (4.4.4). For the left factorization case, the proof of is similar to that of the right case. ∎

Lemma 4.8 *Given the BIBO stable systems $\mathcal{R}(x_0), \mathcal{S}(x_0)$ as defined in Figure 4-21,*

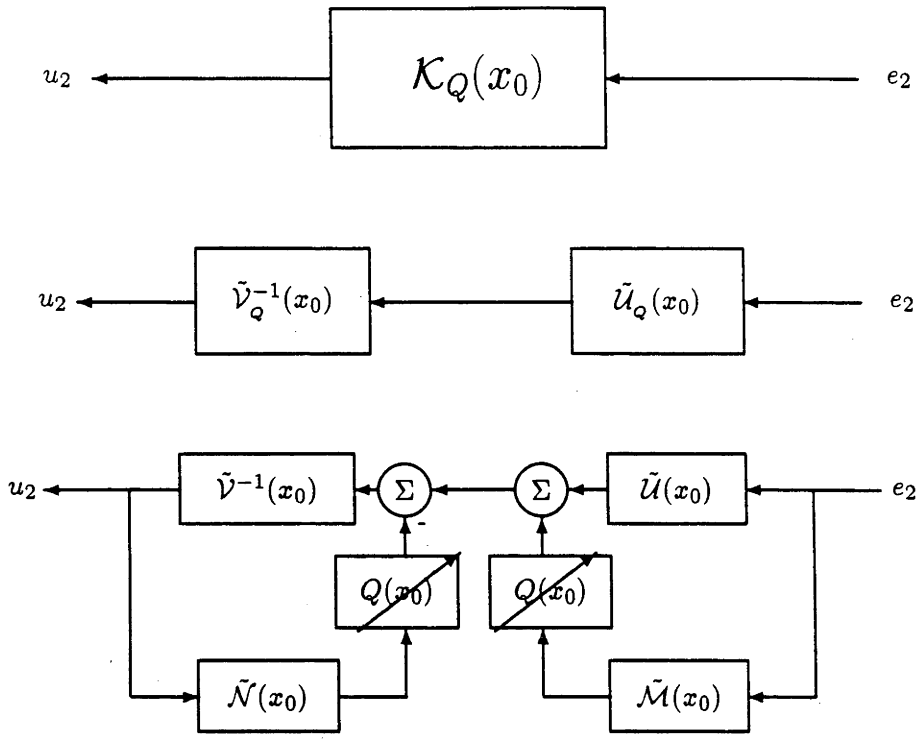

Figure 4-19: The class $\mathcal{K}_Q$

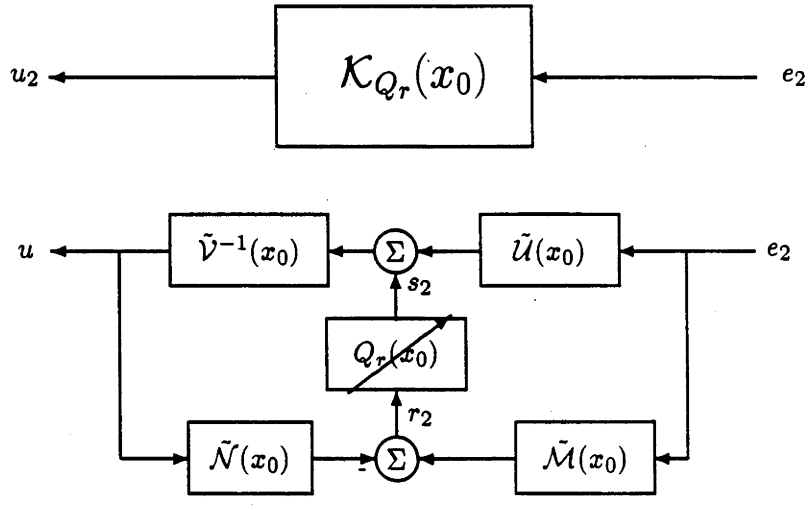

Figure 4-20: The class $\mathcal{K}_{Q_r}$

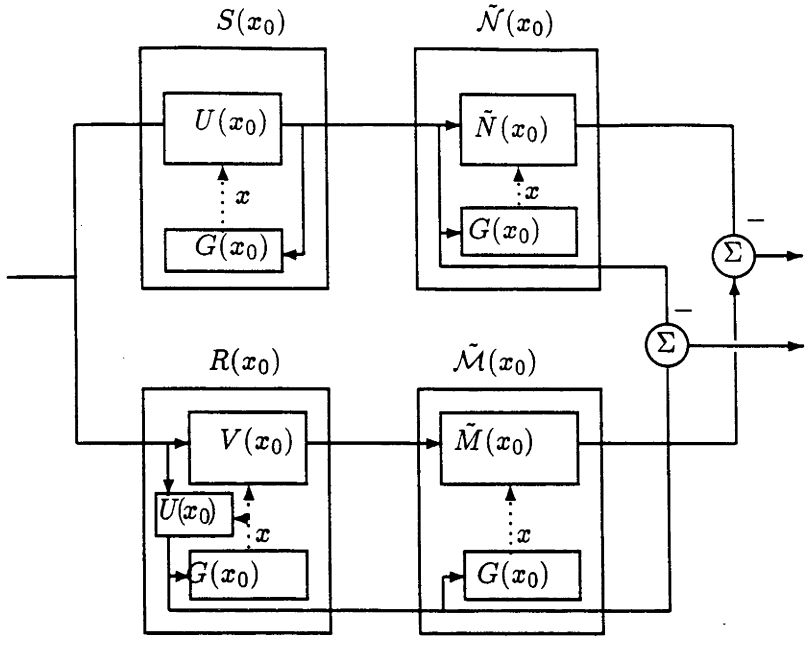

Figure 4-21: The Bezout $\tilde{\mathcal{M}}R - \tilde{\mathcal{N}}S = [I\ 0]'$

and $\tilde{\mathcal{M}}(x_0), \tilde{\mathcal{N}}(x_0)$ *as defined in (4.4.6), (4.4.7), then*

$$\tilde{\mathcal{M}}(x_0)\mathcal{R}(x_0) - \tilde{\mathcal{N}}(x_0)\mathcal{S}(x_0) = \begin{bmatrix} I \\ 0 \end{bmatrix} \tag{4.4.12}$$

Proof. The proof follows from the definitions of the factors in Figure 4-21, and the uniqueness and stability assumptions (4.2.2),(4.2.14), (4.4.8), and the fact that in the linear case $\tilde{M}V - \tilde{N}U = I$. ∎

Remark: In the linear case left coprimeness of $\tilde{M}, \tilde{N}$ follows from the Bezout $\tilde{M}R - \tilde{N}S = I$, since $\tilde{M}, \tilde{N}, R, S$ are BIBO stable. In the augmented nonlinear case, $\tilde{\mathcal{M}}' = [I\ 0]\tilde{\mathcal{M}}$, and $\tilde{\mathcal{N}}' = [I\ 0]\tilde{\mathcal{N}}$ satisfy $\tilde{\mathcal{M}}'(x_0)\mathcal{R}(x_0) - \tilde{\mathcal{N}}'(x_0)\mathcal{S}(x_0) = I$ from (4.4.12) which could be taken as an analogue of left coprimeness for $\tilde{\mathcal{M}}', \tilde{\mathcal{N}}'$. Actually, in the remainder of this chapter, we restrict to stability theory of [47] which does not require left coprimeness of factors $\tilde{\mathcal{M}}, \tilde{\mathcal{N}}$ (or even $\tilde{\mathcal{M}}', \tilde{\mathcal{N}}'$), at least in the proof of the results.

Construction of the class of all stabilizing controllers for a nominal plant

Lemma 4.7 shows that the factorizations (4.4.5)-(4.4.7) have the properties:

$$G(x_0) = \mathcal{N}(x_0)\mathcal{M}^{-1}(x_0) = \tilde{\mathcal{M}}^{-1}(x_0)\tilde{\mathcal{N}}(x_0) \text{ with the factorizations stable.} \tag{4.4.13}$$

$$\mathcal{N}, \mathcal{M} \text{ are right co-prime, and } \tilde{\mathcal{N}}, \tilde{\mathcal{M}} \text{ obey (4.4.12)} \tag{4.4.14}$$

$\tilde{\mathcal{V}}(x_0), \tilde{\mathcal{U}}(x_0)$ are defined such that a Bezout identity (4.3.5) holds. (4.4.15)

In order to establish that the system $\{\mathcal{G}(x_0), \mathcal{K}(x_0)\}$ is robust to small signal injections around the loop we utilize a differential boundedness condition from [22] and exploit results in [47]. **Definition:** a mapping F is said to be *differentially bounded by* θ_F, ε_F iff for all signals a_1, a_2 if $\mid a_1 - a_2 \mid < \varepsilon_F$ then $\mid Fa_1 - Fa_2 \mid < \theta_F$.

Assumptions (4.2.2),(4.4.8) give (BIBO) stability of the left factors of $\mathcal{G}(x_0), \mathcal{K}(x_0)$, and we make further restrictions on the matrices $A(.), B(.), ..., H(.), F(.)$ such that the following property holds:

$\tilde{\mathcal{M}}, \tilde{\mathcal{N}}, \tilde{\mathcal{V}}, \tilde{\mathcal{U}}$ are differentially bounded by $\theta_M, \epsilon_U; \theta_N, \epsilon_V; \theta_V, \epsilon_V; \theta_U, \epsilon_U$ respectively. (4.4.16)

Also, we define Q to be a (BIBO) stable mapping constrained such that

$Q\tilde{\mathcal{N}}$ is differentially bounded by θ_{QN}, ϵ_V, and $Q\tilde{\mathcal{M}}$ is differentially bounded by θ_{QM}, ϵ_U (4.4.17)

Remark: It is beyond the scope of this chapter to give explicit conditions on the matrices $A(.), B(.), ...$ so that conditions (4.4.16),(4.4.17) hold. In the linear case they will hold due to assumptions (4.2.2),(4.2.14), (4.4.8).

Then following [65] let us parametrize

$$\mathcal{K}_Q(x_0) = \tilde{\mathcal{V}}_Q^{-1}(x_0)\tilde{\mathcal{U}}_Q(x_0); \;\; \tilde{\mathcal{V}}_Q(x_0) = \tilde{\mathcal{V}}(x_0) + Q(x_0)\tilde{\mathcal{N}}(x_0); \;\; \tilde{\mathcal{U}}_Q(x_0) = \tilde{\mathcal{U}}(x_0) + Q(x_0)\tilde{\mathcal{M}}(x_0) \tag{4.4.18}$$

and using these parametrizations, we apply a crucial lemma for the stability of the system:

Lemma 4.9 *[47] Consider the augmented plant $\mathcal{G}(x_0)$ and augmented controller $\mathcal{K}(x_0)$ as defined in (4.4.2), with right coprime and stable left factorizations of $\mathcal{G}(x_0)$, and a stable left factorization of $\mathcal{K}(x_0)$ as in (4.4.4), and with the properties (4.4.13)-(4.4.17) and the Bezout (4.4.9) holding. Then*

1. *The system $\{\mathcal{G}(x_0), \mathcal{K}_Q(x_0)\}$, with $\mathcal{K}_Q(x_0)$ defined in (4.4.18), and illustrated in Figure (4-19), will be ϵ_V, ϵ_u bounded-input stable.*

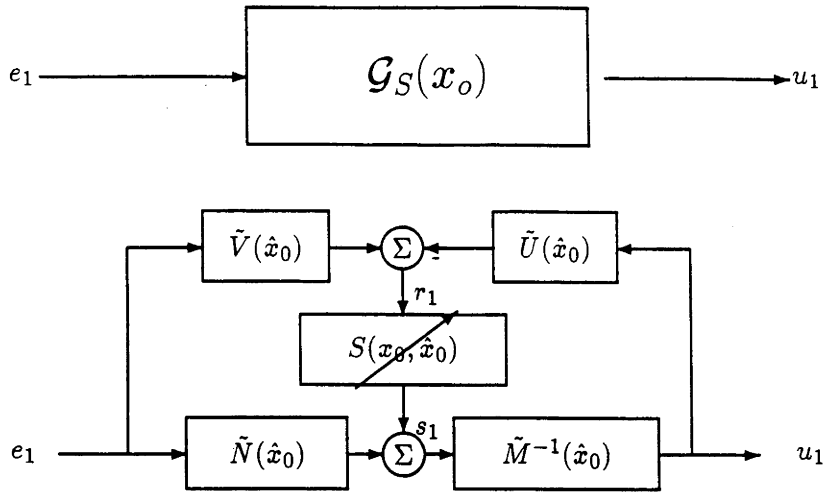

Figure 4-22: The class $\mathcal{G}_S(x_0)$

2. *For every BIBO stable $Q(x_0)$ obeying (4.4.17), there exists a stable $Q_r(x_0)$ given by*

$$Q_r(x_0) = (\tilde{\mathcal{V}}(x_0)\mathcal{K}_Q(x_0) - \tilde{\mathcal{U}}(x_0))(\tilde{\mathcal{M}}(x_0) - \tilde{\mathcal{N}}(x_0)\mathcal{K}_Q(x_0))^{-1} \tag{4.4.19}$$

such that the controllers of Figure (4-20,4-19) are equivalent.

3. *The system $\{\mathcal{G}(x_0), \mathcal{K}_{Q_r}(x_0)\}$ with $\mathcal{K}_{Q_r}(x_0)$ constructed as in Figure (4-20) is ϵ_V, ϵ_U bounded input stable iff $Q_r(x_0)$ is $(\theta_M + \theta_N)$ bounded-input stable.*

The main results are now summarised as a theorem

Theorem 4.2

Consider an augmented plant belonging to the nonlinear class (4.1.2), and obeying assumptions (4.2.2), (4.2.14), (4.4.8). Then left and right factorizations exist as in (4.4.4)-(4.4.7). Given the differential boundedness properties (4.4.16),(4.4.17), then the class of all stabilizing controllers for that plant can be constructed as in Figure (4-20).

Stabilization of plants with unknown initial conditions

An important question remains of stabilization results for plant/controller pairs with non-identical initial conditions, viewed here as working with a non-nominal plant/controller pair. In this section we extend the theory to this case. To this end, we first recall the plant $\mathcal{G}_S(x_0)$ as shown in Figure 4-22. Our aim is to use the S parametrization to characterize the class of plants $\mathcal{G}(x_0)$ in feedback pairs $\{\mathcal{G}(x_0), \mathcal{K}(\hat{x}_0)\}$, over all initial conditions, $x_0, \hat{x}_0$, not necessarily such that $x_0 = \hat{x}_0$ as in earlier results. Here we will assume realistically

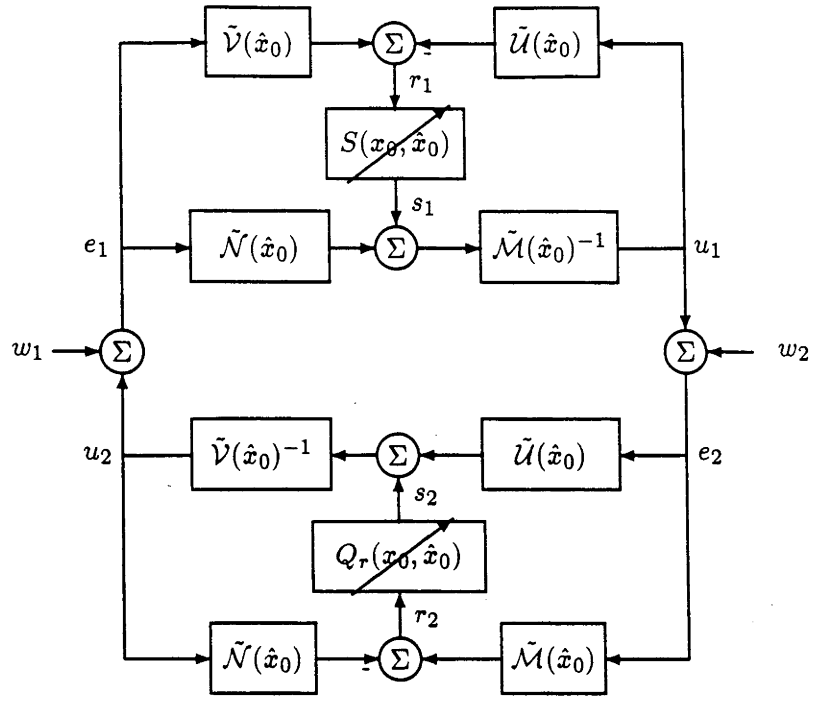

Figure 4-23: The system $\{\mathcal{G}_S(x_0), \mathcal{K}_{Q_r}(\hat{x}_0)\}$

that $\hat{x}_0$, the controller state is known and that x_0 is unknown. Thus we think of our nominal plant/controller pair as $\{\mathcal{G}(\hat{x}_0), \mathcal{K}(\hat{x}_0)\}$ and seek results for the pair $\{\mathcal{G}(x_0), \mathcal{K}(\hat{x}_0)\}$ with x_0 possibly different from $\hat{x}_0$. Thus, consider the following theorem, part of which is a specialization of Theorem 3.1 of [48].

Theorem 4.3

Consider $\mathcal{G}(\hat{x}_0)$ defined in (4.4.2),$\tilde{\mathcal{V}}(\hat{x}_0), \tilde{\mathcal{U}}(\hat{x}_0), \tilde{\mathcal{N}}(\hat{x}_0), \tilde{\mathcal{M}}(\hat{x}_0)$ from (4.4.6), (4.4.7). Then the system $\begin{bmatrix} \tilde{\mathcal{V}}(\hat{x}_0) & -\tilde{\mathcal{U}}(\hat{x}_0) \\ -\tilde{\mathcal{N}}(\hat{x}_0) & \tilde{\mathcal{M}}(\hat{x}_0) \end{bmatrix}$ *is invertible for all initial conditions $\hat{x}_0$, as is $(\tilde{\mathcal{V}}(\hat{x}_0) - \tilde{\mathcal{U}}(\hat{x}_0)\mathcal{G}_S(x_0))$ for all initial conditions $x_0, \hat{x}_0$, for any dynamical system $\mathcal{G}_S(x_0)$ satisfying the assumption (4.2.2) and of compatible dimension. Also $\mathcal{G}_S(x_0)$ has a right factorization*

$$\mathcal{G}_S(x_0) = \mathcal{N}_S(x_0, \hat{x}_0)\mathcal{M}_S(x_0, \hat{x}_0)^{-1} \tag{4.4.20}$$

$$\begin{bmatrix} \mathcal{M}_S(x_0, \hat{x}_0) \\ \mathcal{N}_S(x_0, \hat{x}_0) \end{bmatrix} = \begin{bmatrix} I \\ \mathcal{G}_S(x_0) \end{bmatrix} (\tilde{\mathcal{V}}(\hat{x}_0) - \tilde{\mathcal{U}}(\hat{x}_0)\mathcal{G}_S(x_0))^{-1} \tag{4.4.21}$$

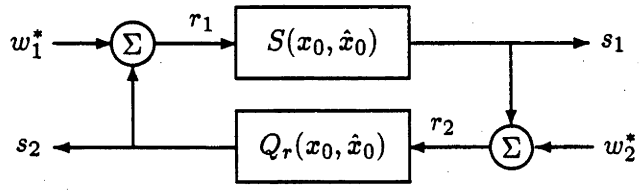

Figure 4-24: The system $\{S(\hat{x}_0, x_0), Q_r(\hat{x}_0)\}$

Define $S(x_0, \hat{x}_0)$ *as*

$$S(x_0, \hat{x}_0) = \tilde{\mathcal{M}}(\hat{x}_0)\mathcal{N}_S(x_0, \hat{x}_0) - \tilde{\mathcal{N}}(\hat{x}_0)\mathcal{M}_S(\hat{x}_0, x_0) \tag{4.4.22}$$

Then the systems $\mathcal{G}_S(x_0)$ *can be organised as depicted in Figure 4-22. Also, its factors* $\mathcal{M}_S(x_0, \hat{x}_0)$ *and* $\mathcal{N}_S(x_0, \hat{x}_0)$ *are given in terms of* $S(x_0, \hat{x}_0)$ *as*

$$\begin{bmatrix} \mathcal{M}_S(x_0, \hat{x}_0) \\ \mathcal{N}_S(x_0, \hat{x}_0) \end{bmatrix} = \begin{bmatrix} \tilde{\mathcal{V}}(\hat{x}_0) & -\tilde{\mathcal{U}}(\hat{x}_0) \\ -\tilde{\mathcal{N}}(\hat{x}_0) & \tilde{\mathcal{M}}(\hat{x}_0) \end{bmatrix}^{-1} \begin{bmatrix} I \\ S(x_0, \hat{x}_0) \end{bmatrix} \tag{4.4.23}$$

Moreover, the factors $\mathcal{M}_S(x_0, \hat{x}_0), \mathcal{N}_S(x_0, \hat{x}_0)$ *and* $\tilde{\mathcal{V}}(\hat{x}_0), \tilde{\mathcal{U}}(\hat{x}_0)$ *obey a Bezout identity*

$$\tilde{\mathcal{V}}(\hat{x}_0)\mathcal{M}_S(x_0, \hat{x}_0) - \tilde{\mathcal{U}}(\hat{x}_0)\mathcal{N}_S(x_0, \hat{x}_0) = I \tag{4.4.24}$$

The factors $M_S(x_0, \hat{x}_0), N_S(x_0, \hat{x}_0)$ *are coprime if they are BIBO stable. Furthermore, given BIBO stability of* $\begin{bmatrix} \tilde{\mathcal{V}}(\hat{x}_0) & -\tilde{\mathcal{U}}(\hat{x}_0) \\ -\tilde{\mathcal{N}}(\hat{x}_0) & \tilde{\mathcal{M}}(\hat{x}_0) \end{bmatrix}^{-1}$ *then*

$$\mathcal{M}_S(x_0, \hat{x}_0), \mathcal{N}_S(x_0, \hat{x}_0) \text{ are BIBO stable iff } S(x_0, \hat{x}_0) \text{ is BIBO stable.} \tag{4.4.25}$$

Proof. The systems $\tilde{\mathcal{V}}(\hat{x}_0) - \tilde{\mathcal{U}}(\hat{x}_0)\mathcal{G}_S(x_0)$ and $\begin{bmatrix} \tilde{\mathcal{V}}(\hat{x}_0) & -\tilde{\mathcal{U}}(\hat{x}_0) \\ -\tilde{\mathcal{N}}(\hat{x}_0) & \tilde{\mathcal{M}}(\hat{x}_0) \end{bmatrix}$ are invertible by similar arguments to that used to prove the invertibility of the system $M(x_0) - U(x_0)S(x_0, \hat{x}_0)$ in Theorem 4.1.

Observe from Figure 4-22 that

$$u = \tilde{\mathcal{M}}^{-1}(\hat{x}_0)[S(x_0, \hat{x}_0)[\tilde{\mathcal{V}}(\hat{x}_0)e - \tilde{\mathcal{U}}(\hat{x}_0)u] + \tilde{\mathcal{N}}(\hat{x}_0)e] = \mathcal{G}_S(x_0)e$$

which yields

$$S(x_0, \hat{x}_0) = [\tilde{\mathcal{M}}(\hat{x}_0)\mathcal{G}_S(x_0) - \tilde{\mathcal{N}}(\hat{x}_0)][\tilde{\mathcal{V}}(\hat{x}_0) - \tilde{\mathcal{U}}(\hat{x}_0)\mathcal{G}_S(x_0)]^{-1} \tag{4.4.26}$$

or equivalently (4.4.22), as claimed.

For each $S(x_0, \hat{x}_0)$ there exists a unique pair $\mathcal{M}_S(x_0, \hat{x}_0), \mathcal{N}_S(x_0, \hat{x}_0)$, and consequently a unique $\mathcal{G}_S(x_0)$. Thus setting $S(x_0, \hat{x}_0)$ to obey (4.4.26) makes the system in Figure 4-22 equivalent to $\mathcal{G}_S(x_0)$.

To show (4.4.24), observe that

$$\begin{aligned}\tilde{\mathcal{V}}(\hat{x}_0)\mathcal{M}_S(x_0,\hat{x}_0)-\tilde{\mathcal{U}}(\hat{x}_0)\mathcal{N}_S(x_0,\hat{x}_0) &= \tilde{\mathcal{V}}(\hat{x}_0)((\tilde{\mathcal{V}}(\hat{x}_0)-\tilde{\mathcal{U}}(\hat{x}_0)\mathcal{G}_S(x_0))^{-1}\\ &- \tilde{\mathcal{U}}(\hat{x}_0)\mathcal{G}_S(x_0)(\tilde{\mathcal{V}}(\hat{x}_0)-\tilde{\mathcal{U}}(\hat{x}_0)\mathcal{G}_S(x_0))^{-1}=I\end{aligned}$$

Also

$$\begin{aligned}\mathcal{N}_S(x_0,\hat{x}_0)\mathcal{M}_S(x_0,\hat{x}_0)^{-1} &= \mathcal{G}_S(x_0)(\tilde{\mathcal{V}}(\hat{x}_0)-\tilde{\mathcal{U}}(\hat{x}_0)\mathcal{G}_S(x_0,\hat{x}_0))^{-1}(\tilde{\mathcal{V}}(\hat{x}_0)-\tilde{\mathcal{U}}(\hat{x}_0)\mathcal{G}_S(x_0))\\ &= \mathcal{G}_S(x_0)\end{aligned}$$

giving (4.4.21). Verification of (4.4.23) follows from,

$$\begin{bmatrix}\tilde{\mathcal{V}}(\hat{x}_0) & -\tilde{\mathcal{U}}(\hat{x}_0)\\ -\tilde{\mathcal{N}}(\hat{x}_0) & \tilde{\mathcal{M}}(\hat{x}_0)\end{bmatrix}\begin{bmatrix}\mathcal{M}_S(x_0,\hat{x}_0)\\ \mathcal{N}_S(x_0,\hat{x}_0)\end{bmatrix} = \begin{bmatrix}\tilde{\mathcal{V}}(\hat{x}_0)\mathcal{M}_S(x_0)-\tilde{\mathcal{U}}(\hat{x}_0)\mathcal{N}_S(x_0)\\ \tilde{\mathcal{M}}(\hat{x}_0)\mathcal{N}_S(x_0)-\tilde{\mathcal{N}}(\hat{x}_0)\mathcal{M}_S(x_0)\end{bmatrix}$$
$$= \begin{bmatrix}I\\ S(x_0,\hat{x}_0)\end{bmatrix}$$

Given unimodularity of $\begin{bmatrix}\tilde{\mathcal{V}}(\hat{x}_0) & -\tilde{\mathcal{U}}(\hat{x}_0)\\ -\tilde{\mathcal{N}}(\hat{x}_0) & \tilde{\mathcal{M}}(\hat{x}_0)\end{bmatrix}$, then by (4.4.23) stability of $S(x_0,\hat{x}_0)$ is equivalent to stability of $\mathcal{M}(x_0,\hat{x}_0),\mathcal{N}(x_0,\hat{x}_0)$. Coprimeness follows from the stability assumption, and the Bezout (4.4.24) via Lemma 2.1 of [47]. ∎

Remarks

1. Theorem 4.3 applies for any plant $\mathcal{G}_S(x_0)$ within the class of interest, and in particular applies to $\mathcal{G}_S(x_0)=\mathcal{G}(x_0)$. A key objective of this chapter is thereby reached, namely to achieve coprime factorizations of $\{\mathcal{G}(x_0),\mathcal{K}(\hat{x}_0)\}$ with $\hat{x}_0\neq x_0$. Thus, we set $\mathcal{G}_S(x_0)=\mathcal{G}(x_0)$, and use the $S(.)$ operator to parametrize over the set of nominal plants $\mathcal{G}(.)$ with varying initial conditions. A dual of Theorem 4.3, holds for any controller $\mathcal{K}(\hat{x}_0)$ with initial conditions $\hat{x}_0$ differing from that of a nominal plant $\mathcal{G}(x_0)$. Thus a $\mathcal{K}_Q(x_0,\hat{x}_0)=\mathcal{K}(\hat{x}_0)$ can be formulated in a dual fashion such that the operator $Q(x_0,\hat{x}_0)$ characterizes the effect of initial conditions of the controller different to those of the nominal plant.

2. Corresponding "left" factorization results are elusive and indeed may not exist to

the generality achieved for right factorizations.

3. This theorem also applies to the factorizations of Section 3.

We next make use of these parametrizations of the set of pairs $\{\mathcal{G}(x_0), \mathcal{K}(\hat{x}_0)\}$ with different initial conditions by recalling a theorem from [47]

Theorem 4.4

Consider the system $\{\mathcal{G}_S(x_0), \mathcal{K}_{Q_r}(\hat{x}_0)\}$ *of Figure 4-23, where* $\tilde{\mathcal{N}}(\hat{x}_0), \tilde{\mathcal{M}}(\hat{x}_0)$,$\tilde{\mathcal{U}}(\hat{x}_0), \tilde{\mathcal{V}}(\hat{x}_0)$ *as defined in (4.4.7), (4.4.6), are stable factorizations of* $\mathcal{G}(\hat{x}_0)$ *and* $\mathcal{K}(\hat{x}_0)$. *Consider also that* $\begin{bmatrix} \tilde{\mathcal{M}}(\hat{x}_0) & -\tilde{\mathcal{N}}(\hat{x}_0) \\ -\tilde{\mathcal{U}}(\hat{x}_0) & \tilde{\mathcal{V}}(\hat{x}_0) \end{bmatrix}^{-1}$ *is BIBO stable, and the differential boundedness conditions (4.4.16) hold. Then the system is* ϵ_v, ϵ_u *is bounded-input stable iff the system* $\{S(x_0, \hat{x}_0), Q_r(x_0, \hat{x}_0)\}$, *of Figure 4-24 ,is* $(\theta_U + \theta_V), (\theta_M + \theta_N)$ *bounded-input stable.*

Remark: This theorem is a powerful robustness theorem, which can be used, for example, in multi-loop controller design strategies as in the linear case [76] and in adaptive control [63].

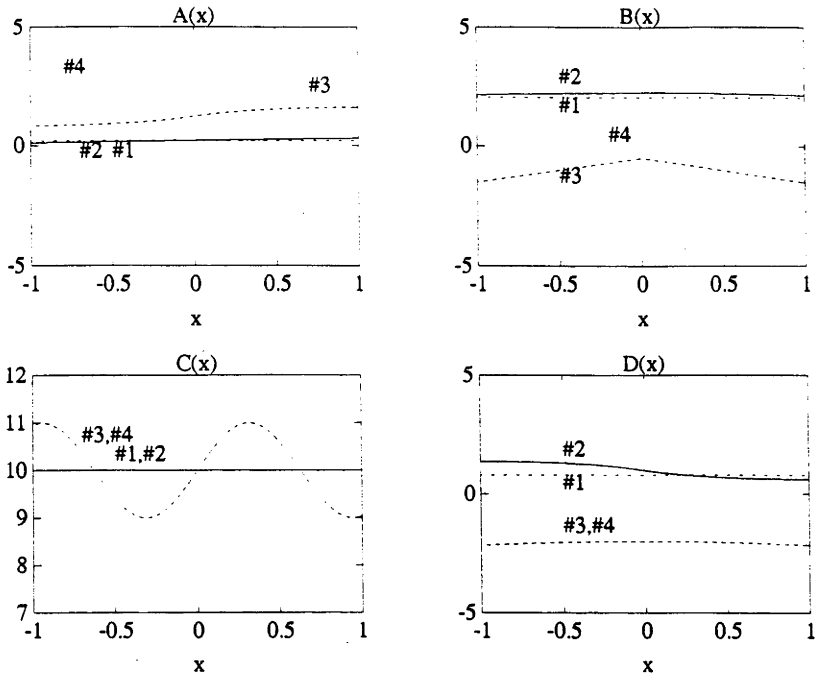

Figure 4-25: The matrix blocks A - D for Plants 1-4.

4.5 Simulation Results

To illustrate nonlinear plant/controller robustness properties developed in this chapter, we present two sets of simulation studies, each consisting of a nonlinear controller designed for a nonlinear nominal plant, and then the pair placed in a feedback loop with stochastic disturbances added. In the first instance, the simulations consist of an augmented controller/plant loop , as in Figure 4-17, with stochastic disturbances added to each of the inputs. The second series of simulations includes a Q parametrised controller in feedback with an unaugmented plant as per Figure 4-13. The idea is to illustrate the tracking, and regulation properties of the controller in the presence of disturbances.

The coefficient functions of the state space formulation of the four scalar variable, first order plants simulated are given in (4.5.1) to (4.5.4).

$$\text{Plant 1: } \left[\begin{array}{c|c} .2 & 2 \\ \hline 10 & .8 \end{array}\right]_{x_0} \tag{4.5.1}$$

$$\text{Plant 2: } \left[\begin{array}{c|c} .2 + .1sin(x) & .2|cos(x)| + 2 \\ \hline 10 & 1 - xe^{-|x|} \end{array}\right]_{x_0} \tag{4.5.2}$$

$$\text{Plant 3: } \left[\begin{array}{c|c} 1.1 + xe^{-|x|} & \text{-min}(|x|, |1/x|) - .5 \\ \hline 10 + sin(5x) & |\text{sinc}(x)| - 3 \end{array}\right]_{x_0} \tag{4.5.3}$$

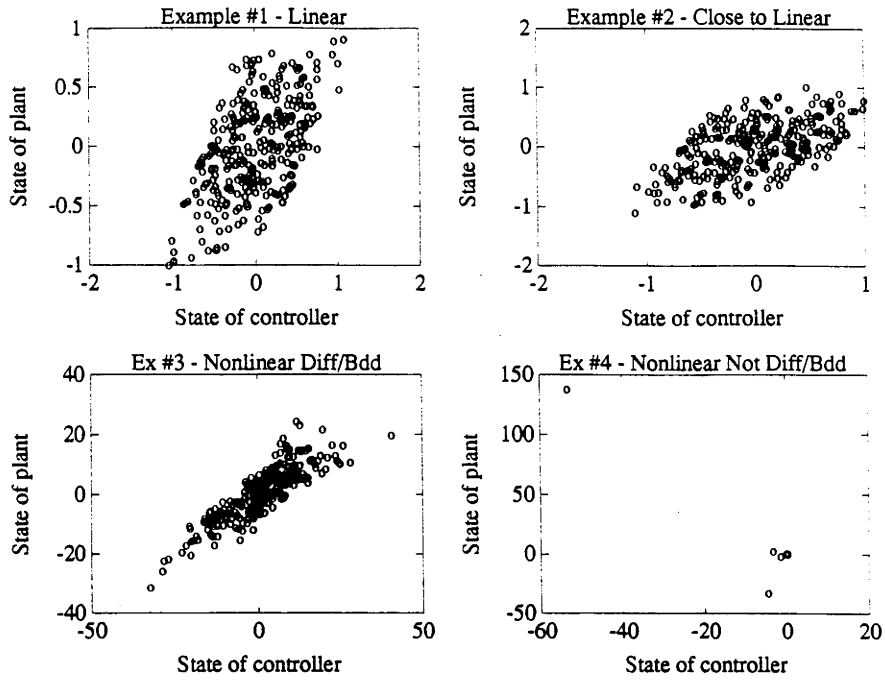

Figure 4-26: The controller and augmented plant states at each time instant.

$$\text{Plant 4:} \left[\begin{array}{c|c} \left\{\begin{array}{ll} -1+\text{sinc}(x), & x \neq 0 \\ 3, & x = 0 \end{array}\right. & \left\{\begin{array}{ll} 2, & \text{integer part of } x \text{ is even} \\ -2, & \text{integer part of } x \text{ is odd} \end{array}\right. \\ \hline 10 + sin(5x) & |\text{sinc}(x)| - 3 \end{array}\right]_{x_0} \tag{4.5.4}$$

The shape of the functions $A(.), B(.), C(.), D(.)$ are depicted in Figure 4-25, where the scalar functions are plotted over the normal operating range of the plant/controller pair.

In each case, specification of the controller requires the definition of the matrix functions $F(.), H(.)$. The choice must give the required differential boundedness conditions in order to guarantee stability of the loop. Here, the differential boundedness is calculated in an L_2 sense, and generally in this case a sufficient condition for differential boundedness is that for two systems with identical input, and unequal but sufficiently close initial states, that the states converge. This condition is facilitated, at least in the zero input case, by any $A(.)$ function of the system which guarantees exponential convergence of the state to zero.

In each case, $F(x)$ and $H(x)$ are chosen for all x such that

$$F(x) = -A(x)/B(x) - .5/B(x) \tag{4.5.5}$$

$$H(x) = -A(x)/C(x) - .5/C(x) \tag{4.5.6}$$

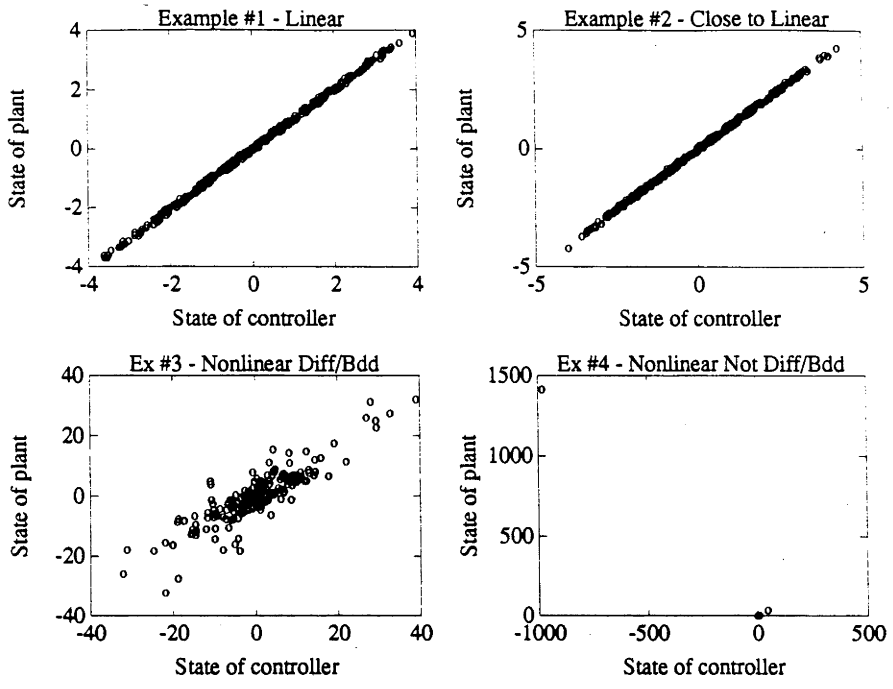

Figure 4-27: The Q-parametrised controller and nominal plant states at each time instant

This sets both $A(x) + B(x)F(x)$ and $A(x) + H(x)C(x)$ to a constant of -0.5 for all x. Thus, as can be seen from (4.4.6),(4.4.7), the $A(.)$ functions of the systems $\tilde{\mathcal{U}}, \tilde{\mathcal{V}}, \tilde{\mathcal{N}}, \tilde{\mathcal{M}}$ are all equal to -0.5, which guarantees exponential convergence for the zero input case.

The controllers in three of these simulations are able regulate the states of the plants close to the zero point. There is a trade off, however, since the $B(.)$ and $C(.)$ functions of the factors $\tilde{\mathcal{U}}, \tilde{\mathcal{V}}, \tilde{\mathcal{N}}, \tilde{\mathcal{M}}$ include $F(.)$ and $H(.)$, and in high input conditions, small $B(.)$ and $C(.)$ functions will, in general, help to achieve differential boundedness, possibly allowing a more variable 'A' function. Further discussion of the properties of nonlinear differential equations which lead to differential boundedness is beyond the scope of this chapter.

The simulations are run with a nominal stochastic disturbance uniformly distributed between $[-.3, .3]$ applied to each input. The systems $\tilde{\mathcal{U}}, \tilde{\mathcal{V}}, \tilde{\mathcal{N}}, \tilde{\mathcal{M}}$ are differentially bounded in the region of interest, of $|x| < 5$, for plants 1,2,3. Plant 4 is not differentially bounded in this region. The simulations extend in the case of plants 1,2,3 for 300 iterations. The simulation results of Plant 4 are shown only for 6 iterations, since the state continues to diverge for all further iterations. The results of the state of the controller plotted against the state of the plant for each time iteration are shown in Figure 4-26.

Further simulations are carried out which include the Q parametrized controller $K_{Q_r}(\hat{x}_0)$ as in Figure 4-20, in a feedback loop with the *unaugmented* nominal plant $G(x_0)$, as in

Figure 4-13. The plants in this case are strictly proper versions of Plants 1,2,3,4 in (4.5.1) -(4.5.4), i.e. identical but with the functions $D(.)$ set to 0. The disturbances are uniformly distributed between 0 and .1. Also, the initial conditions on the plant and controller are not equal, the difference uniformly distributed between 0 and .1. The Q function used in these simulations is $Q_r(x) = sin(x)$. The results are shown in Figure 4-27.

As can be seen from the Figures 4-26 and 4-27, in the three cases where the differential boundedness conditions are satisfied, the controller successfully regulates the state of the plant in the presence of stochastic disturbances, and in the case where the differential boundedness conditions are not met, the system diverges.

4.6 Conclusion

In this chapter we have extended part of the linear factorization theory to a class of nonlinear systems. For these pseudo linear systems with state dependent matrices $A(.), B(.)$, $C(.), D(.)$, cascade and inversion formulas have been introduced which trivially collapse to the well known linear results when $A(.), B(.), etc.$ are not state dependent. Also the approach is such that the nonlinear system factorizations are set up so as to make the corresponding matrices $A(.), B(.), etc.$ identical in all the subsystems in an idealized nominal plant/controller arrangement. In this case results follow directly from the linear time-varying case. This approach excludes corresponding left factorizations in general.

Studies are made of a specialization to the case where the state dependence is rather an output dependence, and to a more general case where the factors are augmented. In these cases stable left factorizations, as well as certain Bezout identities are also generated. These left factorizations are used to generate the class of all stabilizing controllers for a given nominal plant based on earlier theory [47]. Also, an S parametrization is recalled, and then used to parametrize the set of all plants G with different initial conditions, leading to stabilization results for these plants. Simulation results verify the stabilization properties of the nonlinear controllers proposed in this chapter. Thus, for the state dependent class of nonlinear systems, the theory goes quite a way in extending known linear results.

Chapter 5

Time Dependent Switching Controller Design

5.1 Introduction

Averaging theory [57], which allows the study of an "intractable" system by working with an approximation, termed the "averaged" system has found application to the areas of adaptive and robust control. It has provided useful insight and theoretical support for various existing designs, and facilitated the emergence of novel designs. Being such a powerful tool, it seems reasonable for us to explore a dual field of application for averaging theory where an easy-to-analyse system is approximated by an "intractable" system. For example, consider the case of the approximation of a given linear system, the averaged system, by means of a periodic dynamical system. Such "intractable" approximations could be attractive for implementation and perhaps for enhanced robustness in the case of a controller. To lead into such developments, we now review certain results for periodic systems and more general switched systems.

Certainly, it is well known that controllers with periodic gains can lead to more robust performance than time invariant ones, even for time-invariant plants. Gain and phase margin improvement are possible, see for instance [37] and its references for discrete-time results. However, these results do not always generate acceptable inter-sampling performance [20].

For continuous-compensators, averaging theory is used in [41] to explain the superior performance of vibrational controllers by demonstrating that they have zero-placement as well as pole-relocation capabilities. Also [41] extends the discrete-time gain margin

improvement results to continuous time. In the area of decentralised control, it has been shown that periodically switched-gain feedback laws in one feedback channel lead to decentralised controllability and observability in 2-channel systems with fixed modes, whereas time-invariant feedback laws do not, [3, 4]. There is thus a sound theoretical and practical basis for working with periodic controllers, even for time-invariant plants.

A more general class of time-varying/nonlinear controllers are termed state dependent switching controllers. Such may consist of a set of continuous-time or discrete-time controllers , one of which is active at any time. The switched controllers may be time invariant or time varying, or even nonlinear. The switching may be periodic, or may be driven by a rule which assesses which controller will work best according to some measure, given the data. Switching controllers are useful for the control of a system whose dynamics contain jump discontinuities in the dynamics, such as a robot arm which picks up a heavy object. To this end Khargonekar and Poolla [36] state, "in robust multivariable control problems nonlinear time-varying controllers yield advantages ... if there is parametric or structured uncertainty". Again we see that there is strong motivation for switched systems to achieve robustness. How then are such systems analysed ?

In the case of discrete-time periodic systems, methods exist to find an equivalence between discrete-time periodic systems, and higher order time-invariant systems [9, 37, 62]. Standard design results are then applied to the time-invariant representations, and re-interpreted to achieve results for periodic systems. For example, [16] finds the regulator gains for discrete-time periodic systems by solving algebraic Riccatti equations for the associated time-invariant system. For continuous-time plants, these conversion methods are less well understood. Thus [37] reports that the methods of [62] can be extended to continuous-time systems with the drawback that the input and output spaces are in general infinite dimensional Hilbert spaces. Thus there are few explicit results dealing with the convergence of continuous-time switched systems. In fact, short of an infinite series (the Peano-Baker series), there is no analytic solution to the calculation of the transition matrix of a time-varying system unless the update matrix is semi-proper [75]. However approximations exist for the cases where the switching speed is high or low with respect to the dynamics of the system. Thus the stability of high frequency periodically switched systems has been tackled in [69, 70] where the author uses an approximation result on the exponentials of certain matrices to study the dependence of the stability on the frequency of switching. The author gives an explicit formula which facilitates checking the stability of such systems in the limiting case of high frequency switching. However, these results

only apply to systems with piece-wise constant periodic gains, and there is no development of explicit error bounds or regions of convergence. There is therefore a need for stability results which are not restricted to piecewise constant periodic gains, and for which explicit error bounds and regions of convergence can be calculated.

To help focus ideas in meeting the needs for further work in this area, let us keep in mind an application which seems ideally suited to such developments. One possible application of switched systems is to achieve resonance suppression. Such a task has been tackled [26] where square-law nonlinearities in the control law are used to encourage energy flow from the resonances to the controller, and from one frequency band to the entire frequency band. In [68] there is implemented an adaptive resonance suppression controller/plant system with an unstable resonance, possibly due to a badly modelled plant, or changing plant dynamics. Could there be an advantage to a switching controller design approach?

In this chapter we investigate by means of averaging theory two novel avenues of application of the switched and periodic-structure systems. The first is to use easy-to-implement periodic-structure systems to achieve either low order or discrete-time approximations to a continuous-time controller. Following on from these results, it is shown that the periodic structure can be designed to be equivalent to either a low order, or discrete-time system with no approximation necessary at this step.

Thus, in this chapter, we seek approximations of a linear time-invariant (LTI) system via certain periodic systems. We do not seek improvements in the gain or phase margin. In this way we recover the performance of the *LTI* system without any performance enhancement, but with considerable computational advantages, and with tight bounds on the inter-sampled behaviour.

The theoretical justification for this approach is developed from stability results for certain continuous-time time-varying systems (which may or may not be piece-wise continuous), as well as the calculation of specific error bounds as functions of the speed of time variations (ϵ), and a lower bound on the time-variation to ensure exponential stability of the periodic system. This is achieved via an averaging theoretic approach together with linear theory mathematically reminiscent of that employed by [10]. The results are then extended to ensure low sensitivity with respect to input disturbances. Examples illustrate effective controller simplification and resonance suppression.

We apply the averaging theory results to hybrid control, and demonstrate their application to the generation of explicit performance bounds, valid at and between sampling

intervals, when comparing the performance of a discrete-time controller and a continuous-time controller, each controlling a continuous-time plant.

Another application of switched systems is to achieve effective resonance suppression in the presence of lightly damped resonances for uncertain systems, and in particular the simultaneous control of a number of LTI subsystems, each representing a resonance, via a switching between controllers, each designed to suppress one of the resonances. The plant is viewed as a partial fraction representation, and the specific control objective is to suppress the most excited resonance at each given time. This application is further developed in Chapter 6.

The chapter is outlined as follows. Section 2, provides preliminary definitions and notation, and gives the results linking certain periodic systems and time-independent systems. Section 3 uses these results to prove our main theorems on the approximation of a system (or controller) via fast switching between a set of lower order systems. In Section 4 we present simulation examples of certain periodic systems and of controller order reduction and compare the results with the theoretical bounds set in Section 2,3. Section 5 contains results pertaining to hybrid control, and conclusions are drawn in Section 6.

5.2 An averaging analysis of periodic systems

5.2.1 Introduction

This section presents the theoretical basis for the applications of periodic systems developed later. First we introduce necessary notation and quote a fundamental theorem from averaging theory. Then further results are derived for linear systems. In particular, for certain periodic systems and their time-averaged LTI systems with easily calculable state trajectories, we provide explicit bounds for the norm of the difference between the state trajectories of two systems. These bounds are expressed as ϵQ where ϵ is the switching speed, and Q is a constant derived for the specific systems.

5.2.2 Definitions

1. $\delta_1(\epsilon) = O(\delta_2(\epsilon))$ for $\epsilon \to 0$ if there exists a constant k such that $|\delta_1(\epsilon)| \leq k|\delta_2(\epsilon)|$ for continuous functions, $\delta_1, \delta_2 : \epsilon \to 0$. Also $\delta_1(\epsilon) = o(\delta_2(\epsilon))$ for $\epsilon \to 0$ if $\lim_{\epsilon \to 0} \frac{\delta_1(\epsilon)}{\delta_2(\epsilon)} = 0$. Refer to [57] for additional information.

2. Consider the vector field $f(t,x)$ with $f : \mathbb{R} \times \mathbb{R}^n \rightarrow \mathbb{R}^n$, Lipschitz-continuous in x on $D \subset \mathbb{R}^n, t \in [0,T]$; f continuous in t and x on $\mathbb{R}^+ \times D$. If the average

$$\overline{f}(x) = \lim_{T\rightarrow\infty} \frac{1}{T} \int_0^T f(t,x)dt$$

exists, f is called a KBM-vectorfield.

3. Let r be a scalar, x a vector, and A a matrix. Then $|r|$ is the absolute value of r, $||x||$ is the L_2 norm of x, and $||A||$ is the induced L_2 norm of A.

4. Two time-varying functions $f(t), g(t)$ have *exclusive support* iff $f(t)g(t) = 0 \ \forall t$.

5. We employ a shorthand notation for systems:

$$P: \begin{array}{rcl} \dot{x} &=& A(t)x + B(t)u; \ x(0) = x_0 \\ y &=& C(t)x + D(t)u \end{array} \quad : \quad \left[\begin{array}{c|c} A(t) & B(t) \\ \hline C(t) & D(t) \end{array}\right]_{x_0}$$

6. $f(t,x)$ is *periodic* in t with period T iff $f(t,x) = f(t+T,x), \ \forall x,t$.

7. If $f(t,x)$ is periodic in t with period T, then the average $\overline{f}(x)$ is defined as

$$\overline{f}(x) \equiv \frac{1}{T} \int_0^T f(\tau,x)d\tau \tag{5.2.1}$$

8. Let $A(t)$ be a periodically time-varying matrix. We denote its period by T_A, its average $\overline{A}$, and define $D_A := \sup_t ||A(t) - \overline{A}||$, $S_A := \sup_t ||A(t)|| \geq ||\overline{A}||$, $B_A(t) = \int_0^t A(\tau) - \overline{A}d\tau$. Then $||e^{\overline{A}t}|| \leq C_A e^{-\lambda_A t}, \forall t$, for some $C_A \geq 1$, for some λ_A which may be chosen via Proposition 1, $||B_A|| \leq \frac{1}{2} T_A D_A$.

9. Denote the piecewise constant function

$$\Delta_i(n,t,T) \equiv \begin{cases} n, & (i-1)T/n \leq t - mT < iT/n, \ m \in \mathbb{Z} \\ 0, & \text{otherwise.} \end{cases} \tag{5.2.2}$$

10. Given a square matrix A of size n, we construct a time varying matrix $A^{\#}(t,\epsilon)$ with period ϵ, and average A such that the rows of $A^{\#}(t,\epsilon)$ have independent support by

$$A^{\#}(t,\epsilon) = \begin{bmatrix} \Delta_1(n,t,\epsilon) & \cdots & 0 \\ \vdots & \ddots & \vdots \\ 0 & \cdots & \Delta_n(n,t,\epsilon) \end{bmatrix} A \tag{5.2.3}$$

11. Given a system $P = \left[\begin{array}{c|c} A & B \\ \hline C & D \end{array}\right]$, then $P^{\#}(t,\epsilon) = \left[\begin{array}{c|c} A^{\#}(t,\epsilon) & B^{\#}(t,\epsilon) \\ \hline C & D \end{array}\right]$.

12. Denote the Lie brackett $[A,B] \equiv AB - BA$.

13. Given a continuous time signal $f(t)$, and its discrete-time sampled version $f_k = f(k\epsilon)$ with a sample time of ϵ, then denote the difference between the signal $f(t)$, and the piecewise constant approximation $f^d(t) = f(t) - f_k, \;\; t \in [k\epsilon, (k+1)\epsilon]$.

5.2.3 Proposition

To facilitate calculation, we include the following proposition.

Proposition 5.1 *[10] For any n by n matrix F with $Re[\lambda_i(F)] < 0 \;\; \forall i$, there exist constants $\lambda_F > 0$, $C_F > 1$ such that $||e^{Ft}|| \leq C_F e^{-\lambda_F t}, \;\; \forall t \geq 0$. Furthermore, if $||F|| \leq M$, $Re[\lambda_i(F)] < \alpha$, and $0 < \mu < 2M$ then one choice of C, λ may be generated via the inequality*

$$||e^{Ft}|| \leq (2M/\mu)^{n-1} e^{(\alpha+\mu)t}, \text{ for } t \geq 0 \tag{5.2.4}$$

Proof. See Proposition 3 of Chapter 1 of [10]. ∎

5.2.4 Fundamental Averaging Result.

Theorem 5.1

[Eckhaus/Sanchez-Palencia[56],[57].] Given

$$\dot{x} = \epsilon f(t,x), \;\; x(0) = x_0 \tag{5.2.5}$$

with $x_0, x \in D \subset \mathbb{R}^n$. Suppose f is a KBM-vectorfield producing the averaged equation

$$\dot{y} = \epsilon f^0(y), \;\; y(0) = x_0$$

where f^0 is continuously differentiable with respect to y in D. Let $y = 0$ be an asymptotically stable critical point in the linear approximation with domain of attraction $D^0 \subset D$.

Then for all $x_0 \in D^0$

$$x(t) - y(t) = O(\sup_{z \in D} \sup_{t \in [0, \frac{L}{\epsilon})} \epsilon || \int_0^t [f(\tau, z) - f^0(z)] d\tau ||), \ \ 0 \leq t < \infty$$

for any L *independent of* ϵ. *Furthermore, if* $f(t, x)$ *is periodic in* t, *then*

$$x(t) - y(t) = O(\epsilon), \ \ 0 \leq t < \infty \tag{5.2.6}$$

Proof. See [57] ∎

The main results of this section can be verified by making use of the above averaging theorem. However, here we rederive these results in the context of linear systems. This provides explicit error bounds and regions of convergence in terms of ϵ.

5.2.5 Explicit Averaging Results for Linear Systems

We now introduce lemmas on the trajectories of linear-time-varying systems when compared to the trajectories of their time-averaged linear-time-invariant analogues. These results form the basis for the applications of the following sections.

Lemma 5.1 *Consider the following systems*

$$\begin{aligned} G_1: \ \dot{x} &= \overline{A}x; & x(0) &= x_0 \\ G_2: \ \dot{y} &= A(t\epsilon^{-1})y; & y(0) &= x_0 \end{aligned} \tag{5.2.7}$$

where $Re[\lambda_i(\overline{A})] < 0$, $A(t)$ *is periodic with period* T_A, *average* $\overline{A}$, *and Definition (8) holds. Define*

$$\epsilon_0 = \frac{\lambda_A}{2T_A D_A C_A [||\overline{A}|| + S_A]} \tag{5.2.8}$$

then

$$\begin{aligned} ||y(t) - x(t)|| \ \leq \ & \epsilon T_A D_A C_A ||x_0|| [1 + (||\overline{A}|| + S_A) C_A t)] e^{-\lambda_A t} \\ + \ & (\epsilon T_A D_A C_A)^2 ||x_0|| (||\overline{A}|| + S_A)[t + (||\overline{A}|| + S_A) C_A \frac{t^2}{2}] e^{-\lambda_A t/2}, \forall \epsilon < \epsilon_0 \end{aligned} \tag{5.2.9}$$

Moreover, defining $\phi_y(.,.)$ *as the state transition matrix of* $y(.)$*, then,*

$$\begin{aligned} ||\phi_y(t,t_0)|| &\leq C_A e^{-\lambda_A/4(t-t_0)}\{1+\epsilon T_A D_A(1+\frac{4C_A(||\overline{A}||+S_A)}{e\lambda_A}) \\ &\quad +(\epsilon T_A D_A)^2 C_A(||\overline{A}||+S_A)(\frac{4}{e\lambda_A}+32\frac{(||\overline{A}||+S_A)C_A}{e^2\lambda_A^2}\} \ ,\forall \epsilon<\epsilon_0 \quad (5.2.10) \\ &\triangleq C_y e^{-\lambda_y(t-t_0)} \quad (5.2.11) \end{aligned}$$

Proof. See Appendix. ∎

Remarks

1. There is a trade-off between the constant multiples and the decay rate in the error bounds. This proof is intended to show exponential convergence of the trajectories $x(t), y(t)$ given sufficiently fast time variation within $A(t)$.

2. Inequality (B.1) can be used to considerably simplify the error bounds to constants multiplied by decaying exponentials. The cost of this simplification is further loss of tightness of the bounds.

3. Lemma (5.1) can easily be generalised to the case $x_0 \neq y_0$. Here we keep equal initial conditions since this is the case necessary for our applications.

Lemma (5.1) demonstrates that with the switching rate above some limit, any periodic system, with linear average which is exponentially asymptotically stable, is itself exponentially asymptotically stable. In the next lemmas, we extend these results to systems with input disturbances $\omega(.)$. Thus we consider jointly, and separately the implications of assumptions (5.2.12),(5.2.13) and (5.2.14)

Assumptions on Noise : Disturbances $w(\cdot)$ obey the relation

$$\begin{aligned} ||\int_0^S w(t)dt|| &\leq LS^\alpha, \text{ for some constants L}, 0<\alpha<1, \ \forall S>0 \quad (5.2.12) \\ ||w(t)|| &\leq W; \ \ \forall t \quad (5.2.13) \\ ||\dot{w}(t)|| &\leq \eta; \ \ \forall t \quad (5.2.14) \end{aligned}$$

Lemma 5.2 *Consider the system:*

$$G_3: \ \dot{z} = A(t\epsilon^{-1})z + \omega(t); \quad z(0) = z_0 \quad (5.2.15)$$

with the conditions of Lemma (5.1) and the Definitions (8) and Bound (5.2.8)holding. Then $\omega(.)$ obeying Assumption (5.2.12) implies

$$||z(t)|| \leq 2t^{\alpha}C_yL + C_ye^{-\lambda_y t}||z_0||, \quad \forall \epsilon < \epsilon_0 \tag{5.2.16}$$

and $\omega(.)$ obeying Assumption (5.2.13) implies

$$||z(t)|| \leq C_yW/\lambda_y + C_y(||z_0|| - W/\lambda_y)e^{-\lambda_y t} \tag{5.2.17}$$

where C_y and λ_y are constants defined via (5.2.11) such that

$$||\phi_y(\tau, r)|| \leq C_ye^{-\lambda_y(\tau - r)}, \quad \forall \epsilon < \epsilon_0 \tag{5.2.18}$$

Proof. By (5.2.10), we can set the exponential bounds on $\phi_y(.,.)$. Now

$$\begin{aligned} z(\tau) &= \phi_y(\tau, 0)z_0 + \int_0^{\tau} \phi_y(\tau, r)\omega(r)dr \\ ||z(\tau)|| &\leq C_ye^{-\lambda_y\tau}||z_0|| + ||\int_o^{\tau} \phi_y(\tau, r)\omega(r)dr|| \end{aligned}$$

Integrating by parts the second term in the above expression gives :

$$\begin{aligned} ||\int_0^{\tau} \phi_y(\tau, r)\omega(r)dr|| &\leq ||\phi_y(\tau, r)\int_0^{\tau} \omega(s)ds|_0^{\tau}|| + ||\int_0^{\tau} \frac{d\phi_y(t, r)}{dz}\int_0^{z} \omega(s)dsdz|| \\ &\leq ||C_yL\tau^{\alpha}|| + ||C_yL\lambda_ye^{-\lambda_y\tau}\int_0^{\tau} r^{\alpha}e^{\lambda_y r}dr|| \\ &\leq 2C_yL\tau^{\alpha} \end{aligned}$$

The second inequality follows from Assumption (5.2.12), and the last via Inequality (B.2). Similarly, (5.2.17) follows from Inequality (B.3). ∎

Remarks:

Since the transition matrix $\phi_y(.,.)$ is overbound by a decreasing exponential, the above results and other standard results for stable systems can be applied to give bounds on the magnitude of the trajectories for various classes of disturbances. We have chosen to analyze the stability for several classes of bounded disturbances.

Lemma 5.3 *Consider the following systems*

$$\begin{aligned} G_1 : \dot{x} &= \overline{A}x; \qquad x(0) = x_0 \\ G_2 : \dot{y} &= A(t\epsilon^{-1})y; \quad y(0) = x_0 \end{aligned}$$

where $y(t)$ is uniformly asymptotically stable for all $\epsilon < \epsilon_0$, for some ϵ_0 and $A(t)$ is periodic with average $\overline{A}$. Then $Re[\lambda_i(\overline{A})] < 0$, and $\sup_t ||x(t) - y(t)|| = O(\epsilon)$.

Proof. First note that

$$\begin{aligned} (\dot{x} - \dot{y}) &= A(t\epsilon^{-1})(x - y) + [\overline{A} - A(t\epsilon^{-1})](x(t) - y(t)) + [\overline{A} - A(t\epsilon^{-1})]y(t); \\ & \quad x(0) = y(0) = x_0 \end{aligned}$$

Since $y(t)$ is asymptotically stable then $||\phi_y(t,\tau)|| \leq C_A e^{-\lambda_y(t-\tau)}$ for some C_A, λ_y and the rest of the proof follows similarly to that of Lemma 5.1. Thus integrating the second term by parts and the subsequent application of the Bellman-Gronwall Lemma [72] gives exponential convergence of x and y for all $\epsilon < 1/(C_A^2 D_A T_A)$. Thus, since y is exponentially stable, so is x and the Lemma is established. ∎

Lemma 5.4 *Consider the systems*

$$\begin{aligned} G_3 : \quad \dot{z} &= A(t\epsilon^{-1})z + B(t\epsilon^{-1})\omega(t); \qquad z(0) = s_0 \\ G_4 : \quad \dot{s} &= \overline{A}s + \overline{B}\omega(t); \qquad\qquad\quad s(0) = s_0 \end{aligned}$$

With the conditions of Lemma (5.1), Assumption (5.2.13), and Definition (8) holding for matrices A, B, then

$$\begin{aligned} ||z(t) - s(t)|| &\leq \frac{WC_A}{\lambda_A}\left\{2D_B + \epsilon\frac{D_A T_A}{\lambda_A}[C_A(||A||+S_A) + 2\lambda_A]\right\} \qquad (5.2.19) \\ &\times \quad \left\{1 + \frac{\epsilon(||A|| + S_A)D_A T_A C_A}{\lambda_A - \epsilon(||A||+S_A)D_A T_A C_A}\right\}, \\ \forall W &> \lambda_A||s_0||, \quad \epsilon < \frac{\lambda_A}{D_A T_A C_A(||\overline{A}|| + S_A)} \end{aligned}$$

Proof.

$$\begin{aligned} s(t) - z(t) &= \phi(t,0)[z(0) - s(0)] + \int_0^t \phi(t,\tau)[\overline{A} - A(\tau\epsilon^{-1})]z(\tau)d\tau \\ &+ \int_0^t \phi(t,\tau)[\overline{B} - B(\tau\epsilon^{-1})]\omega(\tau)d\tau \end{aligned}$$

$$
\begin{aligned}
&= -\int_0^t \phi(t,\tau)\dot{B}_A(\tau\epsilon^{-1})z(\tau)d\tau - \int_0^t \phi(t,\tau)\dot{B}_B(\tau\epsilon^{-1})\omega(\tau)d\tau \\
&= \int_0^t \phi(t,\tau)\{\overline{A}B_A(\tau\epsilon^{-1})z(\tau) + B_A(\tau\epsilon^{-1})[A(\tau\epsilon^{-1})z(\tau)+\omega(t)]\}d\tau \\
&\quad -B_A z(t) - \int_0^t \phi(t,\tau)\dot{B}_B(\tau\epsilon^{-1})\omega(\tau)d\tau
\end{aligned}
$$

Then application of Assumption (5.2.13), Definition (8), and the triangle inequality gives

$$
\begin{aligned}
||s(t)-z(t)|| \leq\ & \frac{1}{2}\epsilon D_A T_A[||s(t)|| + ||z(t)-s(t)||] + \frac{1}{2}\epsilon C_2 e^{-\lambda_A t}\int_0^t e^{\lambda_A\tau}||s(\tau)||d\tau \\
& + \frac{1}{2}\epsilon C_2 e^{-\lambda_A t}\int_0^t e^{\lambda_A\tau}||z(\tau)-s(\tau)||d\tau + \frac{1}{2}\epsilon C_1 e^{-\lambda_A t}\int_0^t e^{\lambda_A\tau}W d\tau \\
& + \frac{W D_B C_A}{\lambda_A}
\end{aligned}
$$

where $C_1 = D_A T_A C_A$, $C_2 = (||A|| + S_A)C_1$. Let us define $C_3 = \frac{W}{\lambda_A^2}[2\lambda_A C_1 + C_A C_2]$, $C_4 = 2\frac{W C_A D_B}{\lambda_A}$, $x(t) = ||z(t)-s(t)||e^{\lambda_A t}$, and restrict $\epsilon < \frac{\lambda_A}{D_A T_A C_A(||\overline{A}||+S_A)}$. Furthermore since $||s|| \leq \frac{C_A W}{\lambda_A}$ by Inequality (B.3), then

$$
\begin{aligned}
||s(t)-z(t)|| &\leq \epsilon C_3 + \epsilon C_2 e^{-\lambda_A t}\int_0^t ||z(\tau)-s(\tau)||e^{\lambda_A\tau}d\tau + C_4 \\
x(t) &\leq (\epsilon C_3 + C_4)e^{\lambda_A t} + \epsilon C_2\int_0^t x(\tau)d\tau
\end{aligned}
$$

Then by the Bellman-Gronwall inequality [72],

$$
\begin{aligned}
x(t) &\leq (\epsilon C_3 + C_4)e^{\lambda_A t} + \epsilon C_2(\epsilon C_3 + C_4)e^{+\epsilon C_2 t}\int_0^t e^{\lambda_A\tau}e^{-\epsilon C_2\tau}d\tau \\
||s(t)-z(t)|| &\leq (\epsilon C_3 + C_4) + \epsilon\frac{C_2(\epsilon C_3 + C_4)}{\lambda_A - \epsilon C_2}
\end{aligned}
$$

∎

Remarks:

1. Lemma (5.4) is a powerful sensitivity result. It shows for bounded disturbances, and sufficiently fast time variation, that the averaged and the periodic systems will have trajectories whose difference is tightly bounded. It is a consequence of the low pass nature of an integrator, and the high frequency of the perturbations introduced by $A(t\epsilon^{-1})$.

2. Assumptions guaranteeing the independence of the time variation of the noise, and the matrix $B(t\epsilon^{-1})$ lead to a lower expectation value of the error $||z(t) - s(t)||$. The aim of this chapter is to provide hard bounds on the errors, and as such, stochastic calculations are beyond its scope, except to note that the actual errors will in most cases be much smaller than the bounds calculated.

3. Lemma (5.4) can be proven by a number of methods, each giving a different overbound. For instance, the error can be calculated in terms of $\phi_y(.,.)$. The correct choice is important for a given application, as the differences can be many orders of magnitude apart.

4. The bound $W > \lambda_A||s_0||$ comes from the application of Inequality (B.3), and further simplification. Since W is a bound on the noise, if $W < \lambda_A||s_0||$, then W can be replaced by $\lambda_A||s_0||$, and the proof holds for this value.

Lemma (5.4) does not in general give $||s(t) - z(t)|| = O(\epsilon)$, unless $B(t\epsilon^{-1}) = \overline{B}$. However in the case where the noise has bounded derivative, then

Corollary 5.1 *With the conditions of (5.4) as well as Assumption (5.2.14) holding, then*

$$\begin{aligned} ||z(t) - s(t)|| \leq & \frac{\epsilon}{\lambda_A}\left\{D_B T_B[W\lambda_A + C_A(W+\eta)] + \frac{WC_AT_AD_A}{\lambda_A}[C_A(||A||+S_A) + 2\lambda]\right\} \\ & \times \left\{1 + \frac{\epsilon(||A|| + S_A)D_AT_AC_A}{\lambda_A - \epsilon(||A||+S_A)D_AT_AC_A}\right\}, \\ \forall W > & \lambda_A||s_0||, \ \epsilon < \frac{\lambda_A}{D_AT_AC_A(||\overline{A}|| + S_A)} \end{aligned} \tag{5.2.20}$$

Remarks:

1. When $||w(t)||$ is bounded, then the condition that $\dot{\omega}(t)$ is bounded will be automatically satisfied in the case of low-pass filters being applied to the inputs of a feedback loop.

A further generalization is to systems with disturbances which are bounded by a function of the states:

Lemma 5.5 *Consider the systems $\xi(t), \zeta(t)$ such that*

$$\begin{aligned} \dot{\xi} &= A\xi + \omega(t), & \xi(0) = \xi_0 \\ \dot{\zeta} &= [A + \epsilon L]\zeta + \omega(t) + \epsilon v(t) + h(t), & \zeta(0) = \xi_0 \end{aligned}$$

where Assumption (5.2.13) holds, and $||v(t)|| \leq V||\zeta(t)||$,$Re[\lambda_i(A)] < 0$, $||e^{At}|| \leq Ce^{-\lambda t}$,*and* $||h(t)|| \leq H$. *Define* $F = C[H + \epsilon X(V + ||L||)]/\lambda$, *and* X *via Inequality (B.3) such that* $||\xi(t)|| \leq X$, *and* $C, \lambda_{[A+\epsilon L]}$ *via Inequality (B.4) such that* $||e^{[A+\epsilon L]t}|| \leq Ce^{\lambda_{[A+\epsilon L]}t}$. *Then*

$$||\xi - \zeta|| \leq 2F, \quad \forall \epsilon < \min\{\lambda_A/||L||C, \lambda_{[A+\epsilon L]}/(2CV)\} \tag{5.2.21}$$

Proof. Let $u(t) = \xi(t) - \zeta(t)$, and $s(t) = ||u(t)||e^{\lambda_{A+\epsilon L}t}$.

$$\begin{aligned} \dot{u} &= [A + \epsilon L]u(t) - \epsilon[v(t) + L\xi(t)] - h(t) \\ ||u|| &\leq Ce^{-\lambda_{[A+\epsilon L]}t} \int_0^t e^{\lambda_{[A+\epsilon L]}\tau}||\epsilon[V||u(\tau)|| + (V + ||L||)X] + Hd\tau|| \\ s(t) &\leq \epsilon CV \int_0^t s(\tau)d\tau + Fe^{\lambda_{A+\epsilon L}t} \end{aligned}$$

Then application of the Bellman-Gronwall lemma [72] and standard manipulations gives (5.2.21).

Remark:

A result which leads to a sufficient condition for the stability of $\dot{y} = [A(t) + B(t)]y$ in terms of the stability of $\dot{x} = A(t)x$, and the matrix $B(t)$ is found in Proposition 1 of Chapter 1 of [10].

∎

5.3 Controller Simplification

In this section we apply the results of the previous section to prove that any linear, continuous time stabilizing controller (in a feedback loop with any LTI plant which it stabilizes) can be approximated by certain periodic controllers. These controllers may be designed to have the advantages of simple structure, or of being equivalent to first order systems, and thus much computationally cheaper than the full order controllers they are replacing. Moreover, we will show that as the speed of variation increases, the state trajectories of the feedback systems associated with these controllers, and the indices associated with their corresponding *LQG* cost functions, asymptotically approach those of the full order controller.

To this end we reformulate the results of Lemma (5.4) and Corollary (5.1) into our

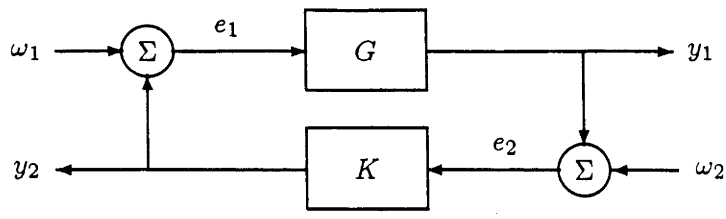

Figure 5-1: The feedback system $\{G, K\}$.

main results on the approximation of controllers:

Theorem 5.2

Consider a plant, and full state feedback controller pair:

$$\begin{aligned} G: \quad \dot{x} &= Ax + Bu + \omega_1(t); \quad x(0) = x_0 \\ K(t\epsilon^{-1}): \quad u &= K(t\epsilon^{-1})x \end{aligned}$$

where $K(t)$ is periodic with period T and average K^0, and $(A + BK^0)$ is exponentially stable, and $\omega_1(t)$ is a noise term obeying Assumptions (5.2.12),(5.2.13). Consider also the "averaged" system

$$\begin{aligned} G: \quad \dot{x} &= Ax^0 + Bu + \omega_1(t); \quad x^0(0) = x_0 \\ K^0: \quad u &= K(t\epsilon^{-1})x^0 \end{aligned}$$

Then the state x, of the system $\{G, K(t\epsilon^{-1})\}$ and x^0 of the system $\{G, K^0\}$ are related by

$$||x(t) - x^0(t)|| \leq \epsilon D, \quad \forall \epsilon \leq \epsilon_0 \tag{5.3.1}$$

where ϵ_0 and D can be calculated from Lemma (5.4).

This result can be extended to controllers employing state estimation.

Theorem 5.3

Consider the feedback loop $\{G^0, K^0\}$ as in Figure 5-1, with the disturbance noise ω_1, ω_2 obeying the Assumptions (5.2.12),(5.2.13), (5.2.14), and the systems G^0, K^0 being

$$G: \left[\begin{array}{c|c} A^0 & B^0 \\ \hline C^0 & D^0 \end{array}\right]_{x_0} ; \quad K^0: \left[\begin{array}{c|c} A^0 + B^0F^0 + H^0C^0 + H^0D^0F^0 & -H^0 \\ \hline F^0 & 0 \end{array}\right]_{\hat{x}_0 = x_0}$$

where the gains H^0, F^0 have been chosen (by LQG design or otherwise) such that $(A^0 + B^0F^0), (A^0 + H^0C^0)$ are exponentially stable.

Consider a second feedback system, $\{G(t\epsilon^{-1}), K(t\epsilon^{-1})\}$ with the systems being:

$$G(t\epsilon^{-1}):\left[\begin{array}{c|c} A^1(t\epsilon^{-1}) & B^1(t\epsilon^{-1}) \\ \hline C^1(t\epsilon^{-1}) & D^1(t\epsilon^{-1}) \end{array}\right], \qquad K(t\epsilon^{-1}):$$

$$\left[\begin{array}{c|c} A^2(t\epsilon^{-1})+B^2(t\epsilon^{-1})F(t\epsilon^{-1})+H(t\epsilon^{-1})C^2(t\epsilon^{-1})+H(t\epsilon^{-1})D^2(t\epsilon^{-1})F(t\epsilon^{-1}) & -H(t\epsilon^{-1}) \\ \hline F(t\epsilon^{-1}) & 0 \end{array}\right]_{\hat{x}_0=x_0}$$

where the matrix blocks have been defined so that

$$\xi^0 = \frac{1}{T}\int_0^T \xi(t)dt; \quad \xi(t+T)=\xi(T) \tag{5.3.2}$$

for ξ being each of the blocks $A^1, A^2, B^1, B^2, \ldots$, as well as the multiples B^1F, HC^1, HD^1F, HD^2F. Define the augmented states of the systems $\{G^0, K^0\}$ and $\{G(t\epsilon^{-1}), K(t\epsilon^{-1})\}$ as $X^0 \equiv [x^{0T}\ \hat{x}^{0T}]^T$, $X(t) \equiv [x^T\ \hat{x}^T]^T$, then

$$||X^0 - X|| \le \epsilon L, \quad 0 \le t < \infty, \quad \forall \epsilon < \epsilon_0 \tag{5.3.3}$$

where L, ϵ_0 are constants and can be calculated via (5.2.20), (5.2.8)

Proof. The feedback system $\{G(t\epsilon^{-1}), K(t\epsilon^{-1})\}$ can be reformulated as

$$\begin{bmatrix} \dot{x} \\ \dot{\hat{x}} \end{bmatrix} = \begin{bmatrix} A^1(t\epsilon^{-1}) & B^1(t\epsilon^{-1})F(t\epsilon^{-1}) \\ -H(t\epsilon^{-1})C^1(t\epsilon^{-1}) & Z(t\epsilon^{-1}) \end{bmatrix}\begin{bmatrix} x \\ \hat{x} \end{bmatrix} + \begin{bmatrix} B^1(t\epsilon^{-1}) & 0 \\ -H(t\epsilon^{-1})D(t\epsilon^{-1}) & -H(t\epsilon^{-1}) \end{bmatrix}\begin{bmatrix} \omega_1 \\ \omega_2 \end{bmatrix}; \quad \begin{matrix} x(0)=x_0 \\ \hat{x}(0)=x_0 \end{matrix}$$

where

$$Z(t\epsilon^{-1}) \equiv A^2(t\epsilon^{-1}) + B^2(t\epsilon^{-1})F(t\epsilon^{-1}) + H(t\epsilon^{-1})C^2(t\epsilon^{-1}) + H(t\epsilon^{-1})(D^2(t\epsilon^{-1}) - D^1(t\epsilon^{-1}))F$$

The averaged system can be expressed as

$$\begin{bmatrix} \dot{x}^0 \\ \dot{\hat{x}}^0 \end{bmatrix} = \begin{bmatrix} A^0 & B^0F^0 \\ -H^0C^0 & A^0 + B^0F^0 + H^0C^0 \end{bmatrix}\begin{bmatrix} x^0 \\ \hat{x}^0 \end{bmatrix} + \begin{bmatrix} B^0 & 0 \\ -H^0D^0 & -H^0 \end{bmatrix}\begin{bmatrix} \omega_1 \\ \omega_2 \end{bmatrix}; \quad \begin{matrix} x^0(0)=x_0 \\ \hat{x}^0(0)=x_0 \end{matrix}$$

The choice of H, F, and the averaging condition (5.3.2), ensures that the averaged system is stable, and consequently the application of Corollary (5.1) gives (5.3.3). ∎

Remarks

1. This result links the state trajectories of any set of plants/controllers obeying the assumptions of the theorem. The power of its application arises from the fact that the matrix blocks of $G(t\epsilon^{-1}), K(t\epsilon^{-1})$ need not be time varying. Thus, we can use Theorem (5.3) to take a stable (time invariant) $\{G, K\}$ system, and link the state trajectories to those of systems where either or both of G, K may be time varying. Furthermore, we can take a stable time-varying system, and design other time variations using concepts such as independent support of Definition (10) to simplify analysis, and provide results pertaining to both systems.

2. Although the states of the time-invariant and time-varying systems are $O(\epsilon)$ close, the same can only be said of the control signals $u(.)$ if $C^1(t\epsilon^{-1}), D^1(t\epsilon^{-1}), F(t\epsilon^{-1})$ are constant matrices. Thus, the choice of these blocks may lead to further system simplification, or to retention of the LQG index to within $O(\epsilon)$ of the LQG index obtained with use of the optimal n^{th} order controller. (This will be elaborated upon in Theorem (5.4)).

3. Theorem (5.3) can be used to give bounds on the control action of feedback pairs chosen from within sets of plants and controllers where each plant and each controller has same time average respectively. Thus, given a limit on the trajectory divergence from some nominal, we can describe a set of time-varying plants/controllers, the elements of which have trajectories satisfying the limit.

We specialize the theorems of this section to the application of controller order reduction,

Theorem 5.4

Consider a linear time-invariant feedback system $\{G, K\}$, where the augmented state update block is exponentially stable, and K has the form

$$K: \left[\begin{array}{c|c} E & F \\ \hline G & 0 \end{array}\right]$$

Consider also $K^{\#}$, a periodic structure controller of the form

$$K^{\#}: \left[\begin{array}{c|c} E^{\#}(t\epsilon^{-1}) & F^{\#}(t\epsilon^{-1}) \\ \hline G & 0 \end{array}\right]$$

where $\#$ is the operation of Definition (10). Then $K^{\#}$ is computationally equivalent to a first order controller. In a given bounded noise environment, with the noise signals obeying Assumptions (5.2.12),(5.2.13),(5.2.14), the LQG indices of the two systems are related :

$$LQG_{\{G,K\}} - LQG_{\{G,K^{\#}\}} = O(\epsilon), \quad \forall \epsilon < \epsilon_0 \tag{5.3.4}$$

where the explicit dependence on ϵ, and the value of ϵ_0 may be calculated via Corollary (5.1).

Proof. Only one state of $K^{\#}$ is changing at any given time since only one row of $E^{\#}$ and $F^{\#}$ is nonzero at any given time. Thus, $K^{\#}$ is computationally equivalent to a first order controller. Moreover, since the augmented system is exponentially stable, then by Lemma (5.1), the difference between the states of the two systems are bounded by $O(\epsilon)$, giving (5.3.4). ∎

Remark:

To further illustrate our claim that a controller with only one state changing at a given time is computationally equivalent to a first order controller, consider the dynamical system

$$\begin{bmatrix} \dot{x}_1 \\ \dot{x}_2 \end{bmatrix} = \begin{bmatrix} a(t) & b(t) \\ c(t) & d(t) \end{bmatrix} \begin{bmatrix} x_1 \\ x_2 \end{bmatrix} + \begin{bmatrix} e(t) \\ f(t) \end{bmatrix} u(t), \quad x_1(0), x_2(0). \tag{5.3.5}$$

where $a(.), b(.), e(.)$ are periodic with period T, and are zero for time $t \in [(2n+1)T/2, nT]$, $n \in J^+$, and which have independent support with respect to the periodic functions $c(.), d(.), f(.)$ which are zero for time $t \in [nT, (2n+1)T/2]$, $n \in J^+$. Then, it is clear that the system (5.3.5)is equivalent to a combination of the two systems:

$$\left.\begin{array}{l} \dot{y}_1 = a(t)y_1 + b(t)C_1 + e(t)u(t) \\ \dot{y}_2 = 0 \end{array}\right\} \quad t \in [nT, (2n+1)T/2], n \in J^+$$

$$\left.\begin{array}{l} \dot{y}_1 = 0 \\ \dot{y}_2 = c(t)C_2 + d(t)y_2 + f(t)u(t) \end{array}\right\} \quad t \in [(2n+1)T/2, nT], n \in J^+$$

(5.3.6)

At $t = nT$, then C_1 is updated to the value of $y_2(nT)$, and when $t = (2n+1)T/2$, C_2 is updated to the value of $y_1((2n+1)T/2)$.

Since $y_1(t)$ and $y_2(t)$ are not updating simultaneously, a single first order system, with a switching of initial conditions and constants at time $t = nT/2, n \in J^+$, can exactly follow the trajectories of $y_1(t), t_2(t)$, which in turn exactly follow the trajectories of $x_1(t), x_2(t)$.

5.4 A Case Study

In this section, we present examples of simulations pertaining to the Lemmas of Section 2,and the Theorems of Section 3.

Example 1: Illustration of Lemma (5.1)

The system studied with reference to Section 2 is adapted from an example [42] of an unstable periodic system, with a stable averaged system. We demonstrate how increasing the frequency of the periodicity will stabilize the system, and also how the bounds between the sates of the fast periodic system, and the averaged system are calculated.

The periodic system simulated is:

$$\begin{aligned} \dot{x} &= A(t\epsilon^{-1})x; \quad x(0) = [-1\ 0]' \\ A(t\epsilon^{-1}) &= \begin{bmatrix} -1 + 3/2\cos^2(t\epsilon^{-1}) & 1 - 3/2\cos(t\epsilon^{-1})\sin(t\epsilon^{-1}) \\ -1 - 3/2\sin(t\epsilon^{-1})\cos(t\epsilon^{-1}) & -1 + 3/2\sin^2(t\epsilon^{-1}) \end{bmatrix} \end{aligned} \tag{5.4.1}$$

The averaged system is:

$$\begin{aligned} \dot{y}(t) &= \overline{A}y; \quad y(0) = [-1\ 0]' \\ \overline{A} &= \begin{bmatrix} -1/4 & 1 \\ -1 & -1/4 \end{bmatrix} \end{aligned} \tag{5.4.2}$$

Thus the averaged system $\overline{A}$ has stable eigenvalues, $\lambda_i(\overline{A}) = -.25 \pm i$, also $||e^{\overline{A}t}|| = e^{-.25t} = Ce^{-\lambda t}$, and the following constants hold for the systems (5.4.1),(5.4.2):

$$||\overline{A}|| = 1.03, \quad S_A = \sup_t ||A(t)|| = 1.78, \quad D_A = \sup_t ||A(t) - \overline{A}|| = .75$$
$$C_A = 1, \quad \lambda = .25, \quad T_A = 2\pi$$

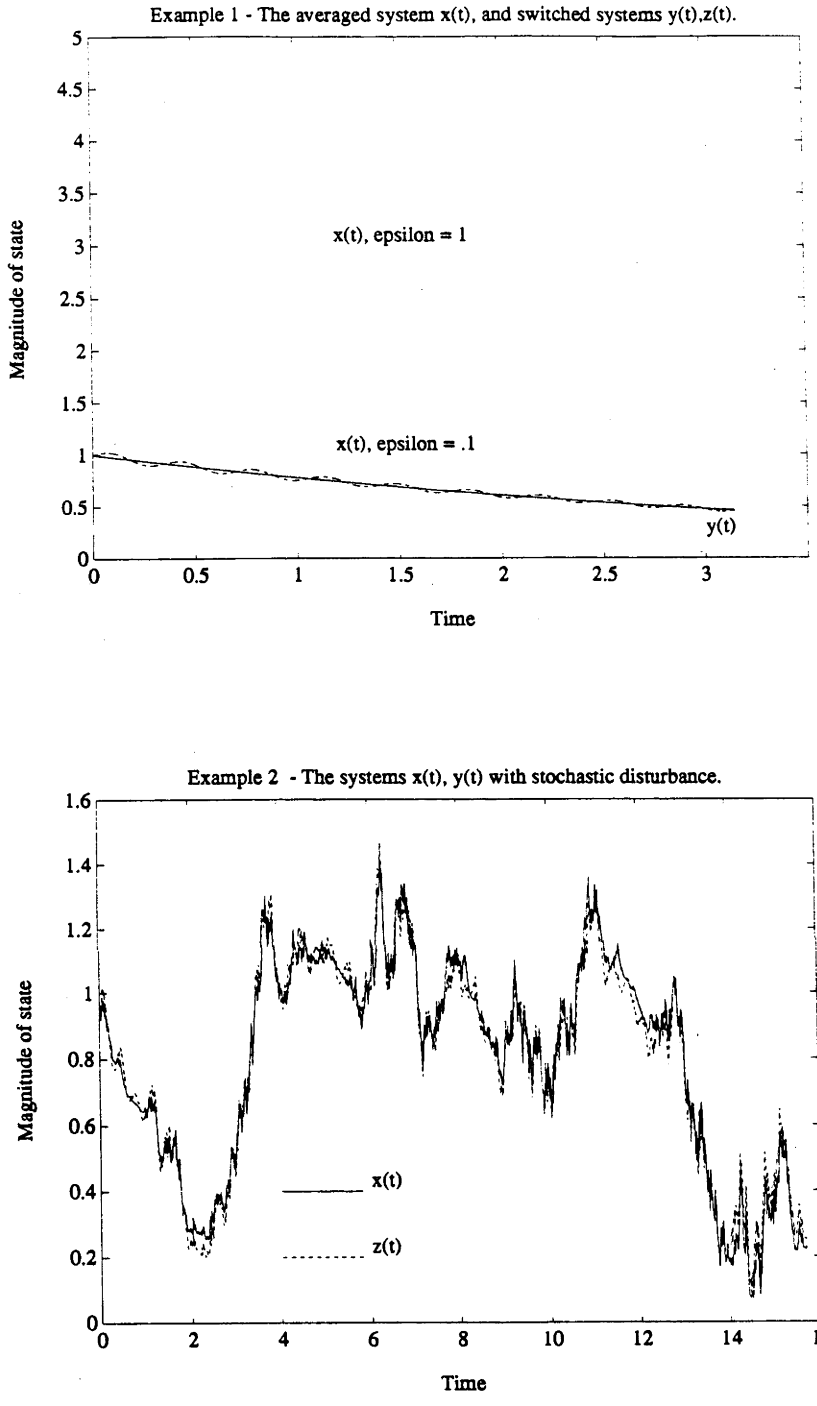

Figure 5-2: Comparison of $x(t), y(t), z(t)$

With $\overline{A}, A(t)$ defined in (5.4.1),(5.4.2), then (5.2.9) and (5.2.10) become:

$$\begin{aligned} ||y(t) - x(t)|| &\leq \epsilon||x_0||[4.71 + 14t + .81t^2]e^{-.125t}; \ \forall \epsilon < \frac{1}{34\pi} \\ ||\phi_y(t, t_0)|| &\leq (1 + 206\epsilon)e^{-.0625(t-t_0)} \ \forall \epsilon < \frac{1}{34\pi} \end{aligned}$$

The trajectories for $x(t)$ with $\epsilon = 1$, $x(t)$ with $\epsilon = .1$, and $y(t)$, all with initial condition $x_0 = y_0 = [-10]'$, are shown in Figure 5-2. It is clear that $x(t)$ will grow exponentially for $\epsilon = 1$, and converge to $y(t)$ for $\epsilon = .1$. Thus this simulation, and others not shown here, illustrate that the region of convergence includes the calculated bound of $\epsilon < 1/144$.

Example 2: Illustration of Lemmas (5.2),(5.4)

In this example, equations (5.4.1), and (5.4.2) are modified by the addition of a disturbance signal, ω, with a uniform amplitude distribution bounded by $|\omega| < 5$.

$$\begin{aligned} \dot{z} &= A(t\epsilon^{-1})z + \omega(t); \quad z(0) = x_0 \\ \dot{x} &= \overline{A}x + \omega(t); \quad x(0) = x_0 \end{aligned} \tag{5.4.3}$$

For the case-study, Lemma 5.2 gives a bound on $z(t)$

$$||z(t)|| \leq 81(1 + 206\epsilon) \tag{5.4.4}$$

and from Lemma (5.4),

$$||z(t) - x(t)|| \leq 2600\epsilon, \ \forall \epsilon < 0.05 \tag{5.4.5}$$

Our case study, as depicted in Figure 5-2 suggests that the theoretically calculated bounds are extremely conservative.

Example 3: A simulation of controller order reduction via Theorem (5.4)

In this section, we describe results obtained by simulation of the procedure outlined in Theorem (5.4) for the reduction of complexity of a given controller.

Consider the plant (transfer function):

$$G : \frac{s^2 + 5s + 6}{s^4 - 1.4s^3 + .75s^2 - .14} \tag{5.4.6}$$

We design a corresponding LQG regulator for the cost index, and noise covariances (5.4.7).

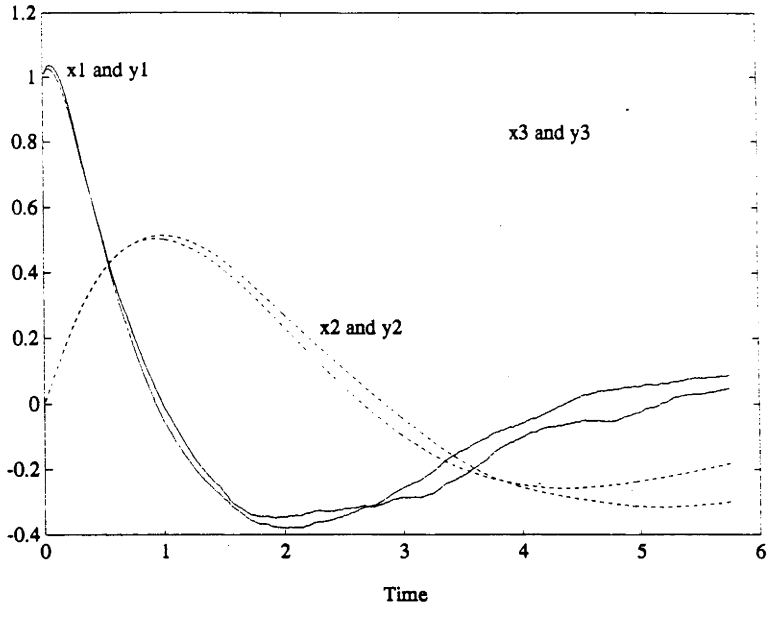

Figure 5-3: Comparison of plant trajectories with the full, and first order controllers.

$$
\begin{aligned}
I &= \int_0^t x'x + u'udt \\
E([\omega_1 \ \omega_2]'[\omega_1 \ \omega_2]) &= \begin{bmatrix} I & 0 \\ 0 & I \end{bmatrix}
\end{aligned} \tag{5.4.7}
$$

Define this optimal LQG regulator K. Then the periodic-structure, first-order controller $K^{\#}$ can be designed via Definition (11) and Theorem (5.4). The feedback systems $\{G, K\}$ and $\{G, K^{\#}\}$ with a switching speed of $\epsilon = .01$ are simulated with an identical noise signal ω which is uniformly distributed between $-.5$ and $.5$.

As can be seen from Figure 5-3, the states of the two systems track each other well, even though for this example Lemma (5.4) only bounds the tracking error for the case $\epsilon \leq 10^{-9}$. The LQG indices calculated for the two systems are : $LQG_{\{G,K\}} = 6.3$, $LQG_{\{G,K^{\#}\}} = 6.5$.

Remark: The differences between the trajectories of the averaged and periodic systems found via simulation are several orders of magnitude smaller than the bounds calculated for the maximum difference. This is because the conservativeness of the bounds is multiplicative, and the theory must at each stage of the calculation bound the maximum possible error.

5.5 Discrete-time control of a continuous-time plant

In this section we apply the results of Section 2 to the problems of discrete-time approximants for continuous-time systems, as well as hybrid control, i.e. the control of a continuous-time plant via a discrete-time controller. In short, our results show that any stable linear continuous-time system can be approximated arbitrarily closely by a discrete-time periodic system, and also that any minimal, linear continuous time system controlled via a continuous-time controller can be controlled via a discrete time controller with only $O(\epsilon)$ increase in the continuous-time performance index.

In order to simplify the presentation, and without loss of generality, we restrict to the class of strictly proper plants. Thus consider a strictly proper plant G^0 : $\left[\begin{array}{c|c} A & B \\ \hline C & 0 \end{array}\right]$, with state $x(t)$, and stabilizing controller K^0 : $\left[\begin{array}{c|c} A+BF+HC & -H \\ \hline F & 0 \end{array}\right]$, with state $z(t)$ and their feedback loop $\{G^0, K^0\}$ as depicted in Figure 5-1. This is the continuous-time feedback system $\{G, K\}$.

Definition:

The system of Figure 5-4 with sampling and a zero order hold applied to the input streams with sampling period of ϵ is denoted $\{_{H(\epsilon)}G, K\}$ (5.5.1)

The state evolution equation of $\{G, K\}$ can be expressed as

$$\begin{bmatrix} \dot{x} \\ \dot{z} \end{bmatrix} = \begin{bmatrix} A & BF \\ -HC & A+BF+HC \end{bmatrix} \begin{bmatrix} x \\ z \end{bmatrix} + \begin{bmatrix} B & 0 \\ 0 & -H \end{bmatrix} \begin{bmatrix} \omega_1 \\ \omega_2 \end{bmatrix}; \quad \begin{bmatrix} x_0 \\ z_0 \end{bmatrix} \tag{5.5.2}$$

and defining

$$\xi = [x^T \; z^T]^T; \mathcal{A} = \begin{bmatrix} A & BF \\ -HC & A+BF+HC \end{bmatrix}, \mathcal{B} = \begin{bmatrix} B & 0 \\ 0 & -H \end{bmatrix}; \omega(t) = \begin{bmatrix} \omega_1(t) \\ \omega_2(t) \end{bmatrix} \tag{5.5.3}$$

gives

$$\dot{\xi} = \mathcal{A}\xi + \mathcal{B}w(t), \quad \xi(0) = \xi_0 \tag{5.5.4}$$

where the minimality of G and subsequent choice of F, H ensure exponential stability of

$\mathcal{A}$.

Application of Definition (13), allows the state evolution equations of the system $\{_{H(\epsilon)}G, K\}$ to be expressed as

$$\begin{bmatrix} \dot{x} \\ \dot{z} \end{bmatrix} = \begin{bmatrix} A & BF \\ -HC & A+BF+HC \end{bmatrix} \begin{bmatrix} x \\ z \end{bmatrix} + \begin{bmatrix} B & 0 \\ 0 & -H \end{bmatrix} \begin{bmatrix} \omega_1 \\ \omega_2 \end{bmatrix} - \begin{bmatrix} 0 & BF \\ -HC & 0 \end{bmatrix} \begin{bmatrix} x^d \\ z^d \end{bmatrix} - \begin{bmatrix} B & 0 \\ 0 & -H \end{bmatrix} \begin{bmatrix} \omega_1^d \\ \omega_2^d \end{bmatrix} \tag{5.5.5}$$

which is equivalent to

$$\dot{\zeta} = \mathcal{A}\zeta + \mathcal{B}w(t) + \mathcal{C}\zeta^d - \mathcal{B}w^d(t);\ \ \zeta(0) = \xi_0, \zeta^d(0) = 0, \omega_0^d(t) = \begin{bmatrix} \omega_1^d(t) \\ \omega_2^d(t) \end{bmatrix} \tag{5.5.6}$$

$$\text{where } \zeta = [x^T\ z^T]^T,\ \ \mathcal{C} = -\begin{bmatrix} 0 & BF \\ -HC & 0 \end{bmatrix} \tag{5.5.7}$$

To apply Lemma (5.5) to equations (5.5.4),(5.5.6) we first must bound the signal $\zeta(t)^d$. To this end, consider the following:

Lemma 5.6 *Given*

$$\dot{\zeta} = A\zeta(t) + \omega(t) + C\zeta^d(t);\ \ \zeta(0) = \zeta_i, \zeta^d(0) = 0$$

where λ_{A+C}, C_{A+C} *are chosen such that* $||e^{(A+C)t}|| \leq C_{A+C}e^{\lambda_{A+C}t}, \forall t \geq 0, ||\omega(t)|| \leq W\ \forall t \geq 0$, *and* $\zeta^d(t)$ *is related to* $\zeta(t)$ *via Definition (13). Then*

$$||\zeta^d(t)|| \leq 4\epsilon C_{A+C}(W + ||A||\zeta(t)),\ \ \forall \epsilon < \min\left\{\frac{1}{2\lambda_{A+C}}, \frac{1}{4||A||C_{A+C}}\right\} \tag{5.5.8}$$

Proof. During the i^{th} time interval,

$$\begin{aligned} \dot{\zeta}^d &= (A+C)\zeta^d + A\zeta_i + \omega(t);\ \ \zeta(0) = 0 \\ \zeta^d &= \int_0^t e^{(A+C)(t-\tau)}[A\zeta_i + \omega(\tau)]d\tau \\ ||\zeta^d(t)|| &\leq 2C_{A+C}[||A\zeta_i|| + W]\epsilon,\ \ \forall \epsilon < \frac{1}{2\lambda_{A+C}} \end{aligned} \tag{5.5.9}$$

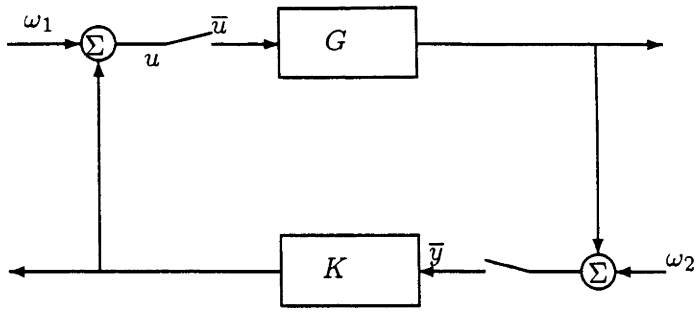

Figure 5-4: Sampled hold system $\{_{H(\epsilon)}G, K\}$.

by the triangle inequality, $||\zeta_i|| \leq ||\zeta^d(t)|| + ||\zeta(t)||$, and (5.5.8) follows. ∎

Theorem 5.5

Consider the stable system $\{G, K\}$, and the system $\{_{H(\epsilon)}G, K\}$ of Definition (5.5.1)with augmented states ξ, ζ respectively, and sampling period of ϵ. Then with Definitions (5.5.3), (5.5.7),(13) holding, their state update equations can be represented as:

$$\dot{\xi} = \mathcal{A}\xi + \mathcal{B}w(t);\ \xi(0) = \xi_0 \tag{5.5.10}$$

$$\dot{\zeta} = \mathcal{A}\zeta + \mathcal{B}w(t) + \mathcal{C}\zeta^d - \mathcal{B}w^d(t);\ \zeta(0) = \xi_0 \tag{5.5.11}$$

Given $\omega(t) \leq W$, $\forall t$, then

$$||\xi - \zeta|| \leq 2C_{\mathcal{A}}[(2||\mathcal{B}||W + \epsilon||\mathcal{C}||(U + XV)]/\lambda_{\mathcal{A}},\quad \forall \epsilon < \min\{\frac{\lambda_{\mathcal{A}}}{2C_{\mathcal{A}}V}, \frac{1}{2\lambda_{A+\mathcal{C}}}, \frac{1}{4||A||C_{A+\mathcal{C}}}\} \tag{5.5.12}$$

where X, V, U are chosen via Inequality (B.3), and Lemma (5.6) such that $||\xi(t)|| < X$, $\forall t \geq 0$; $||\zeta^d(t)|| \leq \epsilon||\zeta(t)||V + \epsilon U$ and $C_{A+\mathcal{C}}, \lambda_{A+\mathcal{C}}, C_A, \lambda_A$ chosen such that $||e^{(A+\mathcal{C})t}|| \leq C_{A+\mathcal{C}}e^{\lambda_{A+\mathcal{C}}t}, \forall t \geq 0$; $||e^{At}|| \leq C_A e^{-\lambda_A t}, \forall t \geq 0$.

Furthermore, if $||\dot{\omega}(t)|| \leq \alpha$, then $||\omega^d|| \leq \alpha\epsilon$, and

$$||\xi - \zeta|| \leq \epsilon 2C_{\mathcal{A}}[XV||\mathcal{C}|| + ||\mathcal{B}||\alpha + ||\mathcal{C}||U]/\lambda_{\mathcal{A}},\quad \forall \epsilon < \min\{\frac{\lambda_{\mathcal{A}}}{2C_{\mathcal{A}}V}, \frac{1}{2\lambda_{A+\mathcal{C}}}, \frac{1}{4||A||C_{A+\mathcal{C}}}\} \tag{5.5.13}$$

Proof. The state equations are derived in (5.5.2) to (5.5.6), and the Theorem follows from application of Lemmas (5.6) and (5.5). ∎

The sampled hold functions force the controller and plant to have constant inputs over each sampling period. Thus the intersample behaviour of the controller has no relevance

to the plant, and consequently the controller can be replaced with a discretised version with no loss of performance. We summarize the preceding discussion:

Theorem 5.6

Consider a feedback loop consisting of a minimal, continuous-time plant G, and associated LQG designed controller K in a feedback loop with bounded disturbance $\omega(t)$ with bounded derivative, obeying Assumptions(5.2.12),(5.2.13),(5.2.14), and with Definition (5.5.1) holding. Then the controller K can be replaced by a zero-order hold function and discrete controller K^D, with sampling period τ with performance:

$$LQG\{_{H(\tau)}G, K\} - LQG\{G, K\} \leq \tau M, \quad \forall \tau \leq \tau_0 \tag{5.5.14}$$

where τ_0, and the constant M may be calculated via Theorem (5.5).

Remarks:

1. Techniques using functions with independent support may be implemented in conjunction with the discretization results of the current section to generate low order discrete-time controllers for high-order continuous-time plants. The optimal implementation will depend on the speed and parallel computing facilities available for a given situation, as well as the performance requirements.

2. Note that this method of hybridization guarantees good inter-sampled behaviour since the state of the plant within the hybrid system is bounded to within $O(\tau)$ of the plant in the continuous-time feedback loop at all times.

3. This system allows any combination of the plant, controller or both to be implemented in continuous or discrete time. A further application is to the simulation of a continuous-time feedback loop by a purely discrete-time feedback loop. This is achieved via defining the factors of $G(t\epsilon^{-1}), K(t\epsilon^{-1})$ such that the factors of $G(t\epsilon^{-1})$ have independent support with respect to the factors of $K(t\epsilon^{-1})$. This loop is exactly implementable on a digital system.

5.6 Conclusion

The idea of using averaging theory for the analysis and design of periodic systems has given us new results on the stability and state dynamics of time-varying systems which are not usually analytically tractable. These results are valid for linear, periodically switched systems where the time scale of the switching is fast compared to the dynamics of the

plant. We calculate in general, and for a specific example, convergence bounds of the switching speed.

A byproduct of these stability results is the comparison of certain time-varying systems and their timewise averaged, time-independent systems. It is shown that, even in certain "stochastic" environments (with bounded disturbances), their states are bounded, with the difference being $O(\epsilon)$ where ϵ is a measure of the switching speed. This linkage gives us further degrees of freedom in the design of controllers/plants, and these are employed to achieve controller simplification, order reduction, and discretization.

Chapter 6

State Dependent Switching Controller Design

6.1 Introduction

Unforeseen external disturbances, model uncertainties, or failure of a component of a plant or controller may lead to unstable behaviour in the form of un-damped or lightly damped resonances. In these cases standard linear time-invariant control techniques may not be applicable, due to model uncertainties, non-linear elements, and high model order.

To focus on a control problem which exhibits these features, consider the design of Large Space Structure (LSS) Controllers. The systems being controlled have the following properties [6]:

1. In theory they are infinite dimensional, and in practise very large dimensional.
2. They have many resonant frequencies, and their natural damping is very low, and very poorly known
3. There is large model uncertainty, since their behaviour in space is markedly different from that on earth.
4. Vibration suppression and other requirements are very stringent.
5. The control may be of a decentralised form, due to competing controllers with objectives such as attitude and pointing control, vibration suppression, shape and thermal control, etc.

In general, to tackle a Large Space Structure control problem, first a finite order model

is created, often by finite element methods [11, 5, 73], and then a controller is designed for the finite order model. However, the model will often be of high order in order to keep the modelling error relatively small. Thus a further reduction in controller order will be necessary since the control commands must be computed rapidly by computers constrained in weight and size (and thereby computational power and memory size) due to pay-load requirements. Model errors will be introduced due to both the order reduction, and the change of environment from earth to space.

A further disincentive to use standard linear time-invariant controllers for (LSS) follows due to their decentralised control property. It is well known [3, 4] that given certain decentralised systems which are minimal with respect to a fictitious centralised control structure, but exhibit "decentralised fixed modes" with respect to all of the decentralised controllers, then for these systems, decentralised control can not be achieved via linear time -invariant controllers, but can be achieved via linear time-varying controllers.

Thus, as a result of the inherent model uncertainties, high order of models, and decentralised control strategies inherent in many Large Space Structures, it is not always possible to utilize standard linear time-invariant control design techniques, and the challenge is to develop alternate control strategies capable of addressing these problems.

Thus there is a need for a control design which is able to suppress as wide a class as possible of vibrations which may arise in an uncertain, possibly nonlinear or time-varying system. This we shall term resonance suppression. Also, the techniques we seek will need to lead to controllers possibly applicable to decentralised control, and of much lower order than the system they are to control.

One tool used to damp resonances in uncertain models is termed passive resonance suppression. This method simplifies control action by, in effect, adding damping terms to resonances, thus increasing the open loop stability of the plant. It is usually based on certain materials which dissipate the vibrational energy to heat, e.g. viscoelectric materials, viscous devices, etc. [35]. Although the determination of damping and stiffness coefficients to optimally damp certain structures can be reformulated, and solved as a feedback control problem [51], in general passive resonance suppression is not designed to be reactive to changing circumstances, and in the case of space structures may be very expensive for pay-load and space considerations.

A nonlinear control design for resonance suppression has been put forward in [26]. A linear compensator is designed to have resonances close in frequency to those of the controlled structure, thus allowing efficient energy transfer from the plant to the controller.

Consequently, if the natural frequencies are not accurately known, then the compensator will have a much smaller effect. To overcome this, a nonlinear feedback controller is proposed [26], where a quadratic term is introduced to promote chaotic motion in the closed loop system. This has the effect of smoothing the frequency components of the signal, allowing energy transfer between each plant mode and many compensator modes at differing frequencies, thus minimising the effect of model uncertainty.

Other methods exist for improving the control of vibrations, and these methods are often used in conjunction with, or as perturbations from standard control methods. An adaptive controller which works as an outer loop around a feedback system and identifies any resonances which may appear, and controls them is investigated in [68]. Frequency shaped cost functionals are used in [52] to increase performance around the resonant frequencies of a system, and Loop Transfer Recovery techniques are blended to improve robustness. Input command pre-shapers [25] have been used as a pre-filter to force tracking signals to induce smaller vibrations, and a Generalized Forecasting Compensatory Control strategy [58] has also been applied to the control of vibrations. This strategy involves the use of a counter excitation to cancel the unwanted vibrations. However, in general, these methods do not reduce the overall computational effort, and do not provide an alternative to standard control design methodologies, since they only supplement rather than replace a given controller.

A control method which has not, to the knowledge of the authors, been applied to *LSS* control is that of Switched Systems. Such systems have however been applied to adaptive adaptive stabilization in discrete [7], and in continuous time [18]. In the latter, the region of plant uncertainty, Σ is partitioned into a finite number of compact sets Σ_i^*, and controller gains K_i are designed such that the gain K_i asymptotically stabilizes any controller from within the set Σ_i^*. The adaptive control consists of switching between the finite number of gains K_i, until a stabilizing one is found for the actual plant. However, here the switching is used as an adaptation method and stopped when the desired control is reached.

In this chapter we explore an alternate switching design, where the switching is used as an integral part of the control design, rather than as an adaptation mechanism. The design we propose involves the creation of simple second order controllers designed for the nominal resonances of the plant, and a switching algorithm which chooses the appropriate controller at a given time. The switching algorithm may simply be a periodic one based on time, or may involve detection of the resonance least well controlled at a given time.

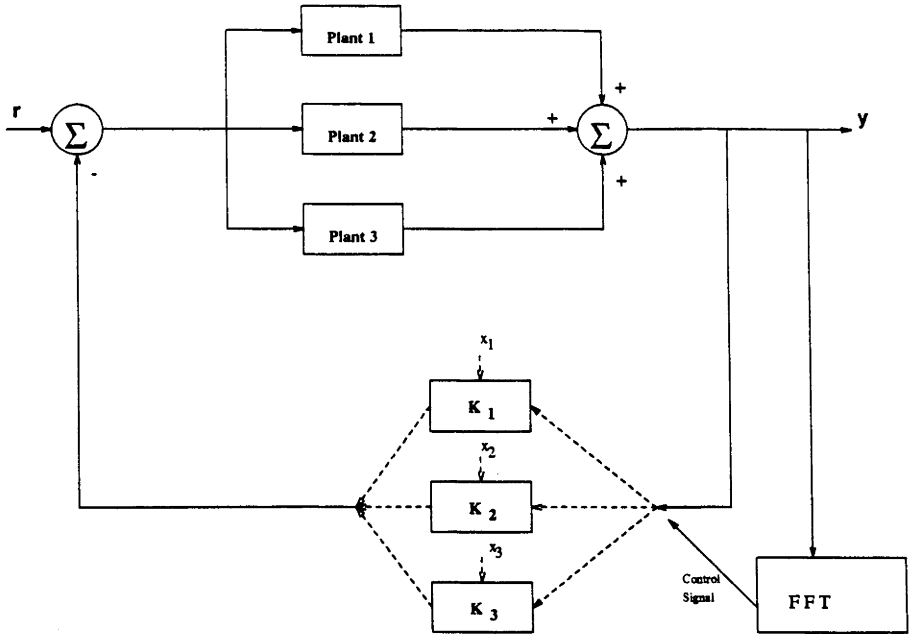

Figure 6-1: Switched control System

The chapter is outlined as follows: Section 2 describes the algorithms used, and Section 3 gives simulation results which support the switched controller method, and Conclusions are drawn in Section 4.

6.2 Switched Controller Algorithms

6.2.1 Introduction

In this section, we introduce the Switched Controller Methodology (SCM) motivated in the introduction, and discuss various implementations of the switching algorithm.

The key idea is first, via a partial fractions expansion, to view a plant as a set of n resonances as in Figure 6-1, and then to design a set of second order controllers, each designed to ,in some sense, optimally suppress one of the resonances.

The controller we propose is a time-varying controller which "switches" its feedback behaviour to that of whichever (second order) controller is deemed to be the "most appropriate" at a given time. The choice is made according to some pre-determined algorithm applied to the current (and past) amplitudes of the plant output around the resonant frequencies.

6.2.2 Aims of Controller Design

An advantage of the switched controller methodology is that after the controllers have been designed and built, the control is still easily adapted via simple and direct modifications to the switching algorithm. The switching algorithm may be designed to achieve certain aims, depending on whether the speed of switching is chosen to be faster, slower, or within the frequency band of the plant. These objectives may include:

1. **Controller Order Reduction via Fast Switching**

   Periodic switching at a rate beyond the pass band of the plant leads to the switched controller asymptotically approaching the performance of a higher order controller. In this way, for instance, n switched second order controllers may asymptotically approach the behaviour of a $2n^{th}$ order controller. Correct choice of the second order controllers enables the averaged controller to be asymptotically close to the optimal controller for the full order system. For full details of this approach, see Chapter 5.

2. **Smoothing of Energy in the Frequency Domain**

   Since sinusoids are eigenfunctions of Linear time-invariant systems, such systems cannot easily move energy between frequency bands. Utilising Periodic switching within the pass band, or decision based switching within an appropriate frequency band, make it possible for energy to be moved between frequency bands.

3. **Slow Switching to Appropriate Controller**

   If the plant is time-varying, or stochastic factors force a certain resonance to be excited at a given time, then the importance of the suppression of resonances within different frequency bands will not be constant. To achieve good control in this situation, a switched controller can simply apply the most appropriate low-order controller at each given time, analyse the results, and then iterate between the choice and analysis stages. A sensible enhancement to this method involves the application of some learning algorithm such as Functional Learning [50], to enable the switching mechanism to "learn" which controller to use at a given time based on past experience.

6.2.3 Description of Controller Design

In order to proceed, we assume that the plant has structured perturbation, or equivalently, is a member of a given set of plants. The number of resonances is assumed known, as well as the approximate frequency of each. Some nominal plant from within the uncertainty class is chosen, and the initial controller design consists of the following three stages:

1. **Partial Fractions Simplification:**

   First a partial fraction description of the plant as a number of lower order components is carried out. For simplicity, we specialize to the case where the lower order components (partial fractions components) are simply second order resonances. However, the methods proposed may be generalised to the control of any group of systems constrained to have the same input, and where the output measured is the sum of the outputs of the individual subsystems, and there is some form of filtering available to detect which subsystem is most highly excited at a given time.

2. **Construction of the Low-Order Controllers:**

   An (optimal LQG) controller for each resonance (sub-plant) is designed for the case where all the other sub-plants are zero. The overall controller is built as per Figure 6-1 as a sum of the low order controllers, with some linear combination of the low order controllers active at any time. This linear combination is accepted as input from the Switching Algorithm.

3. **Design of Switching Algorithm:**

   In its most general form, the switching algorithm maps the current (and past) outputs of the system into a vector of weightings which the Controller uses to weight each Low-Order Controller. This Switching Algorithm, and consequently the weighting vector, may be constrained to only apply a single Low-Order Controller at any given time, or to lead to periodic or even time invariant control.

   The choice of the switching algorithm is critical to the success of the SCM. Thus in the next subsection we give a qualitative discussion of various switching algorithms we have implemented and the reasons for their choice.

6.2.4 Switching Algorithm

We define the *switching rule* as the function which maps the vector of present and past outputs of the system into a vector representing some linear combination of low-order

controllers. The *method of switching* is the way the transient of the controllers is handled, i.e. by either restricting the gains to "smooth" time-varying functions, or allowing them to be piecewise constant, etc.

The *switching algorithm* includes both the switching rule as well and the method of switching. As yet we have few theoretical results on the optimisation of the control as a function of the parameters involved. In fact, simulation results show that there is no overall optimal set, it is entirely dependent on the specific plant and noise environment. Intuition coupled with simulation gives a broad starting point, and fortunately simulation results show, in the most part, that many of the parameters are not critical to the control, as long as they are within certain ranges.

The Switching Rule:

The switching decision will either be based on the amplitude, or velocity of some norm over the peaks of the energy in the frequency band at or close to each resonant frequency. The decision rules studied here include :

- Switch to the controller designed for whichever frequency has the highest amplitude at a given time.
- Switch to the controller designed for whichever frequency has the amplitude which is growing fastest at a given time.
- Periodically switch the controllers.

Estimation Algorithm:

In order to supply the switching algorithm with the information related to the amplitude of the output at each resonant frequency, as well as measured frequency of maximum amplitudes, we apply an "almost" maximum likelihood estimation algorithm [54, 55]:

1. Given a vector $x(k), k = 1, ..., N$ of real data of length $N = 2^m, m \in \mathbb{Z}$ sampled at a rate T, calculate the Hilbert Transform $z(k), k = 1, ..., N$.
2. Apply a Fast Fourier Transform to $x(k)$, generating $X(k)$, and use a search technique around the nominal frequencies to estimate the actual peaks in the frequency spectrum.
3. Find ω_i near to each nominal frequency N_i which maximises:

$$A(\omega) = \frac{1}{N}\Sigma_{n=0}^{N-1} z_n e^{-jn\omega T} \tag{6.2.1}$$

4. The "almost" maximum likelihood frequencies are ω_i, the amplitude estimates are $A(\omega_i)$, and the phase estimates are $arg(A(\omega_i))$.

If the frequencies are well separated, then a computationally less intensive approach based solely on the amplitude of the Fast Fourier Transform, $X(k)$, can be implemented as an alternative. In this case, the magnitude of the FFT is calculated at or close to each nominal frequency.

6.2.5 Parameters of switching system:

As this chapter forms an initial investigation into the applications of switched controllers, our aim is to motivate the SCM via demonstrating certain key variants on the switching procedure, and possible applications of each. These variants are generated via the following parameters:

1. **Transition Time** - After a controller is chosen, the switch to the controller may be smoothed by applying a linear combination of the old and the new controllers. This linear combination is of the form:

$$C = \alpha C_{old} + (1 - \alpha) C_{new} \tag{6.2.2}$$

   where C is the current controller, and α is updated smoothly from 1 to 0 over the transition time.

2. **Data length** - When the switching mechanism calculates the amplitude at each frequency, it uses the last n data samples. The longer this length, the more accurately it is able to ascertain the amplitude at each frequency, however a longer data length will have a less sharply defined time of validity.

3. **Method of decision** - This is the function used to generate the chosen controller from the data samples. It includes the method used to generate the amplitudes at each frequency, as well as the subsequent choice based on those amplitudes. Some examples include decisions based upon which resonant frequency has the largest amplitude, the largest growth in amplitude, periodic switching, etc.

6.3 Simulation Results

In this section we include simulations to illustrate the efficacy of the techniques proposed, as well as to explore some of the consequences of the proposed control approach. As yet, we do not have complete theoretical results able to quantitatively predict whether a given system can be improved by the application of a switched controller, but some qualitative observations do hold.

First note that Linear Time-Invariant controllers are a subset of switched controllers, and consequently the optimal switched controller is at least as good as a LTI controller of the same order, and in some cases can be shown to improve the control. Alternatively, in Chapter 5 we have proved that a number of switched low order controllers when applied to a high order plant, can lead to an LQG index which asymptotically approaches that of the "optimal" n^{th} order controller. Thus, for a high order system, a switched low order controller will be optimal amongst the class of all controllers of the same order.

Hence, the objective of this section is to demonstrate certain situations where switched systems may be of use, and to motivate further research in this area.

6.3.1 Example of Stabilization via Switching and Mixing

It is well known, that there exist time varying systems where if the system is "frozen" at any time, the time-invariant frozen system will be stable. The converse also holds in many simple theoretical systems. Consider the simple example of the following systems :

$$\begin{aligned} A &: \dot{x}_1 = x_1, \ \dot{x}_2 = -2x_2 \\ B &: \dot{x}_1 = -2x_1, \ \dot{x}_2 = x_2 \end{aligned}$$

It is immediate that if either of system A or B is used, that $\lim_{t\to\infty} |x| \to \infty$, but if systems A and B are interchanged with equal times of usage, then $\lim_{t\to\infty} |x| \to 0$.

Of course, for uncertain or time-varying systems, such an analysis and the subsequent generation of the optimal switching schedule may not be tractable. To this end, we investigate such a system in this example with the following properties:

1. The system has two pairs of complex conjugate poles, each of which generates exponentially growing oscillations in the open loop case.

2. With a controller designed for either pair of poles applied, the other trajectory still

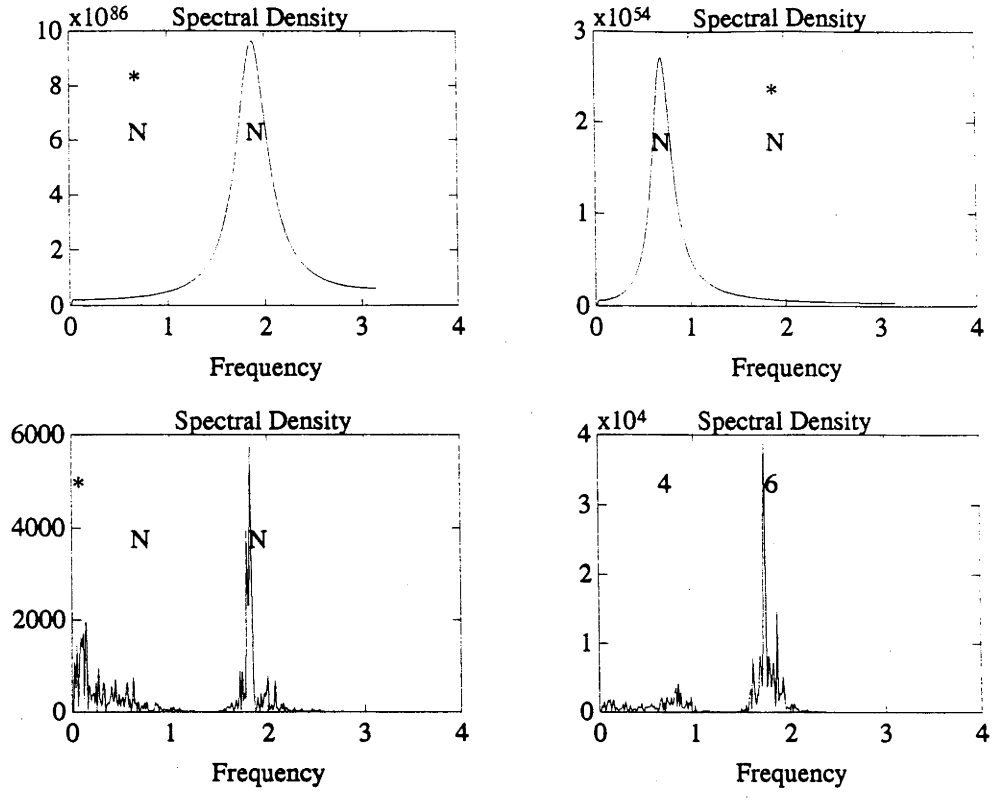

Figure 6-2: Spectral Density of Controllers as per Example 1

exhibits exponential growth in the frequency band of the alternate poles.

3. The plant has structured uncertainty both in the frequency and phase of the poles.

The values of the Plant parameters for this simulation are shown in Table (6.3.1).

Simulation Data for Example 1:

The simulation is run for 512 iterations, with a transit time of 8 iterations, and a data length of 16 iterations. The Switching mechanism chooses the controller each 8 iterations.

Result of Example 1:

The Frequency spectrum of the plant output can be seen in Figure (6-2). In each plot, the asterisk designates the frequency of the nominal controller, with the asterisk at zero indicating the full order LQG designed controller. The plot with numbers is of result

		Resonance 1	Resonance 2
Frequency:	Nominal	0.60	1.8
	Actual	0.61	1.81
Radius:	Nominal	0.99	0.99
	Actual	1.0957	1.0737

Table 6.3.1: Plant Parameters for Example 1:

from the switched controller, with the numbers representing the proportion of times each controller is used.

Note that each low-order controller satisfactorily controls the output close to the frequency of the resonance it is designed for, but fails to stabilize the alternate resonance. The switched controller stabilizes both, as does the higher order optimal *LQG* designed controller.

The LQG indices for the controllers can be seen in Table (6.3.2). These results clearly demonstrates that for the System of Example 1, neither controller 1 nor controller 2 alone, can stabilize the plant, but a switching controller which chooses either of the two, coupled with a smoothing function to ensure bumpless transitions can.

Table 6.3.2: Value of LQG indices for Example 1:

Controller	1	2	Switched
LQG Index	1E67	7E57	0.2778

6.3.2 Switching control of a stable Plant

In this subsection we introduce an example of the control of a 10^{th} order uncertain plant by a switching between a number of second order controllers. Here the motivation is to utilize a switching mechanism to facilitate significant reduction in the order of the controllers employed.

The nominal plant is:

$$19.8\left\{\frac{z+1}{z^2-1.66z+0.81}+\frac{z+1}{z^2-1.56z+0.81}+\frac{z+1}{z^2-0.97z+0.81}+\frac{z+1}{z^2-1.41z+0.81}+\frac{z+1}{z^2-1.75z+0.81}\right\}$$

The actual plant is:

$$19.8\left\{\frac{z+1}{z^2-1.83z+1.00}+\frac{z+1}{z^2-1.71z+0.98}+\frac{z+1}{z^2-0.98z+0.98}+\frac{z+1}{z^2-0.53z+0.98}+\frac{z+1}{z^2-0.99z+0.98}\right\}$$

An *LQG* controller is designed for each part second order component of the nominal plant. These controllers are designated $C_i, i = 1..5$. A switching algorithm is employed. The controller is chosen each 8 iterations, and the choice is performed by the maximum likelihood estimation routine of Section (6.2.4), with a data length of 16. For this example, the controllers are not mixed during transitions.

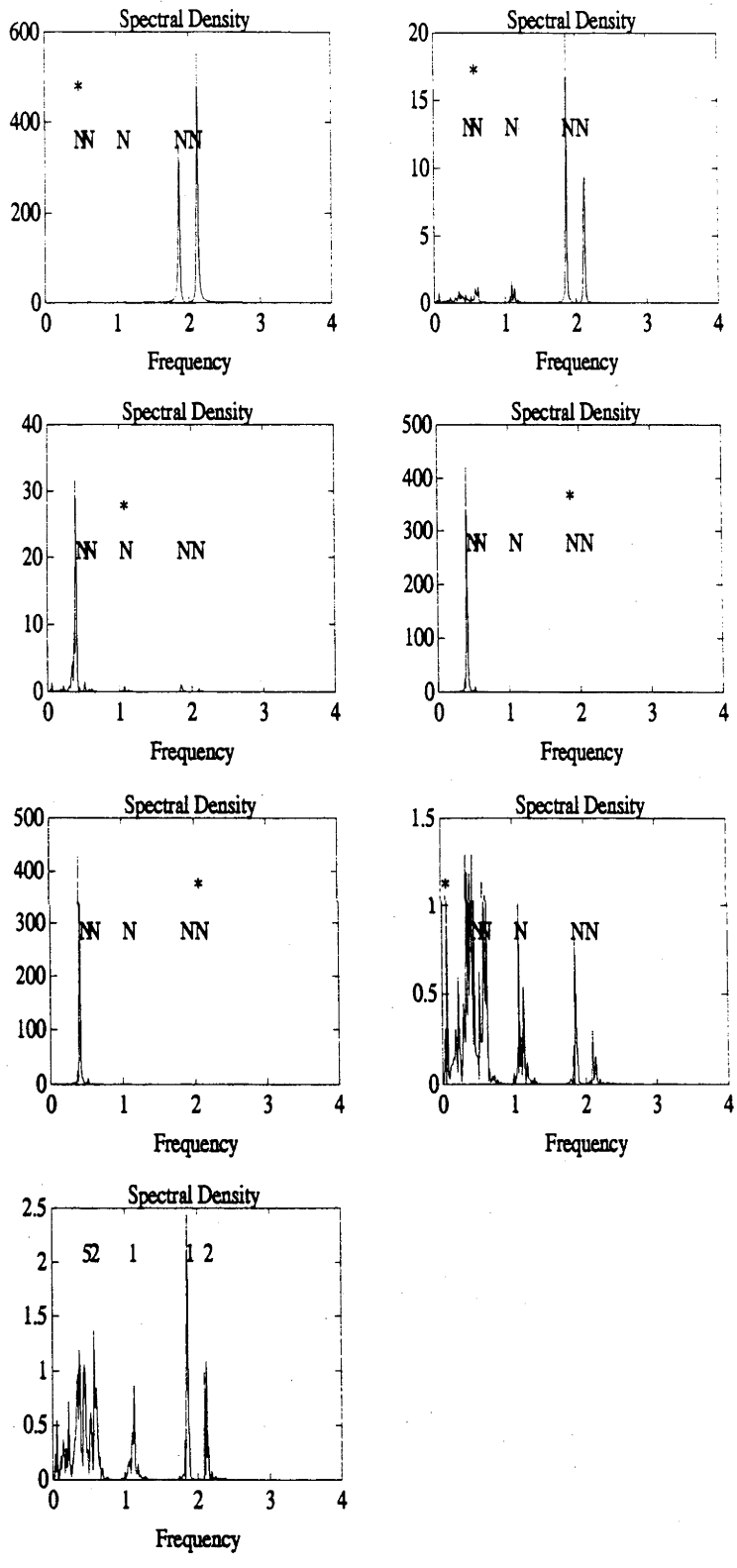

Figure 6-3: Spectral Density of Controllers as per Example: 2

The spectrum of the outputs for Example 2 can be seen in Figure (6-3), with the notation of Example 1 applying. Similarly to Example 1, each controller is capable of controlling resonances close in frequency to the one it was designed for, but does not control the others as well. Both the full order (20^{th}) LQG controller, and the switched controller (2^{nd} order), satisfactorily control all the resonances.

The *LQG* indices for the controllers of Example 2 are shown in Table (6.3.3). From these results, as well as Figure 6-3, the following observations can be made it can be seen that the switched controller significantly beat any of the others of the same order, with the difference in *LQG* index being at least an order of magnitude better.

Table 6.3.3: LQG indices for the controllers of Example 2:

Controller	1	2	3	4	5	Full Order LQG	Switched
LQG INDEX	58.6	1.7	0.6	4.0	4.0	0.3	0.4

6.4 Conclusion

We have developed arguments to demonstrate the efficacy of switching control, specifically, but not restricted to the control of Large Scale Flexible Space Structures. Furthermore a natural method for the design of such controllers is put forward, and simulation results demonstrate its efficacy.

Chapter 7

Conclusion

7.1 Overview of The Thesis

In this thesis we have explored new methods for the analysis of adaptive, learning and switching controllers, and proposed novel areas of application for such schemes based on the analysis results. We present arguments which illustrate an important connection between these controllers - that they are all elements of a subclass of nonlinear systems termed here state-dependent systems, defined as systems having a state space description in matrix form with the matrices themselves functions of the state of the system.

New stability results are generated for periodic time-dependent controllers, and for nonlinear controllers expressed as linear systems augmented (in the Q, S formalism) with nonlinear filters. Also derived here are new factorization results for state-dependent controllers, which together with known stability results lead to a description of a class of all stabilizing state-dependent controllers for a given plant, and the dual.

The stability results obtained advocate new applications of the controllers. We demonstrate one method for the effective blending of adaptive and learning (closed-loop) controllers with *a priori* designed optimal (open-loop) controllers, leading to performance/ robustness enhancement. Furthermore, switched controllers are shown to effectively diminish resonant behaviour in large-scale uncertain systems. The stability results also point to a means for the implementation of low order, discrete-time controllers for continuous-time plants of arbitrary order.

7.2 Overview of Original Results

We now summarize some of the important contributions of this thesis. They are described here in terms of both theoretical results and applications.

7.2.1 New Theoretical Results

Theoretical results are derived which extend stability results to certain classes of systems whose members include many of the controllers proposed in this thesis. They include the following:

- Stability results for the Q, S parametrization are extended from the linear case to the case where the filters Q, S, and consequently the actual plant and controller may be nonlinear.

- Coprime factorizations are constructed for state-dependent systems, and blended with known stabilization results, thus leading to a parametrisation of the class of all state-dependent stabilizing controller/plant pairs which exhibit certain differential boundedness conditions.

- Averaging theory is normally used to tie the trajectories of a complicated (often time-varying) system to those of a much simpler (time-invariant) system. This permits an approximate analysis of the behaviour of the analytically intractable time-varying system. Here the process is applied in reverse, with a class of time-varying systems defined whose performance is linked with that of their time-averaged, time-invariant system. A serendipitous property of the time-varying systems, compared to their time-averaged analogue, is their extra degree of freedom. This is exploited here to design a time-varying system which is equivalent, from an input-output point of view, to a low order time-invariant system. We use this link to formulate results leading to an approximation of a given (linear) controller of arbitrary order by a low-order controller. Moreover, the time-varying system can be designed to provide performance asymptotically close to that of the high-order controller as the time-variations increase.

7.2.2 New Algorithms

In this thesis, we develop several algorithms which pertain to the control of high-order and uncertain systems. The algorithms are based upon the adaptive, learning, and switched

controllers analysed here, and provide improvements in the areas of controller robustness, performance, and implementation. They include the following:

- Two new algorithms are developed which improve the performance and robustness properties of (open-loop) optimal controllers. The algorithms are based on the Q, S parametrization. In the first instance, the inclusion of an adaptive-Q parametrised controller is shown to substantially improve the control of an open-loop optimal controller compared with both the standard open-loop design, and the open-loop design blended with a standard LQG feedback scheme. The algorithm is further developed to the case of a functional-learning-Q controller. This second version allows the controller to be parametrised as a function of the state space, possibly leading to a more accurate compensation for unmodelled dynamics. This algorithm is not as yet as effective as the adaptive-Q scheme, but has computational advantages.

- A new method is proposed for the control of high-order uncertain systems. The control is implemented by a state-dependent switched controller in the form of a a bank of low-order controllers. Only one of the controllers is active at a given time, chosen via some switching algorithm. The switching algorithm investigated is based upon a Fourier analysis of the plant's output to determine the location of the most excited resonance, and the subsequent choice of the low-order controller which best dampens that resonance. The proposed method is computationally cheap when compared to high-order alternatives, and simulation studies, as well as intuitive arguments, indicate that this method of controller design may be advantageous for certain high-order applications with large model uncertainty such as Large-Space-Structures.

- Chapter 5 presents an algorithm which permits the approximate implementation of a continuous-time high-order controller by a low-order controller implementable in either continuous, or discrete time. Proven by our novel averaging results, the performance of the new controller can be designed to be as close as required to that of the high-order controller, limited only by the speed of computation available.

7.3 Areas For Further Research

In this thesis, we have investigated some applications of adaptive systems. The remaining challenge is to take the analytical results, and areas of application presented, and to

formulate conditions under which they may be of greater use.

- It is possible to represent the state-dependent switched controller of Chapter 6 as a linear nominal controller augmented by a nonlinear-Q filter. When coupled with a plant representation in the form of a linear nominal augmented via a linear or nonlinear-S filter, this permits application of the stability results of Chapter 2. The limitation with this approach is the fact that often the Q, S system remains sufficiently complicated to disallow obvious stability results. Work is in progress to determine areas and formulations in which the resulting simplification may be of greater use.

- There are many forms of controllers which modify their behaviour as some function of their experience, including of course the adaptive, learning, and switching controllers examined in this thesis. The fact that, for the cases examined, the learning-Q controller of Chapter 3 did not provide improved performance when compared with the adaptive-Q controller of Chapter 2 leads to questions pertaining to which areas of application are suited to each type of controller, and also to the existence of modifications, such as truncation coupled with finer grid spacings, which may lead to improved performance in the learning controller. As a starting point, further simulation and theoretical work is called for to investigate conditions under which the current learning-Q controller is superior to the adaptive for the case of stabilization around an optimal trajectory.

- The nonlinear stability results quoted in Chapter 4 require a *differential boundedness* condition on the factors. This condition constrains the factors to being 'close' in some sense to linear. Relaxing this condition or exploring other forms of such a condition could increase the class of stable systems described by the analysis, although we would not expect a complete removal of this condition since highly nonlinear systems can exhibit chaos and related behaviour. Independent of this condition, the schemes of Chapter 4 will work when the states of the factors are equal. In this case, the systems function similarly to the linear time-varying systems factorized in [63]. Thus it makes sense to investigate state-dependent systems under the assumption of the existence and inclusion of nonlinear state estimators which lead to bounded state tracking, and hence bounded differences between the states of the factors.

Bibliography

[1] B.D.O. Anderson, R.R. Bitmead, Jr. C.R. Johnson, P.V. Kokotovic, R.L. Kosut, I.M.Y. Mareels, L. Praly, and B.D. Riedle. *Stability of Adaptive Systems, Passivity and Averaging Analysis.* The MIT Press, Cambridge, 1986.

[2] B.D.O. Anderson and J. Moore. *Optimal Control Linear Quadratic Methods.* Prentice Hall, 1990.

[3] B.D.O. Anderson and J.B. Moore. Time-varying feedback laws for decentralised control. *IEEE Transactions on Automatic Control*, AC-26 NO. 5, 1981.

[4] B.D.O. Anderson and J.B. Moore. Decentralised control using time-varying feedback. *Control and Dynamical Systems*, 1985.

[5] A. Balakrishnan. *Applied Functional Analysis.* Springer-Verlag, 1976.

[6] M.J. Balas. Trends in large space structure control theory: Fondest hopes, wildest dreams. *IEEE Transactions on Automatic Control*, AC-27 No. 3, 1982.

[7] Er-Wei Bau. Adaptive regulation of discrete-time systems by switching control. *Systems & Control Letters*, 11:129–133, 1988.

[8] Boyd and Barrat. *Linear Control Design - limits of performance.* Prentice Hall, 1991.

[9] Colaneri. Discrete time linear periodic systems stabilization and zero error regulation. *Proceedings of IFAC World Congress*, 1990.

[10] W.A. Coppel. Lecture notes in mathematics. In *Dichotomies in Stability Theory*, volume 629. Springer-Verlag, 1978.

[11] R. Curtain and A. Pritchard. *Functional Analysis in Modern Applied Mathematics.* New York: Academic, 1977.

[12] G. Cybenko. Approximation by superposition of a sigmoidal function. *Mathematics of Control, Signals and systems*, 1989.

[13] J. C. Doyle, K. Glover, P. Khargonekar, and B. Francis. State space solutions to standard h^2 and h^∞ control problems. *IEEE Trans. Automatic Control*, AC-34:831–834, 1989.

[14] J. G. Doyle and J. G. Stein. Robustness with observers. *IEEE Trans. Automatic Control*, 24-4:607–611, 1979.

[15] M. E. Fisher, J. B. Moore, and K. L. Teo. A constrained h^∞ smooth optimisation technique". *Optimal Control Applications and Methods*, 11:327–343, 1990.

[16] Flamm. A new shift-invariant representation for periodic linear systems. *Systems & Control letters*, 17, 1991.

[17] B. A. Francis. *A course in H^∞ Control Theory.* Springer, New York, 1987.

[18] M. Fu and B. Ross Barmish. Adaptive stabilization of linear systems via switching control. *IEEE Transactions on Automatic Control*, AC-31, No. 12:1097–1103, 1986.

[19] K. Glover. All optimal hankel-norm approximations of linear multi-variable systems and their l error bounds. *Int. J. Control*, 39:1115–1193, 1984.

[20] G. Goodwin and A. Feuer. Linear periodic control: A frequency domain viewpoint. 1991. Submitted for Publication.

[21] J. Hammer. Nonlinear systems stabilization and coprimeness. *International Journal of Control*, 42(1):1–20, July 1985.

[22] J. Hammer. Stabilization of nonlinear systems. *International Journal of Control*, 44(5):1349–1381, November 1986.

[23] J. Hammer. Fraction representations of nonlinear systems: a simplified approach. *International Journal of Control*, 46:455–472, 1987.

[24] J. Hammer. Fraction representations of non-linear systems and non-additive state feedback. *International Journal of Control*, 50:1981–1990, 1989.

[25] J. M. Hyde and W. P. Seering. Inhibiting multiple mode vibration in controlled flexible systems. *Proc. ACC*, pages 2449 – 2454, 1991.

[26] D.C. Hyland. A nonlinear vibration control design with a neural network realization. *Proc. 29th CDC*, 1990.

[27] J. Imae and K. Hakomori. A second order algorithm for optimal control assuring the existence of riccatti solutions. *SICE*, 23-4:410–412, 1987.

[28] J. Imae, L. Irlicht, G. Obinata, and J.B. Moore. Enhancing optimal controllers via techniques from robust and adaptive control. *Int. Journal of Adaptive Control and Signal Processing.* Accepted for Publication.

[29] J. Imae, L. Irlicht, G. Obinata, and J.B. Moore. Enhancing optimal controllers via techniques from robust and adaptive control. *Proc. IEEE Conference on Decision and Control*, 1991.

[30] L. Irlicht, I.M.Y. Mareels, and J.B. Moore. Switched controller design. Submitted - 1993 IFAC World Congress.

[31] L. Irlicht, I.M.Y. Mareels, and J.B. Moore. Periodic structure controller design. 1992. Submitted IEEE Trans. Auto. Control.

[32] L. Irlicht, I.M.Y. Mareels, and J.B. Moore. Periodic structure controller design. *To appear Proc. 31st CDC*, 1992.

[33] L. S. Irlicht and J. B. Moore. Functional learning in optimal non-linear control. *Proc. American Control Conference*, 1991.

[34] A. Isidori. *Nonlinear Control Systems, 2nd ed.* Springer Verlag, 1989.

[35] C.D. Johnson. Passive damping technology using viscoelastics. *Proc. 30th CDC*, pages 2546–2551, 1991.

[36] Khargonekar and Poolla. Robust control of linear time-invariant plants using switching and nonlinear feedback. *Proc. 28th CDC, Florida*, 1989.

[37] Khargonekar, Poolla, and Tannenbaum. Robust control of linear time invariant plants using periodic compensation. *IEEE Transactions on Automatic Control*, AC-30, No. 11, 1985.

[38] R. Kosut, D. Meldrum, and G. Franklin. Adaptive control of a nonlinear oscillating system. *Proc. 1989 American Control Conference, Pittsburgh, PA*, 1989.

[39] A. J. Krener and Yi Zhu. The fractional representation of a class of nonlinear systems. *Proc. of the 28th CDC*, pages 963–968, 1989.

[40] V. Kucera. *Discrete Linear Control: The Polynomial Equation Approach.* Wiley, New York, 1979.

[41] S. Lee, S. Meerkov, and T. Runolfsson. Vibrational feedback control: Zeros placement capabilities. *IEEE Transactions on Automatic Control*, AC-32, No. 7:604–611, 1987.

[42] L. Markus and H. Yamabe. Global stability criteria for differential systems. *Osaka Math J.*, 12:305–317, 1960.

[43] J. B. Moore and L. Irlicht. Coprime factorization over a class of nonlinear systems. *International Journal of Robust and Nonlinear Control.* Accepted for Publication.

[44] J. B. Moore and L. Irlicht. Coprime factorization over a class of nonlinear systems. *Proc. American Control Conference*, 1992.

[45] C. N. Nett, C. A. Jacobson, and M. J. Balas. Fractional representation theory: Robustness with applications to finite-dimensional control of a class of linear distributed systems. *Proceedings of the IEEE Conf. on Decision and Control*, pages 268–280, 1983.

[46] A. D. B. Paice and J. B. Moore. On the Youla-Kucera parameterisation for nonlinear systems. *Systems and Control Letters*, 14:121–129, 1990.

[47] A. D. B. Paice and J. B. Moore. Robust stabilization of nonlinear plants via left coprime factorizations. *Systems and Control Letters*, 15:125–135, 1990.

[48] A. D. B. Paice, J. B. Moore, and R. Horowitz. Nonlinear feedback stability via coprime factorization analysis. Accepted by Journal of Mathematical Systems Estimation and Control, October 1991.

[49] A.D.B. Paice. *Stabilization and Identification of Nonlinear Systems.* Ph.D. Thesis, A.N.U., 1992.

[50] J. E. Perkins, I.M.Y. Mareels, R. Horowitz, and J.B. Moore. Functional learning in signal processing via least squares. *Int. Journal of Adaptive Control and Signal Processing.* Accepted for Publication.

[51] T. Posbergh, M. Trimboli, and J. Duke. A control formulation for vibration absorbers. *Proc. ACC*, pages 2481–2482, 1991.

[52] Prasad, Calise, and Byrns. Active vibration control using fixed order dynamic compensation with frequency shaped cost functionals. *Proc. ACC*, 1991.

[53] V. Wertz R. Bitmead, M. Gevers. *Adaptive Optimal Control - The Thinking Man's GPC.* Prentice Hall International Series in Systems and Control Engineering. Prentice Hall, New York, 1990.

[54] D.C. Rife and R.R. Boorstyn. Single tone parameter estimation from discrete-time observations. *IEEE Trans. on Information Theory*, IT-20 No. 5, 1974.

[55] D.C. Rife and R.R. Boorstyn. Multiple tone parameter estimation from discrete-time observations. *Bell System Technical Journal*, 55, No. 9, 1976.

[56] E. Sanchez-Palencia. Methode de centrage et comportement des trajectories dans l'espace des phases. *Compt. Rend. Acad. Sci., Ser. A*, 280:105–107, 1975.

[57] J.A. Sanders and F. Verhulst. Averaging methods in nonlinear dynamical systems. *Applied Mathematical Sciences, Springer-Verlag*, 59, 1985.

[58] J.J. Shi and S. M. Wu. A generalized forecasting compensatory control strategy and its applications in vibration control. *Proc. ACC*, pages 1414 – 1415, 1991.

[59] J.J. Slotine and Weiping Li. *Applied Nonlinear Control.* Prentice-Hall International Editions, Englewood Cliffs, New Jersey, 1991.

[60] E. D. Sontag. Smooth stabilization implies coprime factorization. *IEEE Transactions on Automatic Control*, 34:435–443, 1989.

[61] E. D. Sontag. Some connections between stabilization and factorization. *Proc. 28th CDC*, pages 990–995, 1989.

[62] Sz.-Nagy and Foias. *Harmonic Analysis of Operators on Hilbert Space.* American Elsevier, New York, 1970.

[63] T. T. Tay and J. B. Moore. Adaptive control within the class of stabilizing controllers for a time-varying nominal plant. *International Journal of Control*, 50:33–53, 1989.

[64] T. T. Tay and J. B. Moore. Enhancement of fixed controllers via adaptive disturbance estimate feedback. *Automatica*, 27 No. 1:39–53, 1989.

[65] T. T. Tay and J. B. Moore. Left coprime factorizations and a class of stabilizing controllers for nonlinear systems. *International Journal of Control*, 49:1235–1248, 1989.

[66] T. T. Tay and J. B. Moore. Performance enhancements of two-degree-of-freedom controllers via adaptive techniques. *Adaptive Control and Signal Processing*, 4:69–84, 1990.

[67] T. T. Tay, J. B. Moore, and R. Horowitz. Indirect adaptive techniques for fixed controller performance enhancement. *International Journal of Control*, 5:1941–1959, 1989.

[68] A. Telford and J.B. Moore. Adaptive stabilization and resonance suppressio n. *International Journal of Control*, 52, No. 3:725–736, 1990.

[69] J. Tokarzewski. Stability of periodically switched linear systems and the switching frequency. *Int. J. of Systems Science*, No. 4:697–726, 1987.

[70] J. Tokarzewski. Stability of linear systems with periodic feedback and sampled-data systems. *Int. J. of Systems Science*, No. 11:2339–2366, 1988.

[71] M. S. Verma. Coprime fractional representations and stability of nonlinear feedback systems. *International Journal of Control*, 48:897–918, 1988.

[72] M. Vidyasagar. *Control system synthesis: A Factorization Approach.* MIT Press, Cambridge, 1985.

[73] P. K. C. Wang. Advances in control systems. In *Control of DPS.* New York: Academic, 1964.

[74] Z. Wang, I.M.Y. Mareels, and J.B. Moore. Adaptive performance enhancement in the presence of unmodelled dynamics. Technical Report TR90-44, University of Newcastle, 1990.

[75] D. Wiberg. *State Space and Linear Systems.* Schaum Outline Series. Mcgraw Hill, 1971.

[76] W. Y. Yan and J. B. Moore. A multiple controller structure and design strategy with stability analysis. *Automatica.* Accepted for Publication.

[77] D.C. Youla, H. Jabr, and J. J. Bongiorno. Modern wiener-hopf design of optimal controllers, part ii; the multivariable case. *IEEE Transactions on Automatic Control*, 21:319–338, 1976.

Appendix A

A.1 Proof of Lemma 3.1 of Chapter 3

Proof.

$$e = \sum_{N^2} \int_{y_0}^{y_0+r/N} \int_{x_0}^{x_0+r/N} (\hat{f}(x,y) - f(x,y))^2 \, dx \, dy \tag{A.1.1}$$

The worst case approximation to $f(x,y)$ of a level function will be when $f(x,y)$ is at its maximum gradient within a grid square. Also, the worst error will be the same for each grid square. To calculate a worst case error then, consider the "worst case" functions $f(x,y) = f_0 \pm Cx \pm Cy$. In this case,

$$e = N^2 \int_{y_0}^{y_0+r/N} \int_{x_0}^{x_0+r/N} (\hat{f}(x,y) - f(x_0,y_0) \pm Cx \pm Cy)^2 \, dx \, dy \tag{A.1.2}$$

Now, the region of that square is $\{x,y : x_0 < x < x_0 + r/N, y_0 < y < y_o + r/N\}$. Set $\hat{f} = f(x_0,y_0)$. Then a substitution of variables gives:

$$e = \frac{7}{6} N^2 C^2 (\frac{R}{N})^4 = O(\frac{C^2}{N^2}) \tag{A.1.3}$$

∎

Appendix B

B.1 Preliminary Results of Chapter 5

Inequality B.1 *Let $n \in \mathbb{N}$, $\lambda_A > 0$. Then*

$$t^n e^{-\lambda_A t} \leq (2n/e\lambda_A)^n e^{-(\lambda_A/2)t}; \ \ t \geq 0$$

Proof. Equivalently $t^n e^{-\lambda_A t/2} - (2n/e\lambda_A)^n \leq 0, \quad t \geq 0$, and verification follows via showing that the maximum value is less than zero via the use of elementary calculus. ∎

Equivalence B.1 *Given constants L, α, and a signal $\omega(t)$, then*

$$\int_0^T \omega(t)dt \leq LT^\alpha, \ \forall T > 0, \Leftrightarrow \int_0^T \omega(\epsilon t)dt \leq \epsilon^{\alpha-1} LT^\alpha; \ \ \forall T > 0, \ \forall \epsilon > 0$$

Proof. The proof follows via a substitution of variables. ∎

Proposition B.1 *Let $A(t)$ be a periodic matrix with average $\overline{A}$ and period T_A. Then using Lie bracket notation*

$$\int_t^{t+T_A} [A(u), \overline{A}]du = 0$$

Proof. Let $D(t) = A(t) - \overline{A}$. Then $\int_t^{t+T_A} D(u)du = 0$. Now

$$\begin{aligned} \int_t^{t+T_A} [A(u), \overline{A}]du &= \int_t^{t+T_A} (\overline{A} + D(u))\overline{A} - \overline{A}(\overline{A} + D(u))du \\ &= \int_t^{t+T_A} D(u)du\overline{A} - \overline{A}\int_t^{t+T_A} D(u)du \\ &= 0. \end{aligned}$$

Inequality B.2

$$\lambda e^{-\lambda t} \int_0^t e^{\lambda \tau} \tau^n d\tau \leq t^n, \quad \forall n \geq 0, \lambda \geq 0 \;\; t \geq 0$$

Proof. Equality holds at $t = 0$, and differentiation verifies that the right hand side increases faster than the left for all $t \geq 0$. ∎

Inequality B.3 *Given $w(t), |w(t)| \leq W$, and η such that*

$$\dot{\eta}(t) = A\eta(t) + w(t); \;\; \eta(0) = \eta_0$$

Then with the definitions of (8) holding, and $Re[\lambda_i(A)] < 0$,

$$||\eta(t)|| \leq C_A W/\lambda_A + (||\eta_0|| - W/\lambda_A) C_A e^{-\lambda_A t} \tag{B.1.1}$$

Proof. The proof follows via use of the transition function $e^{\overline{A}t}$, and the consequent generation of an expression for $\eta(t)$,

$$\eta(t) = e^{At}\eta(0) + \int_0^t e^{A(t-u)} w(u) du$$

∎

Inequality B.4 *Given square matrices A, L with $||e^{At}|| \leq C_A e^{-\lambda_A t}$, then $||e^{(A+\epsilon L)t}|| \leq C_A e^{(-\lambda + \epsilon ||L|| C_A)t}$.*

Proof. Define a square matrix $x(t)$ such that,

$$\dot{x} = Ax + \epsilon Lx, \;\; x(0) = I$$

Note that $x(t) = e^{(A+\epsilon L)t}$. Then defining $z(t) = ||x||e^{\lambda t}$, and using the Bellman-Gronwall lemma [72] gives

$$z(t) \leq C_A + \epsilon ||L|| C_A \int_0^t z(\tau) d\tau \leq C_A e^{\epsilon ||L|| C_A t}$$

Substitution for $x(t)$ gives $||x(t)|| \leq C_A e^{(-\lambda+\epsilon||L||C_A)t}$. ∎

Proof. [of Lemma (5.1)]:

With the definitions T_A, D_A, S_A, C_A, B_A of (8) holding, then

$$\begin{aligned}
\dot{x}(t) - \dot{y}(t) &= \overline{A}[x(t) - y(t)] + [\overline{A} - A(t\epsilon^{-1})]y(t); \qquad x(0) = y(0) = x_0 \\
x(t) - y(t) &= -\int_0^t e^{\overline{A}(t-u)} \dot{B}_A(u\epsilon^{-1})y(u)du \\
&= -B_A(t\epsilon^{-1})y(t) + \int_0^t e^{\overline{A}(t-u)}[\overline{A}B_A(u\epsilon^{-1}) + B_A(u\epsilon^{-1})A(u\epsilon^{-1})]y(u)du \\
&= -B_A(t\epsilon^{-1})C_A e^{-\lambda t}x_0 + \int_0^t e^{\overline{A}(t-u)}[\overline{A}B_A(u\epsilon^{-1}) + B_A(u\epsilon^{-1})A(u\epsilon^{-1})]x(u)du \\
&\quad - \int_0^t e^{\overline{A}(t-u)}[\overline{A}B_A(u\epsilon^{-1}) + B_A(u\epsilon^{-1})A(u\epsilon^{-1})][x(u) - y(u)]du \\
&\quad + B_A(t\epsilon^{-1})[x(t) - y(t)]
\end{aligned}$$

Setting $\epsilon < \frac{1}{T_A D_A}$, and defining $C_1 = T_A D_A C_A[||\overline{A}|| + S_A]$,$s(t) = [x(t) - y(t)]e^{\lambda_A t}$, $C_2 = T_A D_A C_A$ gives

$$s(t) \leq \epsilon C_2||x_0|| + \epsilon C_1 C_A||x_0||t + \epsilon C_1 \int_0^t s(\tau)d\tau \tag{B.1.2}$$

Then by the Bellman-Gronwall Lemma [72],

$$\begin{aligned}
s(t) &\leq \epsilon||x_0||[C_2 + C_1C_At] + \epsilon^2 e^{\epsilon C_1 t}C_1||x_0|| \int_0^t [C_2 + C_1C_A\tau]e^{-\epsilon C_1\tau}d\tau \\
&\leq \epsilon||x_0||[C_2 + C_1C_At] + \epsilon^2 e^{\epsilon C_1 t}C_1||x_0||[C_2t + C_1C_A\frac{t^2}{2}]
\end{aligned} \tag{B.1.3}$$

which verifies (5.2.9) for $\epsilon C_1 < \frac{\lambda_A}{2}$.

Also note that since $||\overline{A}|| > \lambda_A$, and $C_A \geq 1$, then $\epsilon C_1 < \frac{\lambda_A}{2} \Rightarrow \epsilon < \frac{1}{T_A D_A}$.

To verify (5.2.10), first note that $y(t) = \phi_y(t, t_0)y(t_0)$, and also $||x(t)|| \leq Ce^{-\lambda_A t}||x_0||$. Then (5.2.9) and the triangle inequality ,$||y(t)|| \leq ||y(t) - x(t)|| + ||x(t)||$, give a bound for $y(t)$, and consequently for $\phi_y(.,.)$, application of inequality (B.1) then verifies (5.2.10). ∎